MECHANICAL EFFECTS OF ALKALI SILICA REACTION IN CONCRETE STUDIED BY SEM-IMAGE ANALYSIS

THÈSE N^{O} 3516 (2006)

PRÉSENTÉE LE 5 MAI 2006

À LA FACULTÉ SCIENCES ET TECHNIQUES DE L'INGÉNIEUR

Laboratoire des matériaux de construction

SECTION DE SCIENCE ET GÉNIE DES MATÉRIAUX

ÉCOLE POLYTECHNIQUE FÉDÉRALE DE LAUSANNE

POUR L'OBTENTION DU GRADE DE DOCTEUR ÈS SCIENCES

PAR

Mohsen BEN HAHA

ingénieur en Infrastructures et Bâtiments Ruraux, diplômé de l'INAT, Tunisie
et de nationalité tunisienne

acceptée sur proposition du jury:

Prof. P. Muralt, président du jury
Prof. K. Scrivener, directrice de thèse
Prof. E. Brühwiler, rapporteur
Prof. O. Coussy, rapporteur
Dr G. Darbre, rapporteur

ÉCOLE POLYTECHNIQUE
FÉDÉRALE DE LAUSANNE

Lausanne, EPFL
2006

« On prend chacun dans le monde pour ce qu'il se donne;
mais il faut se donner pour quelque chose. On supporte plus
volontiers les gens incommodes que les hommes insignifiants. »
Johann Wolfgang von Goethe, Maximes et réflexions

À celle qui m'a appris mes premières lettres et a consacré sa vie à notre éducation (mon frère, ma sœur et moi), à maman Amina (en photo), avec tout mon amour, je dédie cette thèse.

À celui qui m'a appris ma première table de multiplication et qui m'a fait aimer la science, à mon papa Boubaker, avec tout l'amour et le respect que je lui dois, je dédie cette thèse.

À la mémoire des mes chers oncles Hachemi (en lui disant : « j'ai réussi notre pari ») et Hammouda qui me manquent énormément, je dédie cette thèse.

À celui avec qui j'ai partagé les plus grands moments de ma vie et qui était toujours avec moi depuis notre enfance, mon très cher frère Zied, avec tout mon amour, je dédie cette thèse.

À celle qui n'a cessé d'apporter du bonheur dans notre famille et qui m'a encouragé tout le long de ma thèse, à ma très chère sœur Jihène, avec tout mon amour, je dédie cette thèse.

À celui qui était et qui est toujours présent parmi nous dans notre famille, et qui m'a raconté les meilleurs contes de fée, à mon cher oncle Habib. Avec tout mon amour, je dédie cette thèse.

À celle qui a supporté mes sauts d'humeur durant la rédaction et qui m'a aidé à corriger toute cette thèse, à ma très chère Regina, avec tout mon amour, je dédie cette thèse.

Mohsen Ben Haha

Acknowledgments

I would like to express my gratitude for the many helpful comments and suggestions I have received over the last four years regarding the experimental and data analysis of my thesis, and especially for those comments which bear directly on various arguments central to the thesis. I am indebted to several people in this regard.

Most importantly, I would like to thank my supervisor Professor Karen Scrivener for her nearly four years of supervision, and especially for her commitment to guiding me through my doctoral research, as well as her endless patience in improving my writing and for the time she has spent reading the "various drafts" of this thesis. Her critical commentary on my work has played a major role in both the content and presentation of my discussion and arguments.

I also extend my gratitude to the OFEG for providing financial support for the project during the period of this research and I specially thank Dr. Georges Darbre for his valuable comments during several meetings in the course of the project.

I would like to express my thanks to the thesis defence committee: Professor Eugen Brühwiler, Professor Olivier Coussy and the president of the Jury Professor Paul Muralt.

I would like to address special thanks to Dr. Amor Guidoum for his personableness, support and advices.

I would like to thank Dr. Emmanuel Gallucci for providing me the technical support and very useful tools for the image analysis development.

I would like to thank Dr. Andreas Leeman from EMPA for his help for the petrography and the characterisation of the aggregates.

I would like to thank the laboratory technical staff: Mr. Simonin, Antonino, Mr. Dizerens for all the advice and help given during the experimental programme. Special thanks go to Lionel from the technical staff for the time that we spent together both while collecting the aggregates in the mountains and during the experiments in the laboratory.

I shall not forget the LMC team and especially "***The Untouchables***" members of my first office MXG241 and the "paradise" office MXF210 namely Frederic Heger, Julien Kighelman and Shahsank Bishnoi for their friendship and the atmosphere that they created. I should not forget "***les oiseaux de passage***" that were coming to our office time to time: thanks to Thomas Studer, Nicola Sodini and Tsyoshi Saito "San". Special thanks to the best secretary ever seen and one of the best friends I had in Switzerland Laurence Gallone for the facilities that she gave me during the thesis.

Last but not the least special thank to the Studer family for their hospitality, their support and their "***vieille prune***".

Abstract

The occurrence of alkali-silica and alkali-silicate reactions causes damage in concrete. Even though the reaction has been known for some time, the progress of reaction in affected structures is difficult to predict. This research programme aims to study the relationship between the progress of the reaction and the mechanical properties of the concrete in order to support better prognosis of the effect of ASR on affected structure.

The basic principal of the research programme is to characterise the chemical, microstructural and mechanical state of the concrete, the degree of expansion in the initial and final states and how the rate of change of the chemical reaction is related to the changes in mechanical properties

In practice this is difficult to do because:

- In the field the induction and reaction periods are very long necessitating accelerated testing in the laboratory.
- The amount of reactive material in the aggregate is usually small, and hence difficult to measure.
- The relation between the degree of reaction, expansion and the change of mechanical properties is not known.

The microstructural characteristics of some Swiss aggregates have been studied and quantified using microscopic techniques. Mortar and concretes samples were made with the aggregates and subjected to ASR. Image analysis of SEM-BSE obtained from polished samples was used to quantify the reaction degree.

In this project, a series of mechanical tests, in parallel to the chemical reaction were undertaken in order to determine the effect of ASR on the mechanical properties of concrete. The principal objective of this research is the development of a tool relating laboratory results to real structures.

Important aspects of the research were:

- A multidisciplinary approach to chemical, microstructural and mechanical characterisation to increase the chances of finding a combination of techniques which can be used to assess the degree of reaction
- Use of modelling approach to link between microstructural changes and mechanical properties, which can in turn, be used to extrapolate the evolution of properties in the long term

The results show a strong relationship between the observed reactivity and the degrees of expansion in the concretes and mortars. The presented micromechanical modeling is able to correctly reflect the laboratory results and sheds further light on the mechanism of ASR pertinent to field structures.

Keywords: alkali silica reaction, SEM-image analysis, expansion, alkalinity, micromechanical modelling, degree of reaction, mechanical properties

Résumé

L'occurrence des réactions alcali silice et alcali silicate cause des endommagements des bétons. Bien que la réaction soit connue depuis un certain temps, il est difficile déterminer l'avancement de la réaction sur les structures affectées. Cette thèse vise à étudier le rapport entre l'avancement de la réaction et les propriétés mécaniques du béton afin de mieux pronostiquer l'effet de la RAS sur les structures.

La base du programme était ainsi de caractériser l'influence de certains paramètres sur la chimie, la microstructure et les propriétés mécaniques du béton. Il était aussi prévu de trouver un lien entre les expansions initiales et finales et comment le taux d'avancement est lié aux changements des propriétés mécaniques

Produire une telle approche à partir des résultats sur les structures est difficile parce que :

- la période d'induction et de réaction sont très longues, ainsi elles doivent être accélérées dans le laboratoire.
- la quantité de matériau réactif dans les granulats est petite, et par conséquent difficile à mesurer
- la relation entre le degré de réaction, l'expansion et les changements des propriétés mécaniques n'est pas connue.

Les caractéristiques microstructurales de quelques granulats suisses ont été étudiées et mesurées en utilisant des techniques microscopiques. Des échantillons de mortier et de béton ont été confectionnés avec ces granulats et soumis à la réaction alcali silice. L'analyse des images microscopiques obtenues à partir des échantillons polis a été utilisée pour mesurer le degré de réaction.

Dans ce projet, une série d'essais mécaniques, en parallèle à la réaction chimique a été entreprise. Les essais mécaniques ont comme objectif la description du comportement de quelques propriétés mécaniques en présence de l'alcali silice. Selon les résultats de laboratoire, la tâche principale actuelle était d'extrapoler les résultats obtenus en laboratoire à l'échelle de la structure.

Les aspects importants de la recherche étaient:

- L'approche multidisciplinaire : la caractérisation microstructurale et mécanique pour trouver une combinaison des techniques qui peuvent être employées pour évaluer le degré de réaction
- Modéliser par une approche micromécanique les changements microstructuraux et les propriétés mécaniques engendrées.

Les résultats montrent une relation prometteuse entre la réactivité observée et les expansions dans les bétons et les mortiers. L'approche de modélisation micromécanique présentée a pu reproduire correctement les résultats de laboratoire et permet un éclaircissement des mécanismes de la réaction alcali silice et peut être utilisée dans les bétons de structures.

Zusammenfassung

Das Auftreten von Alkali-Silika-Reaktionen (ASR) verursacht Schäden im Beton. Obwohl diese Reaktionen seit einiger Zeit bekannt sind, ist der genaue Reaktionsablauf in den betroffenen Strukturen schwierig vorherzusagen. Diese Dissertation hat zum Ziel, den Zusammenhang zwischen dem Reaktionsablauf und den mechanischen Eigenschaften des Betons zu untersuchen, um bessere Vorhersagen über die Wirkung der ASR auf betroffene Strukturen machen zu können.

Grundlegend für dieses Forschungsprogramm ist, den chemischen, mikrostrukturellen und mechanischen Zustand des Betons wie auch den Ausdehnungsgrad im Anfangs- und Endzustand zu beschreiben. Weiter soll die Frage behandelt werden, welcher Zusammenhang zwischen der Ablaufsgeschwindigkeit der chemischen Reaktion und den mechanischen Eigenschaften besteht.

In der Praxis ist dies aus folgenden Gründen schwierig durchzuführen:
> Die Induktions- und Reaktionsperioden sind sehr lang, was eine beschleunigte Testung im Labor erforderlich macht

- Die Menge des reaktiven Materials im Aggregat ist normalerweise klein, und folglich schwierig zu messen
- Die Beziehung zwischen dem Reaktionsgrad, der Ausdehnung und den Veränderungen der mechanischen Eigenschaften ist nicht bekannt

Die Eigenschaften der Mikrostruktur einiger Schweizer-Aggregate wurden mit Hilfe von mikroskopischen Techniken untersucht und gemessen. Mit den Aggregaten wurden Mörtel- und Betonproben hergestellt und einer ASR unterzogen. Anhand der mikroskopischen Bildanalyse der polierten Proben wurde der Reaktionsgrad gemessen.

In diesem Projekt wurden eine Reihe mechanischer Test parallel zu den chemischen Reaktionen durchgeführt, um die Wirkung der ASR auf die mechanischen Eigenschaften des Betons feststellen zu können. Das Hauptziel dieser Forschung ist die Entwicklung eines Tools, welches ermöglicht, Laborresultate und reale Strukturen in Beziehung zu setzen.

Die wichtigen Aspekte dieser Untersuchung waren :

- Ein multidisziplinärer Ansatz für das chemische, mikrostrukturelle und mechanische Verhalten von Beton, um schlussendlich die Chancen zu erhöhen, eine Kombination von Techniken zu finden, die verwendet werden kann, um den Reaktionsgrad zu bestimmen.
- Modelisierung der mikrostrukturellen Veränderungen und der dazugehörigen mechanischen Eigenschaften mit Hilfe eines mikromechanischen Ansatzes.

Die Resultate zeigen eine vielversprechende Beziehung zwischen der beobachteten Reaktivität und der Expansion im Beton und im Mörtel. Der hier vorgestellte Ansatz der mikromechanischen Modelisierung ist in der Lage, die Laborresultate richtig wiederzugeben und trägt somit zur weiteren Klärung der ASR-Mechanismen bei, welche für die Strukturbetons von grosser Wichtigkeit sind.

Glossary

Activation energy: is the threshold energy, or the energy that must be overcome in order for a chemical reaction to occur.
Aggregate concentration
Aggregate size
Alkalinity: is a measure of the acid neutralizing capacity of a solution.
ASR: Alkali silica reaction
BSE: Backscattered electron
Bulk modulus of solid: is the inverse of the compressibility.
C/A: cement to aggregate ratio
Compressibility: is a measure of the relative volume change of fluid or solid as a response to a pressure (or mean stress) change.
Compressive strength: the capacity of a material to withstand axially directed pushing forces (Pa).
Concrete: is a composite building material made from the combination of aggregate and cement binders.
Diffusion: is the movement of particles from higher chemical potential to lower chemical potential (chemical potential can in most cases of diffusion be represented by a change in concentration).
Expansion: is the tendency of matter to increase in volume (%).
Flexural strength: Also known as modulus of rupture (Pa).
Image analysis: is the extraction of meaningful information from images by means of image processing techniques.
MIP: mercury intrusion porosimetry
Petrography: is a branch which focuses on detailed descriptions of rocks.
Reaction rate: is defined as the amount (in moles or mass units) per unit time per unit volume that is formed or removed.
Reactivity: refers to the rate at which a chemical substance tends to undergo a chemical reaction in time.
SEM: The scanning electron microscope is a type of electron microscope capable of producing high resolution images of a sample surface.
Tensile strength: Tensile strength measures the force required to pull something to the point where it breaks (Pa).
W/C: water to cement ratio
X-ray crystallography: is a technique in which the pattern produced by the diffraction of X-rays through the closely spaced lattice of atoms in a crystal is recorded and then analyzed to reveal the nature of that lattice.
Young's modulus: (also known as the modulus of elasticity or elastic modulus) is a measure of the stiffness of a given material (Pa).
Micromechanical modelling

TABLE OF CONTENTS

Chapter 1: Introduction

1. Study context and motivations

The use of certain aggregates in concrete may result in a chemical process in which particular constituents of the aggregates react with alkali hydroxides dissolved in the concrete pore solution. These alkali hydroxides are derived mostly from the sodium and potassium in Portland cement and other cementitious materials, and occasionally from certain alkali-bearing rock components within aggregates. The reaction products are hydrous gels whose chemical composition includes silica derived from the reactive aggregates. The damage in concrete is associated with the expansion and cracking that occurs when the reaction product absorbs water and swells.

The alkali aggregate reactions (AAR) were first observed in California in the 1940's but have subsequently been recognised in many countries.

Field evidence for the occurrence of alkali silica reactions (ASR) in a given concrete includes expansion and the development of polygonal or map cracking as a characteristic feature, especially when accompanied by gel deposits exuding from cracks. However, a number of other causes of distress may show superficially similar symptoms, and a petrographic examination of the affected concrete is generally necessary to confirm that ASR is actually present. The distress of concrete is associated with expansion taking place when the gel absorbs water and swells, the swelling pressure generated is sufficient to crack aggregates and propagate cracks in the surrounding paste.

Swiss dams are under permanent monitoring and subject to periodic examinations to better evaluate their serviceability in order to prevent the risks of catastrophic failure.

During the last decade, cracking was observed on the upper levels of the downstream face of some dams. These cracks are mainly horizontal and are then due to structural causes related to the high rigidity of the crest and its geometry. During the first decades of the service life of the Swiss concrete dams,

displacements were recorded by instrumental monitoring installed in the galleries and by geodetic methods. At the beginning of the 1980s, a full inspection and treatment was performed on concrete cores.

Previous investigations referred the existence of alkali–aggregate reactions in the concrete. The inspection of the dam concrete showed the existence of exudations similar to alkali–silica gel and stated that the deterioration of concrete was due to the slow alkali–aggregate reactions.

The present work is part of an investigation program in which it is intended to develop tools for studying concrete in dams. This study links microscopic examination using scanning electron microscopy (SEM), expansion and mechanical performance to identify and to characterise the effect of the reaction product in concrete and mortars.

Despite continuing research, none of the methods of diagnosis of ASR can be relied on independently or collectively to provide a definitive answer especially to the question of whether seriously deleterious reaction should be expected if small amounts of moderately reactive components are discovered. The methods of prognosis are mainly performed on cores and in non-realistic conditions as discussed in the chapter 2.

The modelling of ASR is complex, as there are several coupled processes that determine the kinetics of the reaction. As yet it has not been possible to link mechanical consequences to the microscopic damage. The complexity of interconnecting physico-chemical and mechanical domains necessitates the development of micro-models and macro-models.

The effects induced by alkali silica reactions are also difficult to model due to the random distribution of the reactive sites and the lack of knowledge of the reaction product behaviour when confined. Strength remains the most important property of structural concrete, from an engineering point of view. The Relation between concrete composition and mechanical properties has long been a matter of interest. The strength of the concrete is determined by the characteristics of the mortar, coarse aggregate, and the interface between them. Nevertheless in ASR expansion occurs at the structural level of the mineral and may cause relatively localised deterioration in the original material. During this process the properties of the granular material are modified because of expansion and cracking phenomena. Several methods exist to evaluate the mechanical

properties of concrete. These properties linked to fracture behaviour, of granular material are much less known.

2. Thesis content

The thesis contains seven chapters as illustrated in the Figure 1. Chapter 1 is the introduction. In the chapter 2 the state of the art is presented. Chapters 3 to 6 present the results of the experimental campaigns, microscopical investigations, and structural response and introduce a preliminary model including some of the parameters influencing the reaction and the observed mechanical response.

Chapter 2: in the chapter 2, some fundamentals for the thesis are presented. The focus is drawn to the diagnosis and prognosis method of ASR and the structural effect due to this chemical attack.

Chapter 3:.this chapter gives an overview of the aggregates, their reactivity and the different mixes used for this study. It presents also the new method of quantification used in this study

Chapter 4: the results of the experimental study of the expansion and reaction degree are presented; Expansion tests on mortar and concrete are performed to characterise the reactivity of the aggregates. The expansion behaviour of the mortar and concrete subjected to ASR is linked to the degree of reaction observed.

The concrete and mortar tests focus on long term behaviour as well as early age behaviour of ASR-affected concrete. On the basis of the preliminary tests 2 of the aggregates were identified as being reactive.

The experiments were conducted on 3 types of aggregates 2 reactive and one non reactive, concrete and mortars at 3 different temperatures and 3 different alkaline compositions. This allows expansion and other mechanical properties development to be determined under the influences of the different parameters. These parameters are the aggregate size, the alkaline level and the temperatures. Both, the results obtained from the microscopical study as well as the one obtained from experimental study are used. A simple model is presenting relating the kinetics to the activation energy and the alkaline level.

Chapter 5: the results on the mechanical properties are given. The mechanical properties were linked to the observed reactivity. A first approach to

link the chemical observations to the mechanical properties is then developed. Tensile and compressive strengths as well as Young's modulus of the material were studied.

Chapter 6: in chapter 6, we try to model both the effect of aggregate concentration on the expansion through a micromechanical approach for the affected aggregates.

Chapter 7: the thesis document ends with the conclusions and some recommendations for future work in the chapter 7.

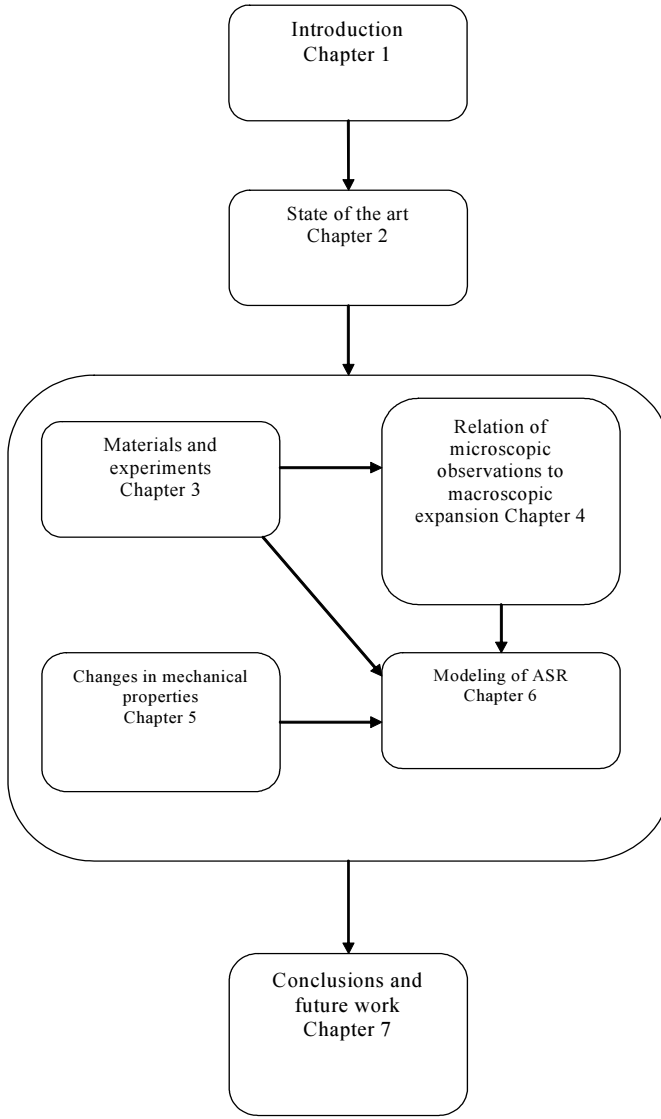

Figure 1: thesis structure

.

3. Significance of the study for practice

The delayed deformations as well as the loss of mechanical properties play a very important rule in the dimensioning of the concrete structures and in determining their long-term behaviour. Disorders may appear in different manners: variation of the stress distribution, increase in the deformations, appearance and propagation of cracks, which directly affect the state of service and the durability of the concrete structure.

In ASR, the reaction sites are distributed randomly within the concrete. Moreover the reaction starts at different times for different reactive sites. The length change is considered to be one of the most reliable methods for assessing the degree of degradation in concrete.

Testing in laboratory is monitored at elevated temperature that causes a faster expansion initiation and a higher level of final expansion. It results in a problem for the good exploitation of the obtained results in the level of the structures where the phenomena occur at low temperatures.

In the absence of a more reliable procedure to evaluate the ASR induced effects in affected structures, it is common to consider the results given from the laboratory assessment (materials mechanical properties) for the design of new concrete structures incorporating reactive aggregates. The performance and long-term durability of concrete structures already affected is one of the most important aspects of the engineering management. Using data from tests in the laboratory and extrapolating them to the site structures under site exposure conditions is a main of interest. This study allows deriving some recommendations that could be for the effective use in structures concrete.

4. Objectives of the study

This research programme aims to study the relationship between the progress of the reaction and the mechanical properties of the concrete in order to support better prognosis of the impact of ASR on the affected structure.

An idealised pattern of ASR is shown in the Figure below:

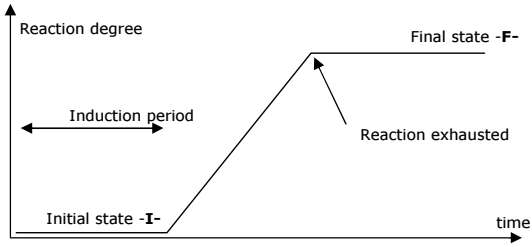

Figure 2: idealised pattern of ASR Curve

The basic principal of the research programme is to characterise the chemical, microstructural and mechanical state of the concrete and the degree of expansion in the initial and final states and how the changes in expansion, mechanical properties are related to the rate of change of the chemical reaction. In practice this is difficult to do because:

- In the field the induction and reaction period are very long, so they have to be accelerated in the laboratory.
- The amount of reactive material in the aggregate is usually small, so the amount reacted is difficult to measure.
- The relation between the degree of reaction, expansion and the change of mechanical properties is probably non linear

Important aspects of the research are:

- A multidisciplinary approach to chemical, microstructural and mechanical characterisation to increase the chances of finding a combination of techniques which can be used to assess the degree of reaction.
- Use of theoretical modelling to understand the link between microstructural changes and mechanical properties, which can be used to extrapolate the evolution of properties in the long term.

5. Research methodology

The development of this study on the diagnosis and prognosis of ASR in the concrete will be done in several steps. These steps can be classified as:

- Experimental study:
  - Chemical tests.
  - Mechanical tests.

- Modelling of the phenomenon.

5.1. Experimental study

ASR depends significantly on the specimen size or on the characteristic dimension of a concrete structure. Generally, there is no simple correlation between the concrete samples examined in the laboratory with the concrete structure under field conditions. Nevertheless it would be of academic and practical interest to appraise the affected concrete structures by the observations obtained using laboratory measurements.

The major tasks that can be obtained by laboratory testing are:

- The evaluation of the aggregates suitability.
- The identification of ASR, its extent and residual potential in possibly affected concrete.

The tests for the examination and the mechanical behaviour prediction that will be used are the Microbar test, mortar bar test, x-ray diffraction and scanning electron microscopy image analysis (SEM-IA).

In the different level of the reaction, the use of a combination of several tests allows more comprehensive and accurate results to be obtained.

The first results to get from these tests or the first concepts on which the tests are based on are the progress of the reaction and the mechanical behaviour linked to.

The microbar test was carried out in the normalised conditions to show the limits of the reactive potential of the aggregates. Some control tests were carried to check the ASR in the bar: SEM images observations.

The mortar bar and concrete prisms was tested at several temperatures 20, 40 and 60 °C in order to obtain the kinetics rate and magnitude of expansion at different temperatures. The activation energy E_A of the reaction is then calculated in order to extrapolate to service temperatures that are lower than the experimental temperatures.

The observed reactivity was calculated using the SEM-IA and linked to the expansion and other mechanical properties.

The monitoring of laboratory concrete prisms provided data to support and facilitate the identification of damage due to ASR and the influence of this reaction in the behaviour of the concrete.

Conventional mechanical parameters such as tensile strength, compressive strength, flexural strength, are frequently used in the modelling of the mechanical behaviour of a concrete structure. To determine these parameters the common standard test methods were employed.

The data needed were:

- The elasticity modulus.
- The strength and the deformation in fracture.
- Tensile strength test.
- The specific fracture energy of the aggregates.

All the mechanical properties are linked to the progress of the reaction.

5.2. The modelling

After getting the results from the experimental study, a theoretical approach is used to better understand the mechanical behaviour of concrete affected by the ASR.

The interest of a model based on the mechanics of the reactive aggregates is to establish the link between internal stresses caused by ASR and the mechanical consequences. The model should provide a basis for:

- Predicting the rate of evolution of the reaction.
- The prediction of the behaviour of the structure affected by the ASR in the future.

In this work the modelling is approached at the material level in order to establish links between durability studies and concrete in real structures.

Before developing the model in macroscopic scale, it is important to define the behaviour in a smaller scale (sample in the laboratory). It is then important to determine the influence of each parameter in the development of the reaction.

The modelling will be done in the microscopic scale by identifying and describing the physic-chemical phenomena that constitute the ASR and The mesoscopic scale by defining a behaviour law that takes the ASR in account. This will allow defining the relation between the reactions and the stresses in the materials, and the quantification of the development of the reaction in the concrete.

Chapter 2: State of the art

1. Introduction

A wide variety of aggregate types in common use across the world, particularly those with a siliceous composition, are vulnerable to attack by the alkaline pore fluid in concrete. This attack, which in wet conditions produces a hygroscopic gel, can cause cracking and disruption of the concrete. The deterioration mechanism is termed Alkali Aggregate Reaction (AAR) or, more specifically, for siliceous aggregates, Alkali Silica Reaction (ASR).

Reactive components may be found in different components of the aggregates such as igneous, sedimentary, or metamorphic components. Sedimentary rocks containing clays, micas have been observed to be reactive. Such rock types include graywackes, argillites, phyllites, siltstones, etc. the reactive component is finely divided quartz or amorphous silica within the rock or the reactions may also involve clay mineral or mica components.

Despite continuing research and improvements, none of the methods of diagnosis of AAR can be relied on independently or collectively to provide an definitive answers especially to the question of the future behaviour of affected structures and reaction and whether reaction should be expected if small amounts of moderately reactive components are discovered.

The basic mechanism of the reaction is well established. Therefore it is not reviewed in details in the present literature review. Furthermore a vast literature on test method exists and is not of our interest to identify potentially reactive aggregates for new constructions.

In this work the focus is the prediction of the behaviour in concrete dams. Thus the main objective of this literature review is to give an overview about what is presently known on the progress of ASR in affected cementitious materials. Attention had been paid to the basics of the chemical reaction, mechanism and product, the method of identification, the related expansion as

well as the structural effects. Prognosis methods are also reported in the present chapter. Previous work on modelling is discussed in chapter 6.

2. Reaction mechanisms

2.1. What's ASR?

Alkali aggregate reactions (AAR) comprise different chemical processes between the alkali ions of concrete pores and the aggregate materials. Three types of AAR are distinguished in the standard classification (Grattan-Bellew 1992a):

- Alkali silica reaction (ASR) can be considered in a simplified manner as an acid-base reaction between the alkaline pore solution and amorphous or reactive silica content of the aggregate.
- Alkali silicate reaction (ASSR) occurs between interlayer precipitous of phyllosilicates and the alkaline pore solution (Hobbs 1988). The kinetics of the reaction is much slower than ASR.
- Alkali carbonate reaction (ACR) is a reaction between the carbonates of the aggregates and the alkaline pore solution of the concrete.

The primary substances participating in ASR are the alkaline pore solution of the concrete and siliceous aggregates material. The pore solution contains various concentrations of hydroxyl ions OH^-, calcium ions Ca^{2+}, sodium ions Na^+, potassium ions K^+, and sulfate ions SO_4^{2-} that interact with the siliceous aggregate material. The reactivity of the aggregates depends essentially on the degree of order of the silica structure. Hobbs (Hobbs 1988) described the reaction mechanism as a penetration of hydroxide ions OH^-, into the disordered structure breaking up siloxane bridges and attacking terminal silanol groups

$$Si_2O + OH^- \rightarrow SiOH + SiO^-$$
$$Si_2O + 2OH^- \rightarrow 2SiO^- + H_2O$$
$$SiOH + OH^- \rightarrow SiO^- + H_2O$$

at the same time, sodium and potassium ions migrate into the silica framework and neutralise the negative anion charges building an alkali silica gel

$$SiO^- + Na^+ \rightarrow SiONa$$

The alkali silica gel is able to imbibe considerable quantities of water. The corresponding volume increase is referred to as the gel swelling process. The internal stresses caused by the growth of the gel cannot be dissipated by

migration of the gel. This internal stresses cause microcracking and damage in the concrete.

The expansion process according to Jones (Jones 1988) can be subdivided into 2 interacting sub-stages:

- Gel hydration and swelling with a volume increase
- Dissipation of the gel from the generation site.

Expansion can only result if the dissipation processes are slower than the gel generation. Otherwise the product could be dissipated without causing internal stresses and concrete damage.

An important property governing the gel mobility is its viscosity (Poole 1992). The gel products exhibit a wide range of viscosities depending on the amount of water incorporated. At the beginning of the reaction the gel is very viscous. As the reaction progresses the gel becomes gradually less viscous by uptake of water until it is fluid enough to flow along cracks and fill pores and voids in the cement paste but when Ca^{2+} enters it, it becomes more viscous again. The relations between composition viscosity and swelling are not fully understood.

AAR is influenced by many different factors that are:

- Internal factors: material mechanical properties (cement, aggregates) internal state of stress.
- External factors: temperature, humidity, availability of water or external alkalis, time, etc.

Though the coupling of the chemical and the induced expansion is not trivial, it can be assumed a priori to be directly related under all circumstances.

Water is necessary to maintain the alkali aggregate reaction and the expansion process. It can be delivered by environmental humidity or by external water flow. For concrete structures in contact with ample water the reaction rate of the hydroxyl ions attacking the silica framework seems to be the most important for the expansion rate. Interesting new research by the Douai group (Garcia-Diaz, Riche et al. 2006) supported by NMR studies proposes a damage mechanism for the alkali–silica reaction. This mechanism is illustrated from a schematic subdivision of the swelling curve of a mortar given in the Figure 1 obtained in a reactor.

Q0, Q3 and Q4 are $H_2SiO_4^{2-}$, $SiO_{5/2}$ and $^{-}SiO_2$ respectively.

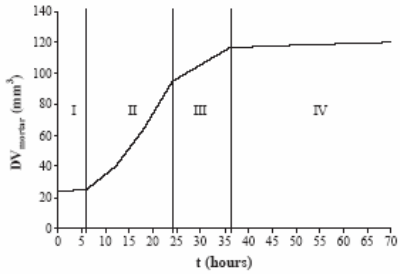

Figure 1: Schematic subdivision of the swelling curve

- period I (first 6 h of autoclaving): the reaction is a dissolution precipitation process: the Q0 tetrahedrons formed from Q4 and Q3 tetrahedrons dissolution react with calcium hydroxide and alkalis these products are called the Q0 products of ASR. The mortar bar does not swell during this period.
- Period II (between 6 h and 24 h of autoclaving): the formation of Q0 products is slowed down and stopped. We observe a regular increase in Q3 tetrahedrons (Q3 products) in the aggregate during this period. The Q4 → Q3 transition is expansive and is responsible for the swelling and cracking phenomena in the aggregate. The pore volume of the aggregate increases. The aggregate swelling is amplified by cracking in the cement paste. a linear relationship between the mortar swelling and the aggregate swelling is observed.
- period III (between 24 and 36 h of autoclaving): the swelling mechanism described above occurs, but the dissolution–precipitation process described in period I starts again: the Q0 products fill part of the cracks generated by the swelling.
- period IV (beyond 36 h of autoclaving): the swelling is asymptotic even though the reaction continues: the Q0 and the Q3 products fill the cracks generated by the swelling. It is a period where the pore volume of the aggregate decreases because of the filling of the cracks.

2.2. Reactions mechanism of highly reactive aggregates

It is frequently reported in the literature that ASR is concentrated in a rim at the surface of the reaction.

Various research programme such as Rivard (Rivard, Ollivier et al. 2002)tried to characterise the ASR rim. In this particular aggregate they observe the development of a dark rim at the internal boundary of the aggregate particles as the reaction progresses and the level of expansion rises. Scanning electron microscopy (SEM) observations showed that the rock was severely cracked at a few places, most likely due to the swelling pressures created by the gel inside the particles. The development of the rim is associated with the progressive disintegration of sandstone particles. Two observations must be highlighted:

- During the process of ASR the intergranular siliceous cement , the recative phase is attacked and dissolved by hydroxides.
- A rim develops as the cement of alkalis and calcium within this rim increases.

Many studies of ASR have been carried out in Opal aggregates. Thus ASR process in these cases can be schematised as a sphere of pure reactive silica attacked by hydroxide ions. However, as is shown by many documented examples, not all rocks react the same way as opal. As a conclusion the reaction can be schematised as:

- Quick penetration of calcium alkali and hydroxide ions into aggregates particles.
- Dissolution of reactive silica.
- Precipitation of some silica within the particles at the interface.
- Densification of the aggregate interface
- Formation of silica gel inside aggregates with a global swelling of the particles
- Aggressive ion penetration into particle cracks.

More work is then needed to gain better understanding of deterioration mechanism and formation of reaction regarding different types of aggregates.

2.3. Aggregate as source of alkali

Some Groups working in ASR (Xu and Hooton 1993; Marc-André Bérubé 2002) suggested that according to their results, very significant amounts of alkalis can be supplied with time by aggregates to the concrete pore solution, particularly by feldspar-rich aggregates (granite, etc), which are widely used in concrete.

Despite a correction being made to take account of the contribution by aggregates in the test method, the results obtained, even at some depth in the concrete, often largely exceed the water soluble alkali content expected to be released by the cement. This confirms that significant amounts of alkalis can be

released with time by the aggregates, particularly feldspar-rich ones, as suggested in their study. Thus, short-term immersion tests in lime-saturated solutions are bound to underestimate alkali concentrations. Long term immersion appears to be more realistic according to the results of their study.

A number of studies suggested that alkalis could migrate and locally concentrate in a concrete element, which can then locally initiate or accelerate ASR. This study gives us a test method to better estimate the amounts of alkalis that can be supplied to the concrete pore solution by the aggregates in the long term, using experimental conditions that better simulate the chemistry of the pore solution in normal concrete.

3. Identification of ASR

3.1. Field evidence of ASR

A detailed field survey is normally the first stage for identifying the possible presence of AAR, and the extent of deterioration. There are two pieces of evidence usually used to identify the ASR, i.e. cracking and the presence of ASR gel in concrete structures. The visual signs to be considered indicating ASR in concrete structures include the following.

Map-cracking: A matrix of fine cracks on the surface of the concrete. Map cracking is seldom distributed uniformly on the surface of concrete. Its appearance can vary from just a few cracks (Figure 2.a) to isolated areas of pattern cracking to fairly severe, closely spaced extensive map cracking (Figures 2.b and 2.c), i.e., the crack density on the surface may vary. It must be noted that it may be difficult to distinguish map cracking due to ASR from the one due to thaw-freezing process in concrete structures.

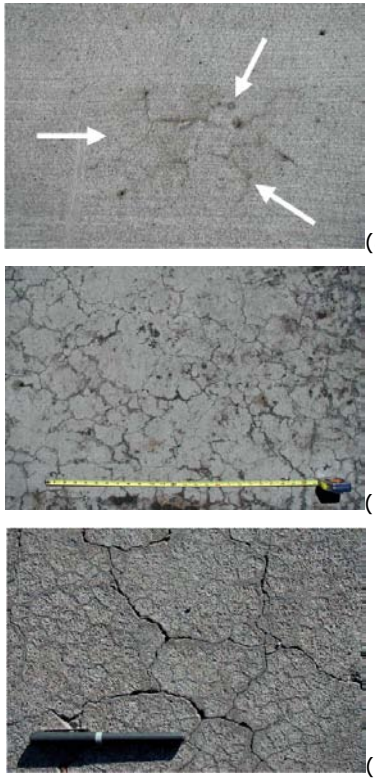

Figure 2: Only a few map cracks (a) to first map cracking (b) and severe map cracking (c): http://www.faa.gov/

Presence of gel: The only indisputable evidence that ASR has developed in concrete is the presence of ASR gel reaction products. However, in the early stages of the reaction, or under conditions where only small quantities of ASR gel are produced, the gel is not easily observed, and is revealed only by microscopy. Thus, ASR may go unrecognized in field structures for some period of time, possibly years, before associated severe distress develops to force its recognition and structure rehabilitation.

Moisture movement through pores and cracks in concrete transports the ASR gel to the surface, where it exudes. However, ASR gel exudation is not very

common, and where present, indicates that there has been sufficient moisture to carry the gel to the surface. This exuded gel is usually greyish white.

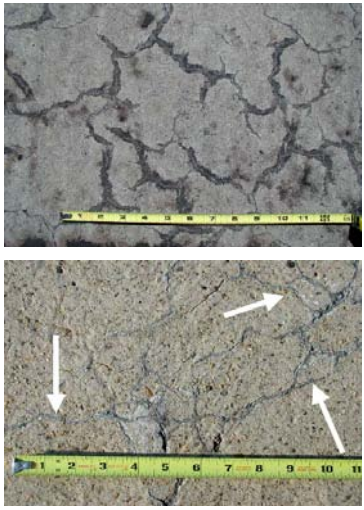

Figure 3: Gel exudation through cracks (picture taken from internet)

3.2. Microstructural evidence

Several methods exist to show the microstructural evidence of the presence of ASR in concrete structures. The most well known are:

3.2.1. Ultra-Violet light diagnosis

The use of uranium acetate and examination by ultra-violet (UV) light to diagnose the presence of ASR has gained acceptance. The gel may be present in varying proportions in aggregate rims and cracks, air voids, fractures, and on the exposed surface of concrete as exudation. By applying uranyl acetate solution to the surface, the gel, if present in an unaltered state, imparts a characteristic yellowish green glow in ultraviolet (UV) light (254 nm) because of uranyl ion substitution for alkali in the gel. Even though the method is sensitive to the presence of ASR gel, results should be interpreted with caution. Cracks may be due to other phenomenon.

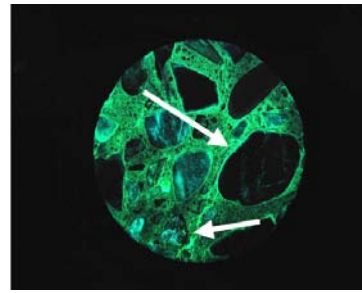

Figure 4: section as viewed under UV light showing ASR gel along cracks and around aggregate periphery (http://www.faa.gov/")

3.2.2. Optical microscopic techniques

Optical microscopy is a highly useful and inexpensive tool for identifying ASR. While optical microscopy offers a relatively rapid means of diagnosing ASR, sample preparation is elaborate, time-consuming, and somewhat demanding. Nevertheless, optical microscopy can reliably serve to identify the deterioration features of ASR. Microscopic examination allows it to be established that substantial ASR has occurred and that the internal cracking has the characteristics of that induced by ASR.

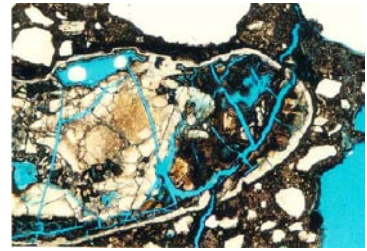

Figure 5: A severely cracked opaline siliceous fine aggregate due to ASR under optical microscopy.

3.2.3. Scanning electron microscopy

Scanning electron microscopy involves identifying ASR gel by its characteristic morphology. Compositions and typical morphologies of gel can be used as diagnostic features to confirm ASR. It would not trust ASR diagnosis on fracture surfaces. Samples can be in any form, provided they can withstand the

high vacuum required in the specimen chamber for the operation of the microscope.

Figure 6: Some ASR gel texture under SEM observations.

3.3. Movements, displacements and deformations

The expansion processes due to ASR often varies throughout the volume of the concrete or within the various concrete elements or parts of the affected structure. The overall, uneven, or differential concrete swelling due to ASR may cause distress such as relative movements, misalignment, distortion, excessive deflection, or separation of adjacent concrete members or structural units. The closure of joints, causing extrusion of jointing and sealing materials and, ultimately, spalling of concrete at expansion or construction joints is a common feature of ASR in concrete pavements.

4. Laboratory identification of ASR

4.1. Number of reactive sites

Some previous research work (Amiet Hélène 2000)presented a microstructural and physico-chemical method approaches of AAR quantification in concrete. The microstructural approach consists in estimating the number of reactive sites over fracture surfaces, recognisable by their specific fluorescence. This method of disorder severity is applied to many cases of work and correlated to the degree of microcracking of concrete. The second approach involves the determination of the distribution coefficient based on specific adsorption of cations on AAR products.

The principle of the first method can be summarised in the following procedure.

The number of positive sites ascertained to contain AAR gels i.e. corresponding to fluorescence areas observed during the uranyl acetate test is used for the evaluation. The reactive sites are referred to as the fluorescence spots observed in concrete specimens whether they are or not associated with gravel. Positive sites associated with gravels concern the fluorescence detected in the gravel themselves, at their interface or in the pore in contact with gravels. The sites detected not associated with gravels are also counted. All aggregate particles studied were used to evaluate the minimum and maximum number of reactive sites. The severity of AAR in the studied specimen is another evaluated factor. This factor is estimated visually.

The microcracking study (2nd method) was carried out using a quantitative procedure. The method involves a stereomicroscopic examination after treatment by impregnation with a coloring agent to reveal all discontinuities in the material. The manual quantification, with magnification between 80 and 100, uses the Stanikov-Stroeven linear counting method.

Quantifying is by linear counts assuming random distribution of the desired phenomena. This method detects and quantifies even minor discontinuities and differentiates between different phenomena.

4.2. Humidity measurement

In situ measurement of relative humidity and expansion of the cracks in damaged structure are also used to diagnose AAR. Jensen (Jensen 2000) presented a method to measure the expansion using electrical humidity probes to measure the humidity. This is a standard method in the wood and paint industry, based on the electrical conductivity of wood. Though the same method was applied on some concrete structures in UK and Denmark, the reliability, uncertainty and limitations of the method are not known. In these experiments, the expansion of the cracks was measured using 3 markers arranged as an equilateral triangle. The distances between the markers were measured every month and average expansion was calculated using a regression analysis.

4.3. NMR spectroscopy

Bulteel (D. Bulteel 2002) proposed a new chemical method for quantitative measurements of the reaction degrees of ASR. Two reaction steps are taken into account in the mechanism: formation of Q3 sites made by breaking up siloxane

bonds of the reactive silica and dissolution of these Q3 sites. The remaining silica is composed of Q4 tetrahedrons and Q3 protonated sites identified by solid NMR spectroscopy. The measurement of the reaction degrees of the step 1 and 2 given before is defined by:

- Quantifying the Q3 sites content by dividing the number of moles of Q3 sites by number of moles of the initial silica.
- Calculating the dissolution degree that corresponds to the number of moles of dissolved silica subtracted from the number of moles of initial silica
- A simple operation can give the number of moles of Q3 sites from the number of moles of the residual silica.

The method of quantification in a model reactor consists of these steps:

- Accelerating the ASR under controlled temperature. in a KOH solution
- First NMR spectroscopy analysis of the aggregate that is constituted by Q4 tetrahedrons that did not react and by the Q3 tetrahedrons that constitutes the altered silica.

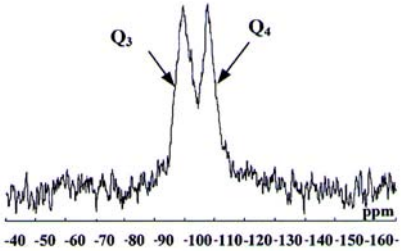

Figure 7: Crossed polarised 29Si solid NMR spectrum of the flint aggregate (from Butleel et al (2002))

- A selective acid treatment to protonate Q3 tetrahedrons to form silanols by release of $K.^{+}$ and all the other alkali cations.
- Thermal treatments of the residual solid at 1000°C to give back silica tetrahedrons Q4 and release water up.

A new identification by the NMR spectroscopy followed this treatment. The weights of the residual silica allow determining the quantity of dissolved silica.

The model reactor approach allows quantifying the number of active Q3 sites created by siloxane bond breaking inside the aggregate and the number of moles of small polymers obtained from Q3 Sites. The limiting step of this method is the

siloxane breaking up. After acid treatment in some aggregates some growth of dark parts which do not allow light transmission in thin sections was observed.

4.4. Digital image using SEM and Other techniques

Some groups (Garcia del Amo and Calvo Perez 2001) presented a method of diagnosis of alkali silica reactivity potential using the digital image analysis of aggregate thin sections. The quartz reactivity index (QRI) values have been obtained by multiplying the percentage of quartz in the aggregate by the specific surface area, which is a characteristic of this mineral phase. In additional to traditional petrography, the calculation of quantitative parameters such as percentage of quartz, perimeter and specific surface area, was carried out by means of digital analysis of images (DAI) on a microscopic as well as macroscopic scale when the grain size allowed it. The process followed for the characterisation of the microscopic samples of the selected rocks has been the following

- To take images on a thin section around 4 times larger than the largest grain size using a camera connected to microscope.
- Acquisition of the image and transformation to a digital form

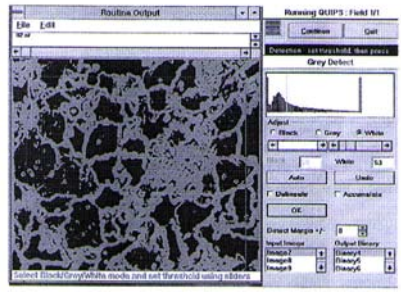

Figure 8: first gradient binary image (from del Amo et Perez (2001))

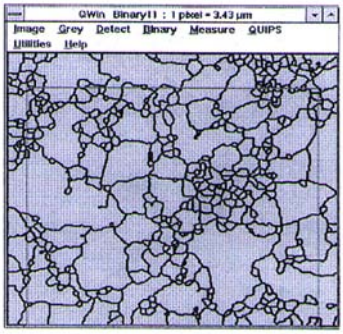

Figure 9: binary gradient image following skeletonization and dilatation (from del Amo et Perez (2001))

- Carrying out the measurements
- Calculation of the quartz reactivity index by multiplying the percentage of quartz in the aggregate by the specific surface area.

The deformation follows expansion of aggregates and their subsequent interactions which lead to ductile or fragile deformation. The digital analysis as proposed by Garcia del Amo (Garcia del Amo and Calvo Perez 2001) is faster than the X-ray diffraction. The results of this test were plotted against a 14 days mortar bar expansion test and it showed an exponential relationship.

5. AAR Structural effects

Due to the gel volume increase an expansion causing internal stresses and microcracks may occur. Therefore the concrete becomes damaged which can be detected by a wide variety of parameters assessing the concrete strength. Many studies have been done to evaluate the properties of affected concrete the following paragraphs will give a short review of the AAR impact on concrete properties and structure behaviour.

5.1. Swelling process

The first structural effect observed is the expansion. Due to the swelling process, the dimensions of ASR affected concrete or mortar prisms increase. The length change of concrete prisms is a function of time. Although the reaction sites are distributed non-uniformly within the concrete. Moreover the reaction

starts at different times for different reactive sites. This implies inherent variations of expansion readings. The length change is considered to be one of the most reliable methods for assessing degree to which the concrete is affected. Swamy (Swamy R.N 1986) indicated that the expansion rate of mortar is much larger than concrete. An elevated temperature causes a faster initiation and rate of expansion and a higher level of final expansion. However the aggregates used for their study were opal "highly reactive aggregate" that is not of common use. The rate of expansion seems to be very useful to determine the potential reactivity of aggregates.

Ballivy (Ballivy G 2000) tried to study the expansion of AAR effected concrete under triaxial stresses. The experimental set-up used a stress that simulated a vertical load of a gravity dam with a confinement due to the dead-weight and horizontal stresses equivalent to those applied by the water. Expansion of the cube was monitored using embedded thermocouples. During the first loading stage, following load application, the expansion was found to cease for a while, but then resumed at about the same rate, i.e. the reaction was delayed but not suppressed completely. An analysis of the temperature distribution inside the cube and its effect on the expansion rates showed that the expansion relative to a fixed temperature could yield a model expansion curve at a normalised age with no thermal effect. This implies a local temperature effect of reaction.

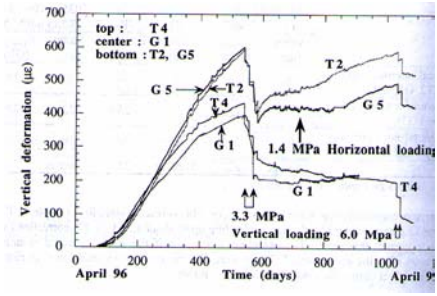

Figure 10: vertical deformation in a triaxial equipment (from Gravel et al 2000)

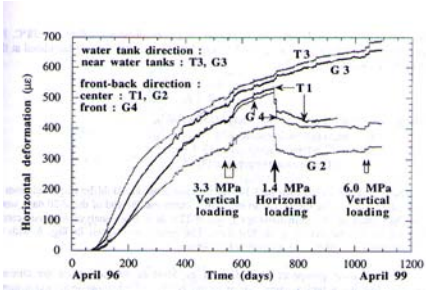

Figure 11: Horizontal deformation in a triaxial equipment (from gravel et al 2000)

5.2. Effect of a loading on ASR

5.2.1. Influence constraints

Rivard (Rivard P 2000) investigated the influence of reinforcement steel on the expansion of AAR affected concrete for both structural and mass concrete cube samples. The results indicated that the confinement by reinforcing steels reduces the overall free expansion. It shows also that vertical deformation is higher than horizontal deformation, and that deformation seems homogeneous. The mechanical properties of both type of concrete were evaluated and show a decrease from the structural concrete. The loading test showed a decrease in elastic modulus for the reactive structural concrete relative to the non-reactive concrete. In mass concrete, mechanical properties after the expansion period show also a reduction in elastic modulus and reduction in compressive strength.

5.2.2. Anisotropy effect of ASR

LCPC group (Larive C 1998; Larive C 2000b) investigated the heterogeneity and anisotropy in ASR affected concrete and their consequences in the structural behaviour. To assess the structure behaviour the following observations have been done:

- Quantifying the ASR heterogeneity.
- Comparing the expansions in the casting and perpendicular direction.
- Taking into account the effect of mechanical stresses (Larive C 1998).
- Comparing the expansion for various specimen sizes.

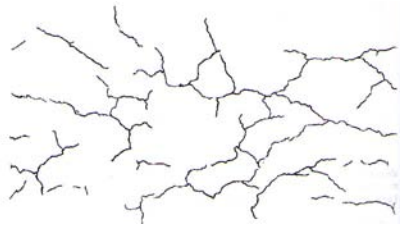

Figure 12: anisotropy of cracks (more cracks in horizontal than in vertical side) (from Larive 1998)

The most important conclusions were:

- For usual sate of stress, recovering may probably be considered as negligible compared with expansions due to ASR.
- Residual expansions test are quite often performed on a small number of cores. As the expansion can at least double from one specimen to another, increasing the number of cores or increasing the number of measurements on each core can improve the results.
- If cores are extracted by horizontal coring, the swelling anisotropy must be taken account to avoid underestimating the residual potential expansion.
- The prediction of structural behaviour via any modelling must not be expected to be more accurate than the input information. Probabilistic framework for mechanical modelling could improve the accuracy of the predictions if relevant statistical data are available.

Léger and al (Leger, Cote et al. 1996)have also tried to investigate the effects of applied stresses on the mechanical properties of concrete (Leger, Cote et al. 1996). In their study they elucidated some influences on concrete expansions resulting from:

- The applied or induced compressive stresses and other constraints/confinement.
- Physico-chemical characteristics of the concrete reactive constituents.
- Distribution of AAR expansion

All these factors were later used for the modelling of AAR.

5.3. Effect on compressive strength

Previous results on ASR (Clark L.A 1990; Ono K 1990) indicated that the compressive strength decreases as the mechanical damage due to ASR increases. The reduction tends to approximately 40% at large expansions. Clark (Clark L.A 1990) emphasised that the compressive strength (on cylinders) of concrete is a more sensitive parameter to ASR than the cube strength. As pointed by Swamy (Swamy R.N 1986) the compressive strength is not good indicator for the beginning and the progress of ASR. Nevertheless it is often used for concrete monitoring due to the simplicity of the measurement.

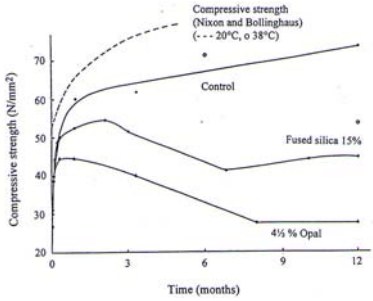

Figure 13: ASR effect on compressive strength (Swamy et Al Asali 1986)

Monette (Monette L.J 2000) investigated the mechanical properties of the materials and studied the ASR under different loading conditions. His conclusion was that compressive strength of the plain concrete was not significantly affected

.

5.4. Effect on tensile and Flexural strength

Previous investigations made by Gallias (Gallias J.L 2000) supplemented autoclaved mortar prisms tests by non destructive and mechanical characterisation to determine the influence of AAR on properties other than expansion damaging such as the variation of ultrasonic pulse velocity, the variation of dynamic modulus of elasticity, the water adsorption and flexural strength. The results obtained showed a strong correlation between expansion values and the variation of the principal physical characteristics of the prisms. Swamy (Swamy R.N 1986; Swamy R.N 1992) showed that AAR significantly

reduces flexural strength since expansion and cracking reduce the flexural capacity of concrete.

Charlwood (Charlwood R.G 1992) indicated a reduction in tensile strength in some cases even if no compressive loss was evident. There are other investigations concluding that tensile strength is more susceptible to ASR deterioration than the compressive strength which has also been confirmed by measurements on concrete structure in service (Al-Asali 1988).

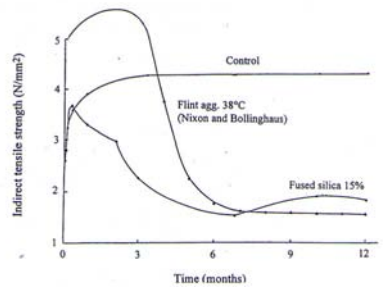

Figure 14 : effect of ASR on tensile strength (Swamy et Al Asali 1986)

Siemes et al (Siemes T 2000) investigated 25 bridges and as results, they found a reducing in mechanical properties up to 85 %. However there was no clear reduction of the tensile splitting strength and the compressive strength. The uniaxial tensile strength was sometimes dramatically lower than the splitting tensile strength.

In Monette's investigation (Monette L.J 2000), the flexural strength and dynamic modulus of elasticity were reduced.

5.5. Effect on Young's modulus and Ultrasonic wave velocity

The behaviour of the dynamic modulus is similar to that of the tensile strength (Swamy R.N 1986). The dynamic modulus seems to be more sensitive to ASR than the ultrasonic pulse velocity. As pointed by the British Cement Association and reported in literature (Rotter H 1996), losses in elastic modulus between 20% and 50% were found for expansions of 1-3mm/m.

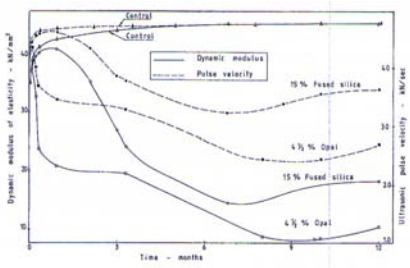

Figure 15: ASR effect on the ultrasonic pulse velocity and dynamic modulus of elasticity (Swamy et Al Asali 1986)

Previous researches (Pleau r 1989; Salomon M. 1993)reported that the ultrasonic pulse velocity is less sensitive to ASR than the length change. On the other hand, other researches (Larive C 1998) concluded that the ultrasonic pulse velocity and young modulus are more susceptible to ASR than length change.

5.6. Effect on Fracture properties

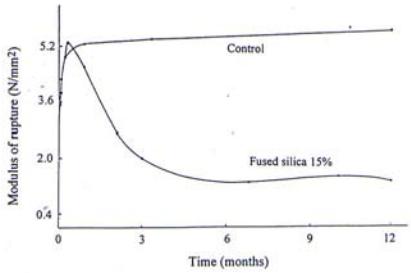

Figure 16: ASR effect on rupture modulus (from Swamy et Al Asali 1986)

Other investigations (Ahmed T 2000) link the effect of alkali aggregate reaction to the load bearing capacity of concrete. The fatigue behaviour of plain concrete tested in compression, indirect tension and flexure was also investigated in this study. The main results were:

- ASR reduces the load bearing capacity and the fatigue life of concrete.
- ASR enhances the shear capacity of reinforced concrete with and without shear reinforcement.

5.7. Effect on structures

Larive (Larive C 2000a)gave an overview of the structural effects of ASR in France on real and laboratory structures. On the hydraulic structures, the swelling causes the bending of the piles and reductions of the gate clearance of some dams. While in one of the dams (Maury) the problems were mainly located in the right abutment, cracks were observed in the piles of another dam. The problems encountered while studying the mechanical properties in this study were:

- The influence of water and stresses on the swelling.
- The prediction of the expansion potential.
- Cracking or map cracking when the cracks opening exceed 0.2 mm because of the risk of reinforcement corrosion and of plastic steel yielding.
- Softening (movements under heavy traffic, unrecoverable and plastic deformations).

Nielsen (Nielsen A 2000)studied the different effect of AAR in concrete structures. The problems that were observed can be classified into:

- Aesthetic phenomena: dark spots on the surface that may create a resin like gel droplet, in some cases the reacting particle has enough stiffness to force open the surface and form a pop out. From cracks on the surface, white staining can flow out because of osmotic effects in the solution in the cracks.
- Functional phenomena: the AAR expansion can cause post-tensioning of reinforcement bars, so that the load-bearing capacity of the member is not reduced.

6. Methodology for prognosis of future expansion

6.1. Methods based on residual expansion

Bérubé (Bérubé 2000) presented a method for calculating further expansion due to the AAR. This method is based on the basic principle which assumes that the AAR and associated expansion and deterioration will continue in the concrete structure as long as the reactive mineral phases within the aggregate particles are not completely consumed, and the two other essential conditions are still satisfied i.e. high humidity and high alkali concentration in the concrete pore solution. Expansions are also a function of temperature and stress level in

service. Their methodology to estimate the potential rate of ASR expansion takes into account the following factors:

- The residual expansion rate of the concrete under study in the laboratory obtained through study of the expansion of cores at 95% RH and 38°C. This rate can be quantified in accordance with a table, where the parameter of the expansion rate varies from 0 to 16.
- The absolute reactivity of the aggregate present in the concrete under study that can be obtained by conducting expansion test on cores in 1N NaOH at 38°C. The expansion obtained after one year when testing cores can be qualified according to a table. The expansion measured can be underestimated if the concrete tested is abnormally cracked.
- Petrographic characteristics of the concrete specimen prior to and after expansion tests on cores, for the correct interpretation of the corresponding results.
- Water soluble alkali content of the concrete under study. The alkali concentration in the pore solution could be estimated knowing the water-soluble alkali content and the original water content of the concrete. However the measured water-soluble content must be corrected to take account of the alkali contribution by the aggregates during the test. The water-soluble alkali is then overestimated. And especially when some amounts of alkali are leached out from the AAR products in the test method.
- Humidity conditions in service by measurement of the humidity inside the concrete.
- Temperature in service.
- Compressive stresses applied to the concrete in service.

Though long-term monitored laboratory experiments may have some inaccuracies induced due to other processes such as leaching, they can give reasonably accurate estimates of the rate of expansion that can be extrapolated to real structures. It must also be emphasised here, as the coefficient of expansion is measured from laboratory tests at a single temperature, the method cannot predict the kinetics of the expansion in a real structure.

6.2. Alkali concentration of pore solution

Kagimoto (H. Kagimoto 2000) presented a method to evaluate the degree of deterioration in AAR damaged concrete along with a method to analyse the pore

solution of the damaged concrete. The study aims at studying the influences of local environmental conditions on the degree of damage in existing ASR damaged structures. The method presented is a combination of two tests, the first measuring the residual expansion of concrete cores as presented by Bérubé (Bérubé 2000) and the second being an analysis of pore solutions in order to predict the degree of deterioration of ASR damaged concrete structures. They proposed a table in which they predict the progress of deterioration in ASR damaged structure within the scope of information and knowledge obtained from the tests

6.3. Damage rating index

Rivard (Rivard P 2000) and Grattan-Bellew (Grattan-Bellew 1992b) presented two different techniques to assess the concrete damage due to the ASR by petrographic analysis. The two techniques are damage rating index (DRI) and a procedure using an image analyser. These methods give an idea about the correlation between expansion and degree of damage. The two methods were compared using polished concrete sections and the data showed that the degree of microcracking correlates well with the expansion of the laboratory test specimens. However no correlation was found between the amount of silica gel measured in the test and the expansion level. The petrographic analysis showed that the degree of damage is lower in the middle part of concrete sample and that the cracking is mainly oriented horizontally. Grattan-Bellew (Grattan-Bellew 1992b) developed a method known as DRI that consists of counting the amount of ASR related petrographic features on polished sections using a stereobinocular microscope at 10X magnification such as:

- Total area of the gel.
- % Area of the gel in each class.
- Total length of the cracking.
- Crack density

A weighting factor is applied to each feature, the factored values thus obtained for each feature are summed and the number normalised for an area of 100 cm^2. The quantitative petrographic analysis consists of placing the polished concrete section on a computer controlled moving stage under a microscope equipped with a high sensitivity black and white camera. A 254-nm UV

illumination is used to enhance the contrast between ASR gel, microcracks and the background. The following information is treated further

The above data is collected for each image, and is then averaged to obtain a global rating for the whole polished section.

7. Summary

The alkali-silica reaction is a phenomenon that affects concretes which is characterised by an internal chemical reaction between amorphous or badly crystallised silica contained in certain aggregates and the ions contained in the interstitial solution.

The fact that it occurs within the concrete, the random distribution of the reactive sites make it difficult to be analysed. If the local reaction mechanisms are well established, the origin of expansion remains a partially source of difference between researches. According to certain authors, it is due to the swelling character of the reaction products (gel). Others advance that it is the rupture of thermodynamic balance and the release of associated energy which is the cause. Swelling could be generated by the destructuration of the siliceous network inside the reactive aggregates.

Most of the current research consists in formulating concretes incorporating of the reactive aggregates. The aggregates used have a great influence on the swelling generated by the reaction. Their reactivity depends on the type of reactive silica that they contain.

Unfortunately, there is very few work in the literature which relates to the influence of aggregate size on the alkali-silica reaction expansion.

ASR affects some mechanical properties such as Young's modulus, the flexural and tensile strength. However its effect on compressive strength remains too limited.

Several testing method exists either to diagnose the concrete affected or for the prognosis of the further development of the reaction.

8. References

Ahmed T, B. E., Rigden, Abu Tair, Lavery (2000). "the behaviour of alkali-silica reactive concrete under high point load and under cycling loading." 11th international conference on alkali aggregate reaction: pp909-918.

Al-Asali, S. a. (1988). "Engineering properties of concrete affected by alkali silica reactions." ACI materials Journal: pp367-374.

Amiet Hélène, H. L. (2000). "quantification of the process of alkali aggregate reaction by microstructural and physico-chemical approaches." 11th international conference on alkali aggregate reaction: pp811-821.

Ballivy G, K., Gravel and Houle D, (2000). "influence of reinforcement steel on the expansion of concrete affected by alkali aggregate reaction." 11th international conference on alkali aggregate reaction: pp919-928.

Bérubé , F., J. Pedneault, A. Rivest (2000). "laboratory assessment of the potential rate of ASR expansion of field concrete." 11th international conference on alkali aggregate reaction: pp821-830.

Charlwood R.G (1992). "a review of alkali-aggregate reactions in hydro-electric plants and dams,." International conference on Alkali aggregate reactions in hydro-electric plants and dams, fredericton, New brunswick, Canada.

Clark L.A (1990). "Structural aspects of alkali-silica reaction." Structural engineering review **2**: pp121-125.

D. Bulteel, E. G.-D., C. Vernet and H. Zanni (2002). "Alkali–silica reaction: A method to quantify the reaction degree." Cement and Concrete Research **Volume 32**(Issue 8).

Gallias J.L (2000). "comparison of damaging criteria for testing aggregtes by autoclaving treatement." 11th international conference on alkali aggregate reaction: pp949-958.

Garcia del Amo, D. and B. Calvo Perez (2001). "Diagnosis of the alkali-silica reactivity potential by means of digital image analysis of aggregate thin sections." Cement and Concrete Research **31**(10): 1449-1454.

Garcia-Diaz, E., J. Riche, et al. (2006). "Mechanism of damage for the alkali-silica reaction." Cement and Concrete Research **36**(2): 395-400.

Grattan-Bellew, P. E. (1992a). "Chemistry of the alkali-aggregate reaction-Canadian experience, in: the alkali aggregate reaction in concrete." Ed. R.N Swamy,Blackie, **Van nostrand Reinhold,**: pp30-53.

Grattan-Bellew, P. E., Danay. A (1992b). "comparison of laboratory and field evaluation of AAR in large dams." proceedings of the international conference on concrete AAR in hydroelectric plants and dams(CEA, Fredericton, Canada): 23 Pages.

H. Kagimoto, M. S., M. Kawamura (2000). "evaluation of the degree of deterioration in AAR damaged concrete and analysis of their pore solution." 11th international conference on alkali aggregate reaction: pp859-868.

Hobbs, D. W. (1988). "Alcali-silica reaction in concrete." Thomas Telford, London: 183pages.

Jensen, V. (2000). "In-situ measurement of relative humidity and expansion of cracks in structures damaged by AAR." 11th international conference on alkali aggregate reaction: pp849-858.

Jones, T. N. (1988). "a new interpretation of alkali-silica reaction and expansion mechanisms in concrete." Chemistry and industry: pp40-44.

Larive C (1998). "apports combinés de l'expérimentation et de la modélisation à la compréhension de l'alcali réaction et de ses effets mécaniques." LCPC **thèse**: 395pages.

Larive C, J. M., Coussy Olivier, (2000b). "hetrogeneity and anisotropy in ASR affected concrete consequences for structural assessment." 11th international conference on alkali aggregate reaction: pp969-978.

Larive C, T. F., Joly, Laplaud, Derkx, Merliot (2000a). "Structural effects of ASR in France on real and laboratory structures." 11th international conference on alkali aggregate reaction: pp979-988.

Leger, P., P. Cote, et al. (1996). "Finite element analysis of concrete swelling due to alkali-aggregate reactions in dams." Computers & Structures **60**(4): 601-611.

Marc-André Bérubé, J. D., J. F. Dorion and M. Rivest (2002). "Laboratory assessment of alkali contribution by aggregates to concrete and application to concrete structures affected by alkali–silica reactivity." Cement and Concrete Research **Volume 32**(Issue 8): pp1215-1227.

Monette L.J, G. N. J., Grattan-Bellew P.E, (2000). "Structural effects of the alkali aggregate reactions on non-loaded and loaded reinforced concrete beams." 11th international conference on alkali aggregate reaction: pp999-1008.

Nielsen A (2000). "alkali aggregate reactions strengthening or total collapse? the different effects of AAR on concrete structures." 11th international conference on alkali aggregate reaction: pp1009-1018.

Ono K (1990). "strength and stiffness of alkali silica reaction concrete and concrete members." structural engineering review **2**: pp121-125.

Pleau r, B. M. A., Pigeon M, Fournier, Raphael S (1989). "mechanical behaviour of concrete affected by ASR." 8th international conference on alkali aggregate reaction: pp721-726.

Poole, A. B. (1992). "introduction to alkali aggregate reaction in concrete, in the alkali-silica reaction in concrete." Ed. R. N. Swamy, Blackie **Van Nostrand Reinhold**.

Rivard P, F., Ballivy (2000). "Quantitative assessment of concrete damage due to alkali-silica reactions(ASR) by petrographic analysis." 11th international conference on alkali aggregate reaction: pp889-898.

Rivard, P., J.-P. Ollivier, et al. (2002). "Characterization of the ASR rim: Application to the Potsdam sandstone." Cement and Concrete Research **32**(8): 1259-1267.

Rotter H (1996). "The impact of alkali aggregate reactions on the fracture mechanics of concrete." Ph-D thesis(T-U Vienna Austria,).

Salomon M., G. J.-L. a. C. J. (1993). "alcalis réactions: mise au point d'un essai d'autoclavage rapide et fiable par lacaractérisation des granulats." Rceherches CEBTP-LCPC sur l'alcalis-réactions : techniques de mesures **N 512**(annales de l'institut technique du bâtiment et des travaux publics).

Siemes T, V. J. (2000). "Low tensile strength in older concrete structures with alkali-silica reactions." 11th international conference on alkali aggregate reaction: pp1029-1038.

Swamy R.N (1992). "testing for alkali-silica reaction in concrete." the alkali silica reaction in concrete ed R N Swamy , Blackie, Van Nostrand Reinhold: pp54-95.

Swamy R.N, a. A.-A. M. M. (1986). "influence of Alkali silica reaction on the engineering properties of concrete." Alkalis in concrete, ASTM STP 930, Ed, V.H. Dodson, American society for testinfg and materials Journal, Philadelphia: pp69-86.

Xu, Z. Z. and R. D. Hooton (1993). "Migration of Alkali Ions in Mortar Due to Several Mechanisms." Cement and Concrete Research **23**(4): 951-961.

Chapter 3: Materials and experiments

1. Objectives

The aim of the experimental programme was to study the suitability of microstructural characterisation for quantifying the degree of alkali silica reactivity in structural concrete. The ultimate goal is to develop tools to enable the transfer of expertise acquired through laboratory experiments to structures affected by alkali silica reaction i.e., to predict the kinetics and the amplitude of swelling of the concrete throughout the course of the reaction in affected structures.

The basic principal of this research programme was to characterise the chemical, microstructural and mechanical state of the concrete and the degree of expansion and to relate the change of the chemical reaction to the changes in mechanical properties.

This objective requires a different approach from that of much research which aims to prilimarily to identify if the aggregates are reactive or not.

In this chapter, the challenges faced in order to implement a good experimental programme are identified. The characterisation of the aggregates chosen for the study is presented. The final section explains the experimental programme adopted and the accompanied microstructural study.

2. Challenges

The extrapolation from the concrete samples examined in the laboratory to the concrete from structures in the field conditions is difficult.

In order to develop a relevant laboratory programme, we need to be aware of the following characteristics of the alkali silica reaction:

2.1. Leaching:

A major problem in the study of alkali silica reaction is the leaching of alkalis. The reaction stops when alkalis leach out. The leaching process depends significantly on the specimen size or on the characteristic dimension of a concrete structure. The alkali concentration is lower in the surface layers of a structure due to leaching effects. Thus the smaller the size of the component the more important becomes the influence of the surface layers due to leaching effects.

2.2. Types of aggregates

The type of aggregate is very important for the alkali-silica reaction. The swelling generated depends on their reactivity, its kinetics and amplitude. Concrete using different types of aggregates will have different expansion behaviour in the same conditions of storage. These differences can be attributed to the distribution and amount of reactive silica contained in the aggregates. Some aggregates generate disorder and expansion only in certain proportions (Pessimum effect). The behaviour depends on the type of reactive silica contained in the aggregates due to the history of deformation that the rock underwent or the internal structure of the siliceous network.

The size of the aggregates has an important influence; it seems that the kinetics of expansion increase with the decrease in diameter of the reactive aggregates. However the granular distribution is important. The extension of granulometry to fines or reactive fine additions makes it possible to decrease the expansion as reported in previous research.

The type of aggregate influences the features of the reaction observed at the microscale for the reaction. A great diversity of features have been observed such as peripheral discoloration, reaction rims observed in opal, or polygonal cracking of aggregates, and micro cracks in paste.

2.3. Timescale

Relating the changes of the microstructural disorder to mechanical properties is difficult in practice. In the field, the induction and reaction period are very long and the amount of reactive material in the aggregate is usually small, so the amount reacted is difficult to measure. Laboratory tests should be shorter and

thus accelerated. Like all the chemical reactions, the alkali-silica reaction is sensitive to temperature. A rise in the temperature increases the kinetics of the reaction. The content of alkali is also an important factor with respect to expansion kinetics.

2.4. Availability of cores

For a reliable study on the effect of alkali silica reaction in structures, we should basically study the concrete on cores from the structure. Getting cores from concrete structures is difficult and costly. Moreover the size of the core specimen is sometimes small relative to the largest aggregate size in the dam. The cores give only one point in the evolution of the structures. Therefore we decided to establish the research programme on laboratory samples from which it is possible to evaluate and develop testing methods as a first step to the in situ prediction of materials-related damage.

2.5. Non linearity

The relation between the degree of reaction, expansion and the change of mechanical properties is probably non linear. The expansion generated by the alkali-silica reaction could have different components such as damage, redistribution of stresses due to the viscoelastic nature of cement paste not only the swelling characteristics of the gel.

3. Aggregates used in this study

3.1. Origin and choice of aggregates

Three Swiss Alps aggregates were studied. The aggregates were used in the construction of 3 dams namely A, B and C that show signs of alkali silica reaction. They were taken from the quarry used for the building of the dams. The reactivity of the aggregates is not excessive and the kinetic of the reaction is slow. In the structure the reaction took from 30 to 50 years to develop for dam A and C.

3.2. Aggregate characterisation

The first step of laboratory testing was the evaluation of the aggregates. A petrographic study was performed to identify the mineralogy of the aggregates.

Both SEM and optical microscopical observations were used to identify whether the reaction took or not place.

The chemical tests were used with the aim of confirm the mineralogy and the effect of alkaline immersion on aggregates. These were chemical immersion in alkaline solution with X-ray diffraction and SEM-Images of the aggregates immersed are given.

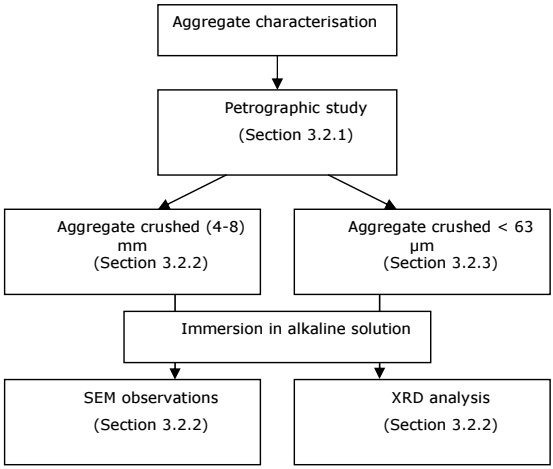

Aggregate characterisation organisation

3.2.1. Petrographic analysis

Petrography is the science of description and classification of rocks. This description or classification is based on their texture, structure and composition which are a reflection of its geological history. Petrographic analysis uses microscopic techniques to determine the constituents of aggregates. The mineral content and the textural relationships within the rock are described in detail.

The petrographic examination of the aggregates was carried out according to SIA 162/1. Additionally, their texture and mineralogy was investigated with thin sections with polarising microscope. These experiments were carried out in the EMPA with the help of Dr. Andreas Leeman.

To produce an accurate representation of the distribution and volume percent of the mineral within a thin section, point counting was used:

POINT COUNT - Count each mineral occurrence along a series of traverse line across a given thin section. For a statistically valid result > 2000 individual points must be counted.

The number of grains counted, the spacing between points and successive traverse lines is dependant on the mean grain size of the sample. Silicates constitute more than 90% of each aggregate type.

Aggregate A

Chlorite schist: The rock is foliated with a thickness of the layers between 0.5 and 3.0 mm. The green layers have a high concentration of chlorite and the white layers a high concentration of quartz and feldspar. Embedded in the layers are agglomerations of feldspar with a length of up to 3 mm and a thickness of up to 0.5 cm.

Table 1: Petrography and silicate mineralogy of aggregate A.

rock type	percent by number	amount of silicates	silicates
chlorite schist	100	> 95	quartz, feldspar, chlorite >>> muscovite > biotite

Most of the quartz (diameter: 10-100 µm) shows well defined boundaries and not a very distinct undulatory extinction. But there are agglomerations of fine grained quartz (diameter of single minerals < 5 µm / figure 1). Approximately 5 % of the quartz consists of such agglomerates. The feldspars present usually are not altered. Chlorite is by far the most common phyllosilicate. Muscovite and some small amounts of biotite are present as well.

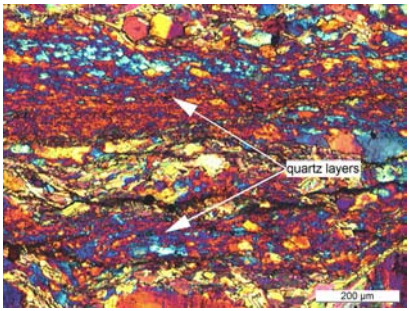

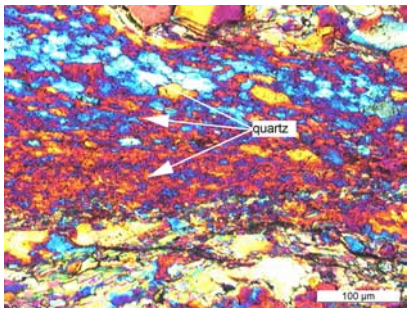

Figure 1: Layers rich in fine grained quartz.

Aggregate B

This contains four different rock types which can be distinguished by their texture and their relative amount of phyllosilicates. Biotite schist 1 contains mostly biotite and only a little muscovite. Biotite schist 2 and 3 are have the same mineralogy, but biotite schist 3 contains feldspar with a diameter up to 1.5 mm. The rocks are foliated with alternating bands of quartz/feldspar rich layers and layers rich in phyllosilicates. The layers have a thickness of 0.5-2.0 mm. the 4^{th} type consists on muscovite schist.

Table 2: Petrography and silicate mineralogy of aggregate B (number of particles analysed: 46).

rock type	percent by number	amount of silicates	silicates
biotite schist 1	14	> 95	quartz, feldspar, biotite >>> muscovite
biotite schist 2	47	> 95	quartz, feldspar, biotite > muscovite
biotite schist 3	9	> 95	quartz, feldspar, biotite > muscovite
muscovite schist	30	> 95	quartz, feldspar, biotite < muscovite

Most of the quartz grains have a diameter between 10-100 µm. They often form bands with a thickness of 0.1-2.0 mm. The boundaries of the single quartz grains are usually well defined (figure 3). They show a weak undulary extinction. Occasionally there are aggregate particles containing quartz minerals with boundaries and size < 5µm (figure 4). Feldspar (K-feldspar) occurs mostly as larger minerals often embedded between bands of quartz or mica. They usually are not altered and contain small inclusions of mica (sericite). Sometimes the

feldspars were severely cracked. Biotite is the most common phyllosilicate present followed by muscovite and some chlorite. Like quartz the phyllosilicates mostly form bands along cleavage plains. Some aggregate grains contain a significant amount (up to 5 %) of pyrite (or marcasite / figure 4 and 6). The larger part of the ore is usually oxidised.

The cleavage planes form along boundaries of bands of quartz and phyllosilicates. They display a thickness between 0.1 mm and 10 mm. The rock is very brittle.

The thin sections contain limestone mainly in the sand fraction. It appears that they are naturally rounded.

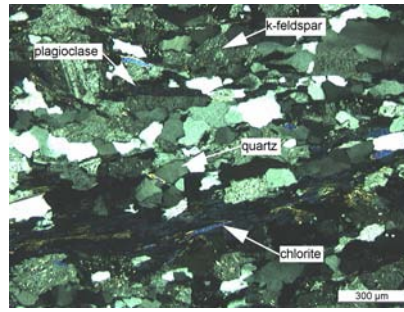

Figure 2: Texture of aggregate B from thin section observations

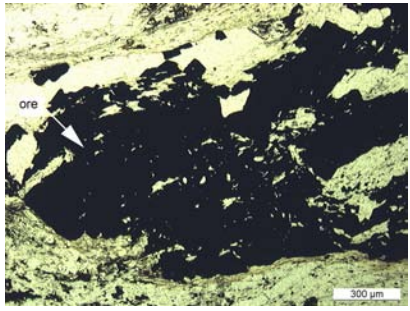

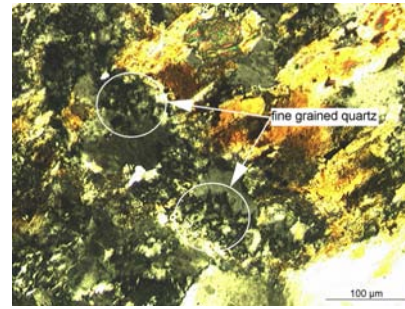

Figure 3: Ore. Fine grained quartz aggregate B

Results of aggregate C

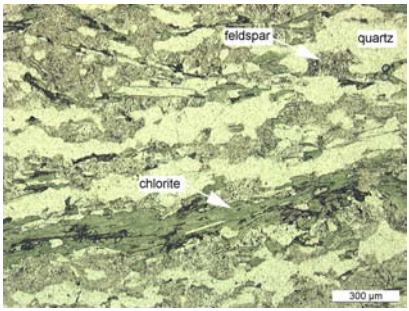

Figure 4: Texture of aggregate C from thin section observations

Biotite schist 1 contains mostly biotite and only a little muscovite. Biotite schist 2 and 3 have the same mineralogy, but biotite schist 3 contains feldspar with a diameter up to 1.5 cm.

The alternating layers of the foliated rocks are between 0.5 and 2.0 mm thick.

Aggregate C is very similar to aggregate B regarding the minerals and the texture present.

Table 3 : Petrography and silicate mineralogy of the aggregate C (number of particles analysed: 61).

rock type	percent by number	amount of silicates	silicates
biotite schist 1	8	> 95	quartz, feldspar, biotite >>> muscovite
biotite schist 2	45	> 95	quartz, feldspar, biotite > muscovite
biotite schist 3	11	> 95	quartz, feldspar, biotite > muscovite
muscovite schist	28	> 95	quartz, feldspar, biotite < muscovite
pegmatite	3	> 95	quartz
Mafite	5	> 95	biotite, amphibole/pyroxene

3.2.2. Observation of dissolution features

The investigation of the reactivity of single components in the aggregates was carried out by the following procedure: Particles (4–8 mm) were embedded in epoxy, cut and polished. For each type of aggregate, two samples with a combined surface area of approximately 40 cm2 were prepared. They were immersed in 1000 ml of 2 M NaOH solution at a temperature of 38 °C in a

calibrated heater without stirring for 2 weeks. NaOH was used to produce the alkaline solution because it is employed in various accelerated test methods to determine aggregate reactivity. The relatively high concentration and temperature of the solution were chosen in order to accelerate the dissolution of silicates.

Dissolution and precipitation phenomena on the polished surfaces were studied with a low vaccum scanning electron microscope. The samples were not coated and the operating conditions of the ESEM were between 15–20 kV and 0.5–1.5 Torr.

Aggregate A

There were a lot of cavities on the polished surface. Some of them could be attributed to the oxidation and removal of ores during weathering. Others may have been due to minerals breaking loose during the sample preparation. Therefore there might be dissolution phenomena but they could not be identified. However, several layers with quartz and feldspar had got a milky appearance after the immersion in the alkaline solution. This might be caused by some kind of dissolution phenomena.

Aggregate B

Biotite-schist 1 + 2 and muscovite-schist were immersed in the alkaline solution. The biotite-schist 2 displayed the strongest dissolution phenomena (quartz > feldspar > biotite / figure 5).

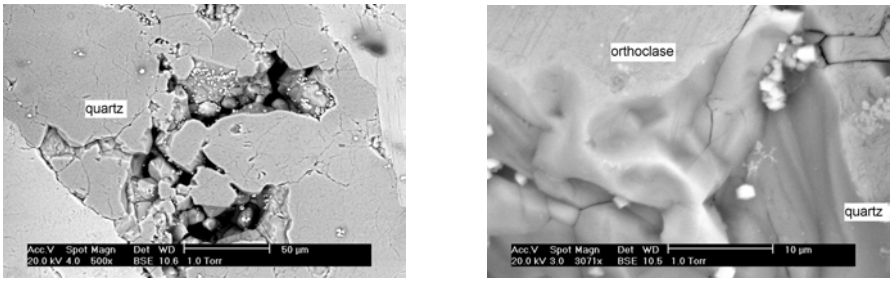

Figure 3: Quartz and feldspar with dissolution phenomena. Biotite-schist 2.

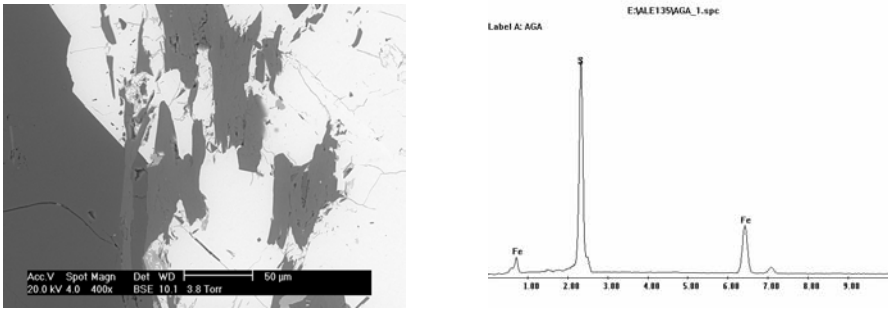

Figure 4: composition of ore: FeS_2 (pyrite or marcasite***).***

Aggregate C

Biotite-schist 1 + 2 and muscovite-schist were immersed in the alkaline solution. The biotite-schist 2 displayed the strongest dissolution phenomena (quartz > feldspar > biotite / figure 7).

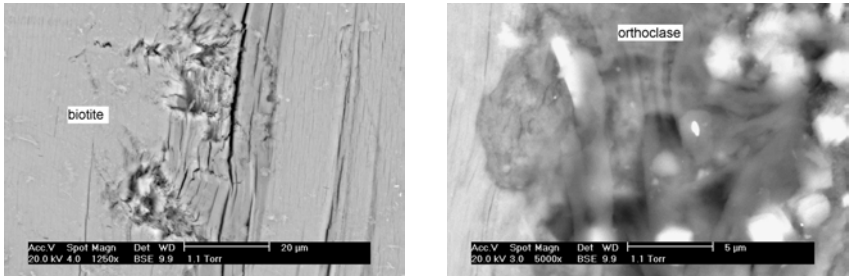

Figure 7: Biotite and feldspar with dissolution phenomena. Biotite schist 2.

3.2.3. Chemically selective dissolution + XRD

Alkali silica reactions in aggregates occur generally via a dissolution-precipitation process, during which amorphous and badly crystallised silica dissolve, and silica gel precipitate. Other researchers showed that the reaction occur via in-situ transformation of network.

The aggregates were crushed then sieved to obtain a fine aggregate powder whose maximum diameter is lower than 63µm. this was done to increase the reactivity of the aggregates, by increasing their specific surface. A part of the aggregates was used to manufacture a pellet which was analysed by X-rays diffraction. Analysis by X-rays diffraction enables us to know the initial composition of the 3 aggregates to be detrmined.

Solutions of 5, 10, 15, and 20 % of KOH were prepared at 95 °C. The solution was constantly agitated using a magnetic stirrer. The aggregates were introduced into the solution and the temperature was maintained at 95°C (to increase the reaction kinetics) for 4 hours.

The aggregates were then recovered by decantation and filtration under a vacuum .then the aggregates were dried for 24 hours. After drying and elimination of any liquid phase, the filtrate was again cracshed to eliminate coagulation then a new X-rays diffraction pattern was obtained. A study in parallel using HCl was undertaken to obtain additional information on the nature of Feldspars as well as the phyllosillicates present in the aggregates.

The patterns were indexed by comparing then it with the (JCPDS) data base containing tens of thousands of reference patterns.

When the diffracting crystals are of nanometric size, the number of planes is not infinite and the corresponding signal present a certain distribution around the Bragg angle. The width of this distribution is directly related to the dimension of the diffracting crystals (Guinebretière 2002). The ideal crystals can be described like a regular stacking of the atomic plans. The rupture of this stacking creates a defect and thus a modification of the signal. This defect modifies the width of the distribution peak

Aggregate A results

The results of the XRD for the aggregate A are shown in the figure 5

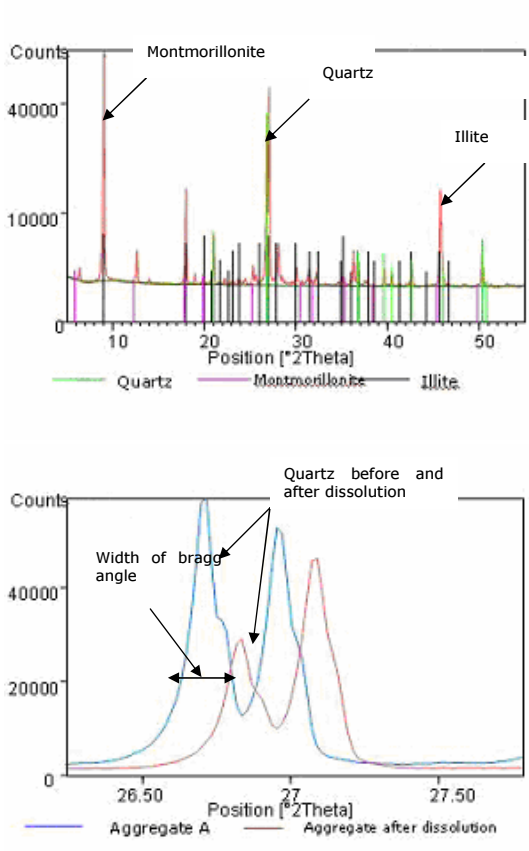

Figure 8: X-Ray diffraction pattern aggregate A (up: aggregate characterisation, down: difference between curves before and after dissolution)

Pattern 1 of the Figure shows the principal phases of aggregate A. It shows preponderance of quartz as well as argillaceous phases (Illite and Montmorillonite). Illite which contains potassium (2 K_2O_3) can constitute a source of additional alkali. The other argillaceous phase, montmorillonite, is a phyllosilicate particularly sensitive to the alkali-reaction ($(Na,Ca)0,3(Al,Mg)_2Si_4$

O_{10} $(OH)_2$ nH_2 O). Water infiltrates easily between the layers and ion exchange may occur which releases alkali to the interstitial solution.

Pattern 2 indicates a strong reduction in the quartz phase after dissolution which indicates that SiO_2 reacted with the KOH. Knowing the petrography of the Swiss Alps and the general process of deterioration of the rocks, the content of amorphous silica is likely to be low or inexistent. This important dissolution of quartz indicates that the siliceous phase is poorly crystallized. The alkaline ions can thus penetrate more deeply into the aggregate and increase the kinetics of the reaction. Thus the poorly crystallised aggregate is potentially reactive.

Aggregate A presents at the same time phyllosilicates and poorly crystallised silica which can be prone to both alkali-silica reaction and alkali-silicate reaction. The peak of the quartz crystal is wide which indicates poor crystalline phases within the silica.

Aggregate B results

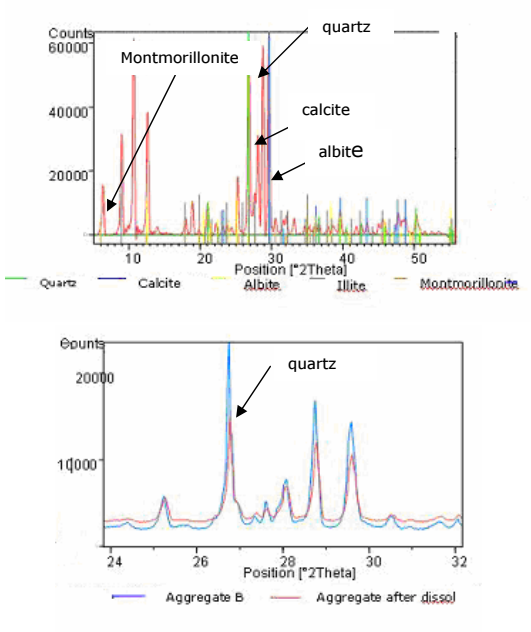

Figure 9: X-Ray diffraction curves aggregate B (up: aggregate characterisation, down: difference between curves before and after dissolution)

Pattern on the top of the Figure shows as in the previous figure the principal phases present in the aggregate B. One notes the presence of quartz, an abundant calcite phase, clays (montmorillonite and illite) as well as a feldspar, $NaAlSi_3O_8$ white feldspar. From the petrographic analysis some of the minerals are known to be potentially reactive however the KOH dissolution indicates a low amount of alkali susceptible material. Indeed, dissolution KOH 10 % has little effect, the concentration was increased up to 20 %, but no difference was noted. The aggregate is thus far from reactive. This can be confirmed by the tests in a cementitious environment which were carried out thereafter such as microbar tests that will be presented in the following chapter.

Aggregate C results

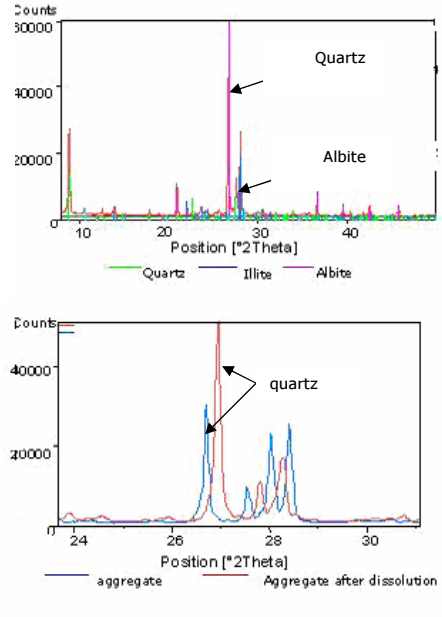

Figure 10: X-Ray diffraction curves aggregate C (up: aggregate characterisation, down: difference between curves before and after dissolution)

The aggregate C has an abundance of calcite with quartz and illite and white feldspar, a Feldspar containing calcium. Dissolution reveals a relatively large fraction of clay. It is noted that the dissolution of quartz with the KOH was high; the aggregate was thus considered reactive. The fraction of clay in this

aggregate is important. This makes the aggregate porous to water and facilitating the ingress of alkaline ions. In the same way the illite present in this aggregate being contains potassium which could constitute an additional source of alkali to the interstitial solution of the concrete.

4. Preparation of cementitious materials

4.1. Introduction

Table 4: tests of aggregates in cement matrix

	microbar	Mortar bar	concrete
Aggregate size	16-63µm	0-3 mm	0-15mm
Formulation C/A (cement/aggregate) ratio	2, 5, 10	1/3	1/6
Specimen size	10 x 10 x 40 mm	40 x 40 x 160 mm	70 x 70 x 280 mm
temperature	150 °C	20,40, 60 °C	20,40, 60 °C
alkalinity	1.5 Na2Oeq	0.8 , 1.2	0.4, 0.8, 1.2
environment	Alkaline environment	Immersed in water	Immersed in water
tests	Microstructure expansion	microstructure expansion Flexural and compressive strengths Young's moduli	microstructure expansion Tensile and compressive strengths Young's moduli

Three types of cementitious material were prepared. Microbars, mortar bars and concrete in order to follow up the evolution of mechanical properties under alkali silica reaction.

The objective at the start was to study variations of several parameters such as temperature and alkaline level content in the cement matrix and aggregate size.

4.2. Mix compositions

4.2.1. Introduction

The experimental methodology followed in order to study the the progress of ASR is described in this section. The results obtained by this study provide the basics of a simple model relating ASR the given parameters.

4.2.2. Principal of tests

Several factors can influence the kinetics and the reactivity of mortars and concrete, which can in turn influence the mechanical behaviour such as expansion. The experimental programme implemented tried to investigate the influence of temperature, alkali content aggregate content and aggregate size on these properties, especially the expansion.

4.2.3. The temperature effect

Like all the chemical reactions, the alkali-silica reaction is sensitive to temperature(Jensen 1982; Swamy R.N 1986; Jones 1988; Pleau r 1989; Salomon M. 1993; Larive C 1998). A rise in the latter involves an increase in the kinetics of the reaction. Previous researches have studied the expansion process occurring due to this chemical reaction either in model reactor or in concrete at different temperatures. It is reported that the effect temperature can be modelled by Arrhenius law.

In order to study this effect, the mortar bars and concrete samples were stored at temperatures of 20, 40 and 60 °C under water. This allows the total rate and magnitude of expansion at different temperatures to be obtained, which used to the activation energy of the reaction. This enables the result to be extrapolated and used for service temperatures that are lower than the experimental temperatures. Microstructural results may also be obtained to measure the degree of reaction.

4.2.4. The alkali effect

The alkaline content has an influence on the reaction(Sibbick and Page 1992; Guedon-Dubied, CADORET et al. 2000). It is thus important to investigate the influence of hydroxyl ions on the kinetics and the magnitude of the reaction. Varying this can have some influence on the expansion. Previous researches have shown a considerable influence of the variation in alkali level on expansion. The impacts on the kinetics order of the reaction was studied for different alkali levels 0.4%, 0.8% and 1.2 % Na_2O_{eq} for concrete samples and 0.8% and 1.2 % Na_2O_{eq} for mortar samples.

To avoid the effect of migration of alkalis, the samples were placed in a saturated environment (under water). Only a small amount of water was added in order to limit the leaching process.

4.2.5. The aggregate size effect

Some previous investigations(Diamond 1974; D. W. Hobbs and Gutteridge 1979; Hobbs 1988; Zhang, Wang et al. 1999; Zhang, Wang et al. 1999; Jin, Meyer et al. 2000) showed that damage induced by ASR is dependent on reactive particle size. In order to investigate this effect two types of aggregate size distribution were fine (0-3mm) for mortars and (0-15mm) for concrete. It allows the measurement of the expansion and some mechanical variation corresponding to the material which approaches dam concrete (in term of properties however the aggregate size remain small compared to the dam one).

The formulation mortar uses also range 0/3 of reactive aggregates. It is used to highlight the influence of aggregates density and diameter on the level and kinetic of expansion and to increase the kinetics of the reactions. In the following graphs and figures in the following chapters of results the name of each composition is referred to its alkali content and temperature of storage (for example a concrete with 0.8% Na_2O_{eq} stored at 60°C is called 60°C Alk 0.8).

4.2.6. Testing procedure

In the microbar test, The kinetics of alkali-reaction were accelerated by increased temperature and by the presence of water and alkali(Chatterji (1989),). The method presented here allowed to give results concerning the reactivity of aggregates at 3 days test duration.

If swelling is lower than a determined threshold, the aggregate is classified "not reactive", if swelling is higher than the determined threshold, the aggregate is classified "potentially reactive" with an uncertainty of 10 % around the value of the threshold.

The classical methods for alkali-reaction evaluation are based on expansion measurements, on mortar or concrete standard prisms (NF P18-585, NF P18-587), typically during 6 to 12 months.

In the present study, a modification of the standard test method was used which consisted essentially of testing concrete and mortar mixes incorporating the reactive aggregates at varying alkali contents and temperatures. The mortar and concrete samples were pre-treated, as follows:

- Immersed in water at 20, 40 and 60°C

- Cooled in humidity chamber at 20°C one day before the measurement of expansion to ensure the stability of the measurements.
- Tests made in humid samples to avoid any difference in measurement state between samples.

The samples were stored for a period of more than a year. The alkali content of the samples was also determined at the beginning and the alkaline level of the water was estimated during the storage. The cement used has an alkali content of 0.4%. To realise these alkali conditions chosen that starts from the limited condition of non reaction to highest alkali content of cement material, alkalis were added in water during the mixing process.

5. Quantification of reactivity using SEM-IA

Polished sections were prepared from the microbar, mortar and concrete prisms after the test and from reference prisms after 3 days which had not experienced alkali silica reaction. The polished sections were observed by Scanning electron microscopy (SEM) to identify the disorder induced by the reaction and to evaluate the reactivity.

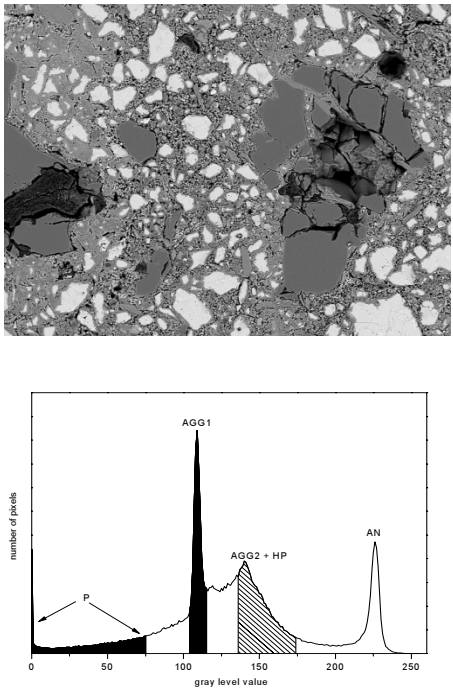

Figure 11: SEM-BSE image (x200) and corresponding grey level histogram (P = porosity and ASR aggregates, AGG1 and AGG2 = aggregate, HP = hydrated products, AN= anhydrous cement grains)

Samples were studied in the Backscattered Electron (BSE) mode in a FEI QUANTA 200 Scanning Electron Microscope. BSE are sensitive to the chemical composition of the analysed materials and lead to the so called 'phase contrast': the higher the average atomic number of a phase, the higher the number of generated BSE, and consequently the brighter the phase will appear in the image. Therefore, the different phases can be distinguished due to the intensity of BSE emit, which results in a difference in their grey level on the acquired images. The phases can be discriminated in the grey level histogram (distribution of the grey level of all pixels of the image).

An example is given in Figure 11. The heaviest phases are the brightest and lie on the right side of the histogram whereas lightest phases are on the left. Thus each peak or each region of the histogram can be attributed to a particular feature in the image. On this basis, aggregate grey levels are found to lie in the following ranges of the histogram:

- between 0 and 75 : region corresponding to porosity and reacted aggregates
- around 110 : region of silicate aggregates
- between 135 and 175 : wide range of variable composition aggregates and hydrated cementitious products (mainly CSH).

The challenge in this approach is therefore to correctly distinguish the aggregates from the cement matrix

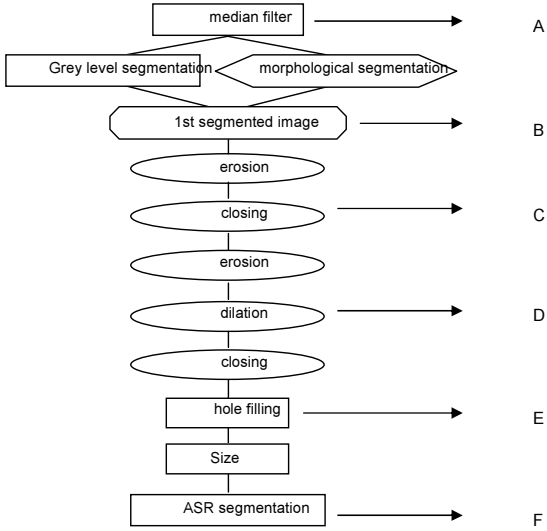

Figure 12: image processing sequence

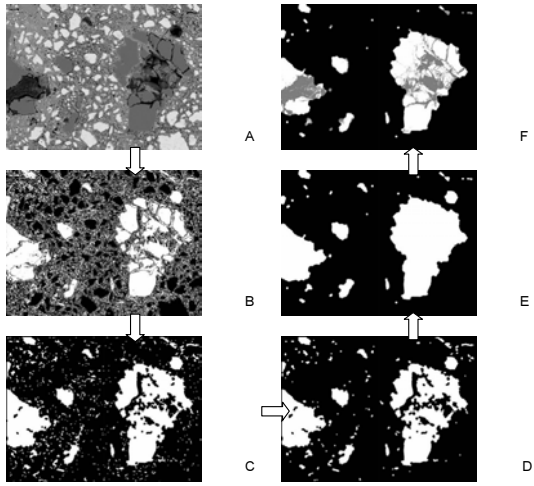

Figure 13: sequence snapshots

As cementitious materials are heterogeneous, phase quantification by image analysis is usually done on a large number of fields in order to take into account

the variations from one field to the other. Some authors have tried to optimize the number of images to be taken, as a function of the magnification, to achieve the lowest standard error on the quantified phases (K.L. Scrivener 1987; Mouret, Ringot et al. 2001). Each aggregate can be considered as an image in itself, in which we aim to measure the ASR degree: At a magnification of 200x, 100 images were found to be sufficient to consider about 5000 aggregates which is large enough to ensure that the results are statistically relevant, as discussed later.

This is similar to the segmentation reported by Young (Yang and Buenfeld 2001). It is not possible to segment the aggregates purely on the basis of grey level on the overlap with the grey level of the cement paste various morphological filters were employed as shown in the figure 11 and 12. It has to be noted that all aggregates really present in one field are not necessarily segmented and counted (this is mainly the case for small sand grains). This is not very important as long as the final number of aggregates considered is high.

5.1. Quantification method verification

5.1.1. Fraction of aggregates in Microbar

The fraction of coarse aggregate in a single microbar or concrete SEM image is unlikely to be representative of the concrete as a whole due to its relatively large size. In order to test many SEM images, the image takes different types of aggregate particles and was in further study used in the mortar and concrete areas. The measured sand fractions in the microbar at different cement/aggregate ratios were compared with those calculated on the basis of the mix proportions of the specimens. The specific gravities of OPC and siliceous sand were taken to be 3.15 and 2.62, respectively. The measured and calculated results are compared in Table 2; a good agreement is observed in all cases.

Table 5: method verification on the mix proportion

C/A ratio	2		5	
	Experimental volume	Images surfaces	Experimental volume	Images surfaces
Aggregate	38cm3	$18.75\ 10^6$	19cm3	$8.51\ 10^6$
Total	162 cm3	$78.03\ 10^6$	174 cm3	$78.03\ 10^6$
fraction	23.7%	24.03 %	10.91%	10.86 %

5.1.2. Porosity of aggregates

The results of the porosity obtained by SEM-IA were compared to the value obtained from MIP. A minimum number of 78 images are required in order to minimise error and to be representative of the sample (due to the small size of pores). The results from the two methods are in good agreement. Further, for the purpose of comparison, the variation of porosity experimentally obtained from SEM-IA was taken as a reference value.

Table 6: method verification on aggregates porosity before reaction

Original porosity	MIP	Microscopy
Aggregate A	4.07%	3.47%
Aggregate B	1.87%	1.53%
Aggregate C	2.07%	1.83%

5.2. Discussion of the method

The BSE image technique offers a simple and reliable method for quantifying the reactivity of the aggregates.

In this research we proposed a new method for quantitative measurements of the reaction degrees of ASR. The measurement of the reaction degrees, porosity and mix composition were given by:

- Quantifying the ASR gel sites content by dividing the number of pixels of crack sites by number of pixels of the initial silica (aggregate).
- Calculating the dissolution degree that corresponds to the number of sites of dissolved silica reduced from the number of cracked surfaces of aggregates present in the beginning.

The methods of quantification consisted of an experimental study containing these steps:

- Accelerating the ASR under controlled temperature.
- SEM-IA of the aggregate that is constituted by cracks and non reacted silica.
- A polishing treatment to obtain well polished thin section at different ages of the reaction.

- SEM-IA treatments for the polished sections to give back the new ratio of microcracks present in aggregates.

The image analysis approach allows quantifying the number of reactive sites created by ASR inside the aggregate. The limiting step of this method is the grey level histograms changing during image acquisition. After taking images in some aggregates some growth of dark parts was observed which did not allow good treatment of the images.

The main limitations of the technique are spatial resolution, which is less than secondary electron imaging (used with fracture surfaces) and the fact that only two dimensional sections of a three dimensional microstructure can be observed.

By microscopic investigations the formation of an internal amorphous product was revealed. This is due to the alkaline diffusion through the porosity of the aggregate. This method allows highlighting the formation of active sites due to dissolution of reactive particles as the ASR progresses.

6. Summary

The results given before showed that aggregates A and C are potentially reactive. The reactivity of aggregate B is marginal. The results of the mechanical tests are given in the following chapters.

7. References

Chatterji ((1989),). "Mechanisms of alkali–silica reaction and expansion. ." In: K. Okada, S. Nishibayashi and M. Kawamura, Editors, Proceedings of the 8th International Conference on Alkali–Aggregate Reaction in Concrete, Kyoto (Japan): pp. 101–105.

D. W. Hobbs and W. A. Gutteridge (1979). particle size of aggregate and its influence upon the expansion caused by the alkali silica reaction. magazine of concrete research. Vol 31: 235-242.

Diamond, S., Ni. Thaulow (1974). a studay of expansion due to alkali silica reaction as conditionned by the grain size of the reactive particle. cement & Concrete research. Vol 4: 591-606.

Guedon-Dubied, J.-S., G. CADORET, et al. (2000). Study on Tournai limestone in Antoing Cimescaut quarry – petrological, chemical and alkali reactivity approach. Proceedings of the 11th ICAAR in concrete: 335-344.

Guinebretière, R. (2002). "Diffraction des rayons X sur des échantillons polycristallins." Lavoisier: 287 pages.

Hobbs, D. W. (1988). "Alcali-silica reaction in concrete." Thomas Telford, London: 183pages.

Jensen, A. D., Chatterji S, Christensen P. Thaulow N and Gudmundsson H (1982). "Studies of alkali aggregate reactions part1 . a comparison of two test methods,." Cement and Concrete Research 12: pp641-647.

Jin, W. H., C. Meyer, et al. (2000). ""Glascrete" - Concrete with glass aggregate." Aci Materials Journal 97(2): 208-213.

Jones, T. N. (1988). "a new interpretation of alkali-silica reaction and expansion mechanisms in concrete." Chemistry and industry: pp40-44.

K.L. Scrivener, H. H. P., P.L. Pratt, L.J. Parrot (1987). "analysis of phases in cement paste using backscattered electron images in: L.J. Struble, P.W.Brown(Eds), microstructural development during hydration of cement." Mater. Res. Soc. Symp. Proc 85: 67-76.

Larive C (1998). "apports combinés de l'expérimentation et de la modélisation à la compréhension de l'alcali réaction et de ses effets mécaniques." LCPC thèse: 395pages.

Mouret, M., E. Ringot, et al. (2001). "Image analysis: a tool for the characterisation of hydration of cement in concrete - metrological aspects

of magnification on measurement." Cement and Concrete Composites 23(2-3): 201-206.

Pleau r, B. M. A., Pigeon M, Fournier, Raphael S (1989). "mechanical behaviour of concrete affected by ASR." 8th international conference on alkali aggregate reaction: pp721-726.

Salomon M., G. J.-L. a. C. J. (1993). "alcalis réactions: mise au point d'un essai d'autoclavage rapide et fiable par lacaractérisation des granulats." Rceherches CEBTP-LCPC sur l'alcalis-réactions : techniques de mesures N 512(annales de l'institut technique du bâtiment et des travaux publics).

Sibbick, R. G. and C. L. Page (1992). Susceptibility of various UK aggregates to alkali-aggregate reaction. Proceedings of the 9th ICAAR in concrete,. Vol2: pp. 980-987,.

Swamy R.N, a. A.-A. M. M. (1986). "influence of Alkali silica reaction on the engineering properties of concrete." Alkalis in concrete, ASTM STP 930, Ed, V.H. Dodson, American society for testinfg and materials Journal, Philadelphia: pp69-86.

Yang, R. and N. R. Buenfeld (2001). Binary segmentation of aggregate in SEM image analysis of concrete. Cement and Concrete Research. 31: 437-441.

Zhang, C. Z., A. Q. Wang, et al. (1999). influence of aggregate size and aggregate size grading on ASR expansion. cement & Concrete research. Vol 29: 1393-1396.

Zhang, C. Z., A. Q. Wang, et al. (1999). "Influence of dimension of test specimen on alkali-aggregate reactive expansion." Aci Materials Journal 96(2): 204-207.

Chapter 4: Relation of microscopic observations to macroscopic expansion

1. Introduction

In this chapter, the results of expansion of mortars and concretes using different alkaline compositions and under different temperatures are presented. The concretes and mortars were placed in water baths at 20 °C, 40 and 60°C. Small batches of samples were placed in sealed containers with a small quantity of extra water to minimize leaching. Specimens from the 3 water baths were tested at various intervals up to 80 weeks for concrete samples. In the following parts, the effects of alkali and temperature on the expansion of concrete and mortar results are presented. Tests were performed for the 3 aggregates. The aggregates characterisation (chapter 3) indicated that aggregates A and C were reactive while the reactivity of aggregate B was marginal.

2. Microbar results

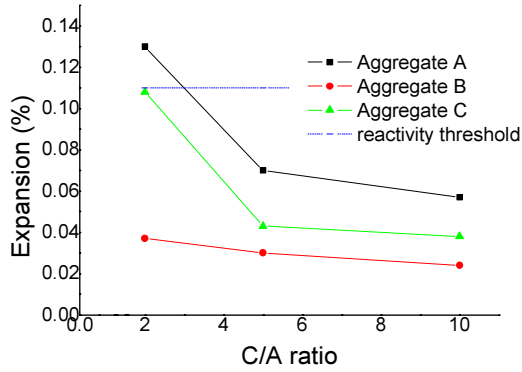

Figure 1: expansion of 3 aggregates under microbar conditions

Figure 1 shows the expansion of the aggregates in the microbars prepared from the three aggregates at the 3 cement to aggregate ratios 2, 5 and 10. The solid horizontal line at 0.11 % indicates the threshold recommended by the test as a criterion of reactivity. From this figure it can be seen that this test confirms the results given in the previous chapter (aggregates A and C as would be identified as reactive and B as unreactive).

Table 1: expansion of the 3 aggregates under microbar conditions

measurement	expansion			
C/A ratio	Aggregate A	Aggregate B	Aggregate C	Mean Errors
2	0.13	0.037	0.108	±0.002
5	0.07	0.03	0.053	±0.003
10	0.057	0.024	0.038	±0.002

As can be seen in Figure 2, the elevated temperature and alkaline environment of the microbar test led to a high degree of reaction of the reactive aggregates, with the formation of holes and voids within the aggregate particles

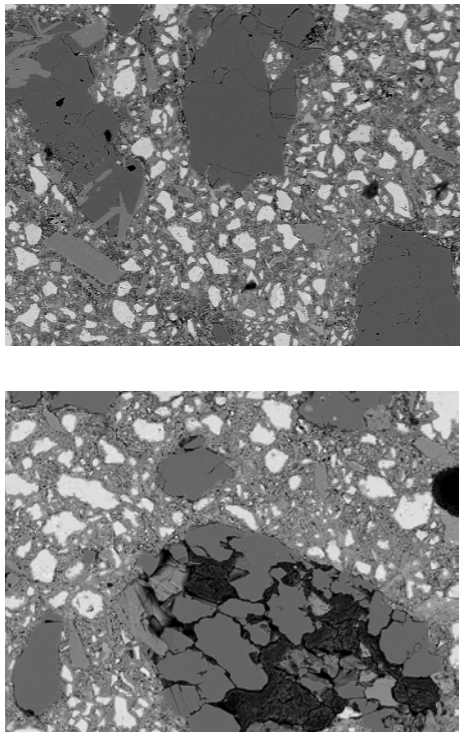

Figure 2 : BSE-Images of microbar samples of aggregate A before and after Microbar test

Microscopy specimens prepared from the microbars for the 3 aggregates and were examined at 3 Cement/Aggregate ratios were examined. 5 specimens of each C/A ratio were prepared, one sample was kept out and not submitted to ASR and the 4 others were submitted.

The image analysis method was used to quantify the amount of aggregate which had reacted during the test. The results are shown in Table 2. It can be seen that relative amount of reaction of the aggregates corresponds well with the amount of expansion at the cement to aggregate ratio of 2. In the microbar test even though the amount of expansion is different at the different C/A levels, the amount of reaction measured in the aggregate is the same at all levels. This

indicates that the chemical reactivity is unaffected by the C/A ratio. However the consequences of this reaction in terms of expansion depend on the cement to aggregate ratio. The microbar test induces a very high level of the reaction as it can be seen from the obtained results.

Table 2: degree of reaction of the different aggregates in the microbar test

	Obtained reactivity using SEM-IA		
C/A ratio	Aggregate A	Aggregate B	Aggregate C
2	12.02	5.71	11.63
5	12.37	4.32	11.67
10	12.51	4.34	11.48

The mean error is equal to ± 0.14

3. Mortar bars

3.1. Effect of ASR on expansion

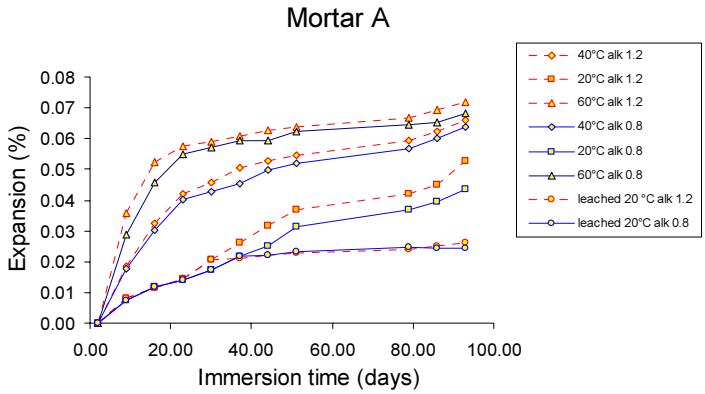

Figure 1 a: mortar bars A expansion vs. time 3 temperatures 2 alkaline content levels

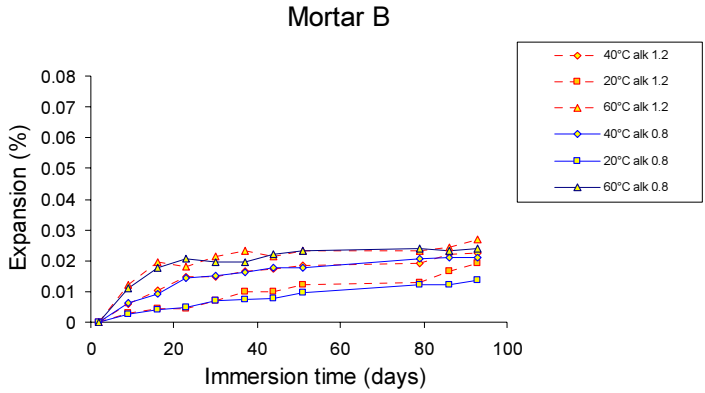

Figure 3 b: mortar bars B expansion vs. time 3 temperatures 2 alkaline content levels

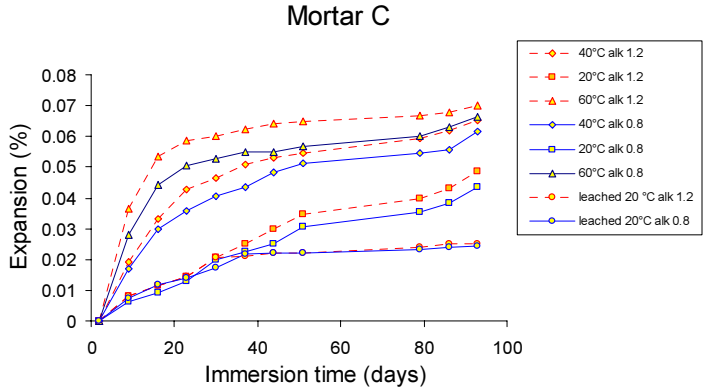

Figure 3 c: mortar bars C expansion vs. time 3 temperatures 2 alkaline content levels

Figure 3 shows the expansion of the mortar prepared from the 3 aggregates exposed at the different temperatures and alkali level. The results are consistent with those found in the microbar test and with the preliminary aggregate characterisation; namely that aggregates A and C show significant reaction while

aggregate B shows low reactivity. Indeed the expansion of the bars made with aggregate B remains low at all temperatures, while those made with aggregates A and C show high expansions at the two higher temperatures after only 20 to 40 days. A loss of alkali occurred in the samples stored at 20°C thus new samples were prepared.

Temperature has a major effect on the rate of reaction and expansion, while the different alkali levels 0.8 and 1.2 seems to have a relatively minor impact especially on the level of expansion. The effects of temperature and alkali level are discussed in more detail in a subsequent section.

3.2. Relation of expansion to reactivity

Polished sections were prepared from the mortar bars at 2, 23, 40, 90 and 180 days and the degree of reaction of the aggregates was measured by the image analysis method presented in chapter 3. The results for the mortars with alkali content of 1.2 and 0.8 are shown in Tables 3 and 4 respectively. The image analysis measurements were time consuming therefore in mortar samples we focused the measurement of A and C. not all the samples of C at 0.8 Na2Oeq were measured.

First it can be noted that the maximum amount of reaction in the mortar bars at the plateau of expansion is much lower than that observed in the microbar test around 3% for aggregates A and C compared to 12 % in the microbar test and only 0.25 % for aggregate B compared to an amount of 5% in the microbar

Table 3: reactivity of mortars at different temperature and an alkaline composition 1.2 % Na_2O_{eq}

Temperatures	Ages (days)	Aggregate A	Aggregate B	Aggregate C
leached 20°C	2	0	0	0
	23	0.24	0.07	0.2
	40	0.38	0.15	0.34
	90	0.39	0.15	0.35
20°C	23	0.24		0.2
(not leached)	40	0.39		0.37
	90	0.57		0.49
	180	0.74		0.68
40°C	23	0.48	0.14	0.39
	40	1.44	0.2	1.07
	90	1.95	0.21	1.78
	180	2.07	0.22	1.91
60°C	23	0.84	0.17	0.61
	40	3.01	0.22	2.06
	90	3.04	0.21	2.08
	180	3.09	0.23	2.15

Table 4: reactivity of mortars at different temperatures and an alkaline composition 0.8 % Na_2O_{eq}

Temperatures	Ages (days)	Aggregate A	Aggregate B	Aggregate C
leached 20°C	2	0		0
	40	0.34		0.32
	90	0.39		0.35
20°C	40	0.38		0.32
	90	0.51		0.41
	180	0.64		0.51
40°C	40	1.02	0.2	
	90	1.45		1.28
	180	1.87		1.81
60°C	40	2.01	0.22	
	90	2.85		2.15
	180	3.09	0.34	2.75

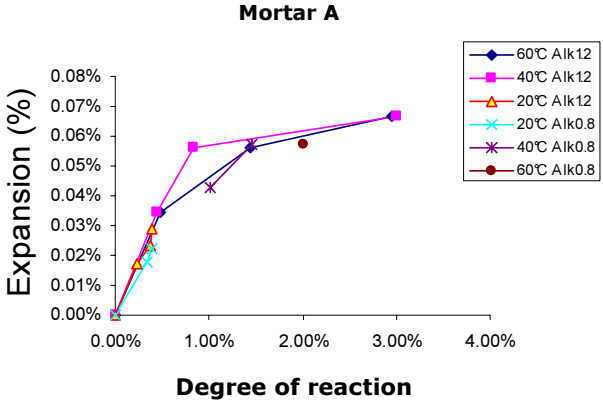

Figure 4 a: expansion vs. observed reactivity for mortar A

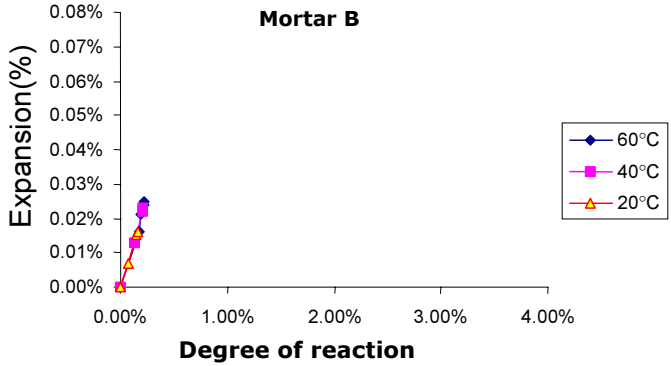

Figure 4 b: expansion vs. observed reactivity for mortar B

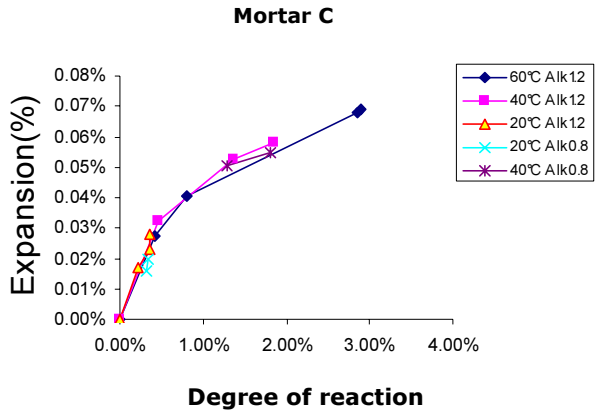

Figure 4 C: expansion vs. observed reactivity for mortar C

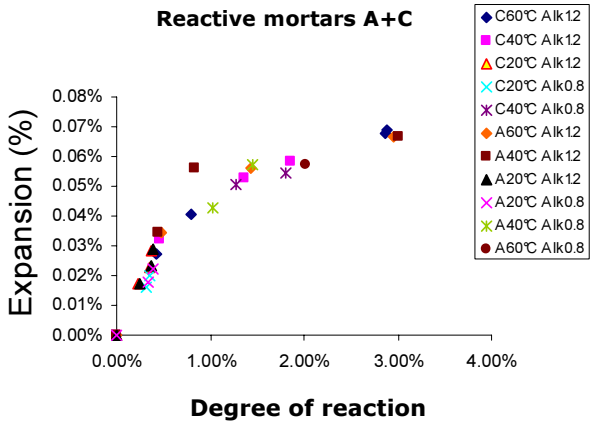

Figure 4 d: expansion Vs observed reactivity for all mortars compositions

In figure 4 the expansion is compared to the observed reactivity for each aggregate. The figure shows an excellent correlation between expansions and the degree of reaction in the aggregates measured by image analysis. The amount of materials in the aggregate disappearing (voids, cracks) is considered proportional to the amount of ASR gel produced in the aggregates on mortars.

Therefore, the correlation between reactivity of aggregates and free expansion suggest that the compressibility of gels and the osmotic pressure caused by the imbibition of water by the gels were not so much different from one aggregate to another for a confined media (aggregates).

The length changes detected under all storage conditions were generally accompanied by an increase in the ASR gel content after several days of storage. The level of observed reactivity in the new 20samples remains low compared to thus of 40 and 60°C. It was stated above from the results of the observed reactivity (presented in table 3 and 4) that the low expansion in the mortars corresponding to the curves at the temperature of about 20°C is due to the slower reactivity of the process at this temperature (the reactivity did not exceed the 0.5%).

No reduction of alkali in the samples stored under laboratory conditions at 40 and 60°C was observed, possibly due to the rapid consumption of alkalis by the silica leading to the formation of gel. It was assumed that no significant changes in the amount of voids and cracks in the aggregates could happen with the dried samples, even when moisture has been entirely eliminated, since the samples were in vacuum for 1 day (No visible cracks with the matrix were recorded as it was shown later).

4. Concrete prisms

4.1. Effect of ASR on expansion

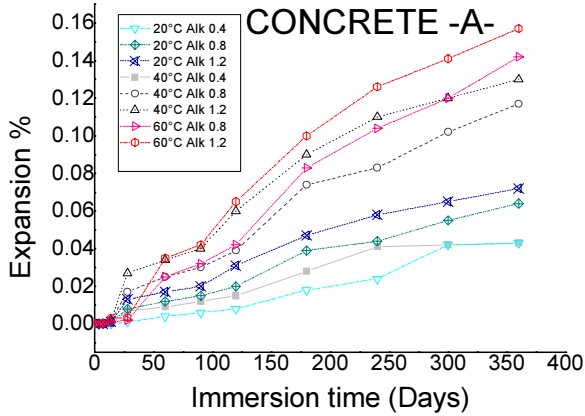

Figure 5 a: concrete prisms expansion vs. time (reactive aggregate A) at 3 temperatures and 3 alkaline content levels

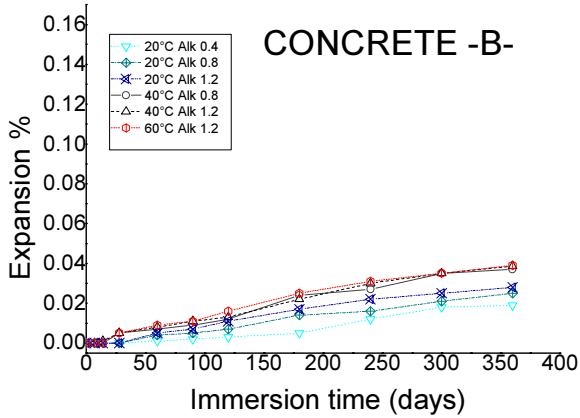

Figure 5 b : concrete prisms expansion vs. time (non reactive aggregate B) at 3 temperatures and 3 alkaline content levels

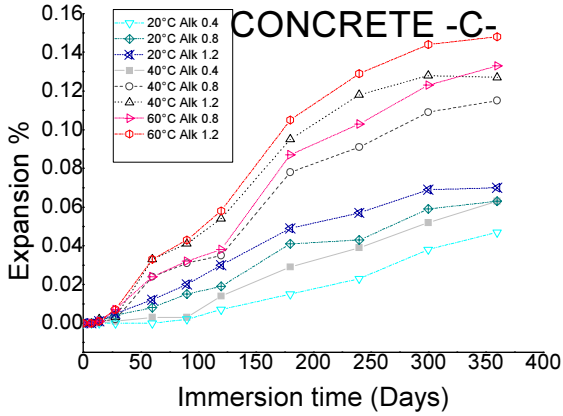

Figure 5 c : concrete prisms expansion vs. time (non reactive aggregate C) at 3 temperatures and 3 alkaline content levels

The expansions measured for concrete at different alkaline content and temperature level are plotted against time, as shown in figure 5. Concrete made with aggregates A and C containing high amount of alkalis at high temperatures showed the highest expansions.

No significant variation in alkali contents occurred during the experiment even for those stored at 20°C which showed significant expansions. For these samples and in order to avoid leaching, the amount of water added was calculated in order to prevent leaching. The pH of the storage bath solutions did not significantly change during the experimental period.

After the initiation of the expansion test, concrete with high alkaline levels rapidly expanded up to about 180 days, and thereafter expanded more slowly. The concrete with 1.2% Na2Oeq at 40°C showed a similar curve to that of concrete with 0.8% Na2Oeq at 60°C. There were only small differences in measured expansions between these both concrete mixes throughout the expansion test.

The concrete with 0.4 % Na2Oeq started expanding after about 28 days, and then expanded slower than all the other concrete mixes. However the concrete

with 1.2% Na2Oeq at 20°C, reached almost the same level of expansion as the concrete with low alkali level at higher temperature.

The expansion curves after 28 days for the concrete specimens given in Figure 5 show that the expansion increases with increasing alkali content for all curing temperatures. The highest rate of expansion was observed at the early ages of storage. Most of the expansion occurred within the first 180 days after the specimens were immersed in the water solution. In the subsequent period up to 300 days, the expansion of the concrete prisms enhanced only by 27% of the specimen expansions at the shorter immersion time.

4.2. Relation of reactivity to expansion

Using the same Image Analysis technique, the reactivity of concrete samples at different time interval was quantified. The samples from aggregate B did not expand significantly and due to the time consuming nature of sample preparation and the image analysis process, the measurement were limited our approach to the two reactive aggregate A and C. Image analysis was performed when changes in expansion and other mechanical properties were observed.

Table 5: reactivity of concrete at different temperatures and different alkaline composition aggregate A

Alkalinity (Na_2O_{eq})	Temperature (°C)	age (days)			
		0	60	120	300
0.4	40	0	--	0.153%	0.238%
	60	0	--	0.212%	--
0.8	20	0	--	--	0.612%
	40	0	--	--	--
	60	0	--	--	2.520%
1.2	20	0	--	--	---
	40	0	0.347%	--	2.104%
	60	0	--	1.571%	2.201%

The results of the concrete quantification are presented in the table 5 and 6 for the aggregate A and C respectively. As for mortar bars, the plot of expansion vs. observed reactivity was derived for the concrete prisms (Figure 6). A very good correlation between the observed reactivity and the expansion is also seen.

Table 6: reactivity of concrete at different temperatures and different alkaline composition aggregate C

Alkalinity (Na_2Oeq)	Temperature(°C)	age (days)			
		0	60	120	300
0.4	40	0	--	0.143%	0.304%
	60	0	--	0.224%	--
0.8	20	0	--	--	0.612%
	40	0	--	---	1.940%
	60	0	--	0.270%	2.220%
1.2	20	0	--	--	---
	40	0	0.260%	--	2.504%
	60	0	0.371%	--	2.601%

As can be observed from the table the limits of reaction of the concrete are similar to those observed in mortars at shorter times. However they are different from those of the microbar. The maximum of reaction obtained at 40 and 60°C at the two high alkaline compositions are almost the same 2.601% and 2.220% for concrete A and C compared with 3.04% and 2.15% in the mortar from same aggregates.

In all concretes with a degree of reaction bigger than 0.3%, the expansion increased with increasing gel content. However with the appearance of cracks the kinetic of expansion changed.

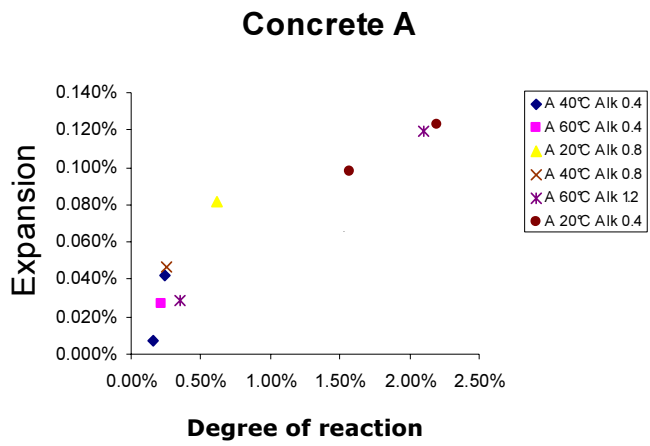

Figure 6 a: expansion vs. observed reactivity of concrete A

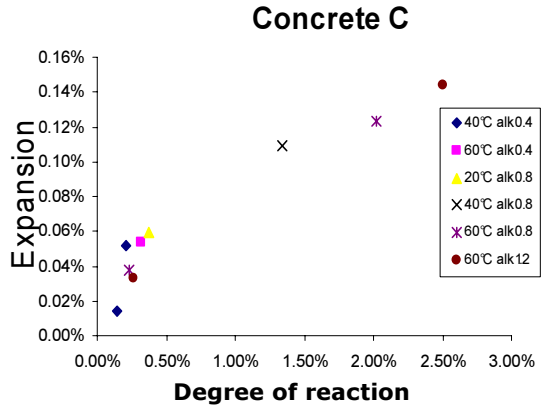

Figure 6 b: expansion vs. observed reactivity of concrete C

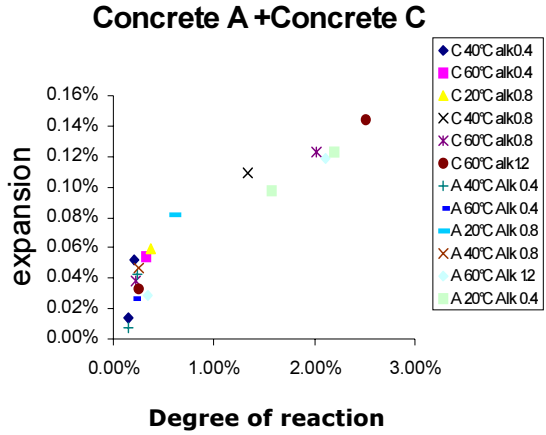

Figure 6 b: expansion vs. observed reactivity of both concretes A and C

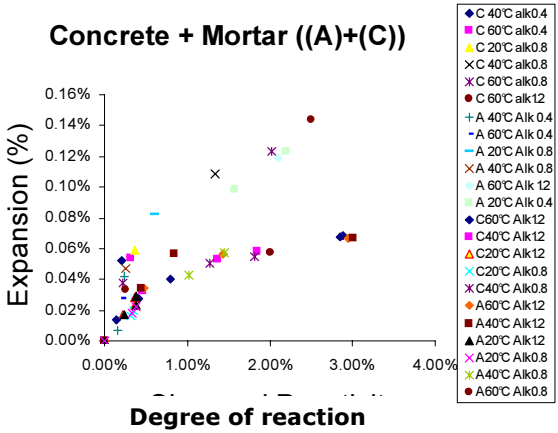

Figure 7: expansion vs. observed reactivity of mortars and concrete samples

Despite a relatively large amount of gel produced in the aggregates, only a low expansion occurred which is due mainly to the fact that the gel formed within a rigid aggregate. The points from curves at different temperatures fall on the same master curve for both aggregates. A small amount of alkali was consumed

in the first reaction stage on the great internal reactive silica surface areas in the reactive aggregates leading to the formation of a small amount of ASR gels but a big expansion rate. Then a cracking process occurred and reduced thus the expansion rates for all the mixes used in this study.

Taking account of the result that differences in expansion between different measurements for the different mortars from the same aggregate were very small, the reliability of the measured expansion in this study is considered very high. Therefore, the scatter of the plot in Figure 7 may be attributed to uncertainly in the estimation of the volume fraction of the gel. However, it may be concluded that the expansive pressure induced in mortar and concrete prisms is generally approximately proportional to the volume fraction of ASR gel

5. Effect of temperature and alkali on rate of expansion

5.1. Introduction

As it was described in the chapter 3, the alkali-silica reaction is sensitive to temperature(Jensen 1982; Swamy R.N 1986; Jones 1988; Pleau r 1989; Salomon M. 1993; Larive C 1998) like all chemical reactions. Previous researches(Dent Glasser and Kataoka 1981; Jones 1988; Gillott 1995; Larive C 1998, D.) studied the expansion process occurring due to this chemical reaction either in reactor (D. Bulteel 2002) or in a concrete (most of the researches) at different temperatures. It can be deduced from these studies that, for the aggregates used, temperature has a purely kinetic effect (A rise in the temperature involves an increase in the kinetics of the reaction.). For most chemical reactions the kinetics can be modelled by the Arrhenius law(Larive C 1998; D. Bulteel 2002). If Arrhenius behaviour is confirmed for ASR the kinetics found in high temperatures can be extrapolated to low temperatures.

Expansion measurements made at different temperatures, using constant alkaline content, allow the effects of temperature to be investigated. In terms of activation energy, a high temperature test is effectively equivalent to a low temperature test (at structural temperatures), enabling the long-term behaviour of the concrete to be observed.

This study also aimed to investigate the role that alkali content has on the ASR expansion rates of concrete and mortar bars at different temperature

conditions. With measurements taken at all of temperatures and alkalinities, these measurements give indications on the kinetic regime of ASR.

5.2. Definition of rate of expansion

The estimation of rate of expansion could be either instantaneous or mean rate. In our case, we calculated the instantaneous mean rate of expansion. These values were applied to determine all the calculations related to the rate (activation energy, etc…).

To determine the rate we calculate the slopes of the regression lines that go through every 3 consecutives measurements for each set of expansion data.

When the rates were calculated, the maximum rate observed within which corresponds generally to the first part of the reaction was used. In the first part of the reaction no cracking happens so the expansion more closed to the product of the reactions. We performed these calculations for all the sets of data that we obtained from the expansion measurements.

5.3. Effect of temperature on expansion

Eight sets of expansion rates were measured, two for each aggregate in mortar and concrete with two different alkali contents. Each of the sets of measurements was used to estimate the activation energies.

The measurements of activation energies at different alkali content were performed to check their dependence on this factor. Expansion rates were dependent on alkali level. Thus, we believe that measured expansion rates observed for each alkali level are consistent with the reality.

The apparent activation energy, E_a, was obtained from the Arrhenius equation, assuming that the expansion rate can be taken as equal to the kinetic constant. The slopes in the Arrhenius plot were calculated by linear regression. The equation at the same alkaline level is given this form

$$\frac{\partial \varepsilon}{\partial t} = k e^{-\left(E_a / RT\right)} \quad (1)$$

In the equation k is the pre-exponential factor and R is the universal gas constant. T is the temperature and ε is the observed expansion.

$$\ln\left(\frac{\partial \varepsilon}{\partial t}\right) = \ln(k) - \frac{E_a}{RT} \qquad (2)$$

Thus, a plot of the natural ln of the time for completion of Stage 1 versus the inverse of the temperature in Kelvin would yield a straight-line relationship with a slope equal to $\frac{E_a}{R}$.

The activation energy can thus be calculated from the slope. The Arrhenius plots for the current study are presented in Figure 8. The experimental data satisfies a straight-line relationship with a high degree of correlation (R^2>.95). This indicates that the mechanism driving the reaction at all temperatures is the same.

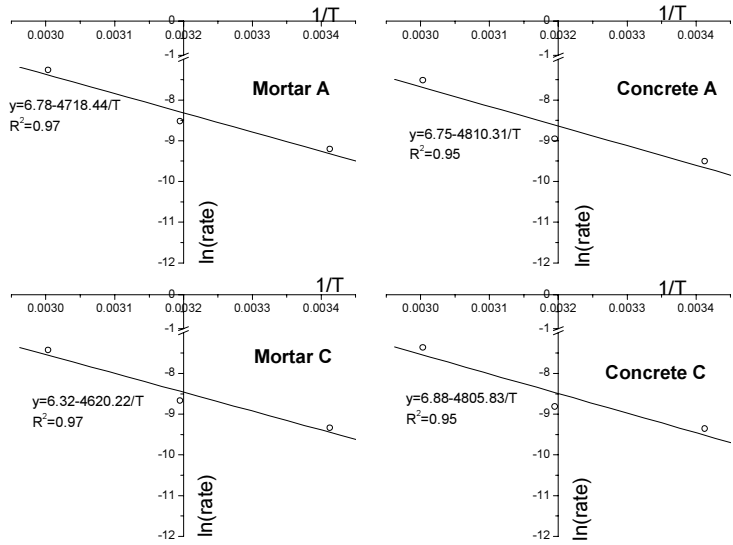

Figure 8: effect of temperature on the rate of expansion of concrete and mortars A and C at 0.8%Na_2O_{eq}

The activation energy is 43.5 ± 2 kJmol^{-1} at alkali content of 0.8 and 1.2 for mortars. For concrete and for both alkaline content, the activation energy shows

almost the same values and is equal to 42.8 ± 3.5, respectively for both aggregates A and C.

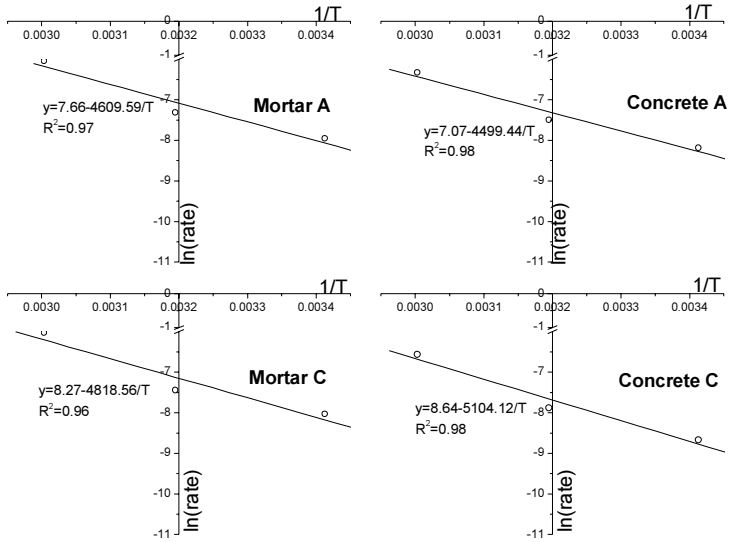

Figure 9: effect of temperature on the rate of expansion of concrete and mortars A and C at 1.2%Na_2O_{eq}

To assess if apparent activation energy depends on the alkaline level, the expansion rate of concrete and mortars was investigated starting with alkali content of 0.8 and 1.2%. The mean values of activation energy obtained for both alkaline levels are 42 and 44 kJ.mol^{-1}. Thus, from the alkaline concentration investigated, the apparent activation energies were found to be similar.

The effects of temperature on the expansion of mortars and concrete due to ASR can be then modelled using simple chemistry-based relationships.

The temperature effect for both aggregates was modelled as an expansion rate law, while an Arrhenius relationship was used to account for the temperature of storage of concrete. Simple regression models were sufficient to explain the variation in expansion with the temperature. Using the results from

these models, modification to evaluate ASR expansion in structures can be possible.

Knowledge of temperature effects provides information on the rate controlling mechanism (Lasaga 1998). It is often considered that values of activation energy below 20 kcalmol^{-1} indicate a diffusion-controlled kinetic regime, while values between 40 and 70 to 80 kcal.mol^{-1} indicate that the kinetic regime is controlled by a mix of surface reaction and diffusion. According to the above scheme, the ASR expansion process is controlled under a diffusion controlled kinetic regime, the rupture of chemical bonds at the surface and the following release of reaction products to the mineral-water interface takes place faster than the diffusion of reaction products through the interface.

5.4. Physical approach for temperatures effect

Previous researchers(D. Bulteel 2002; Yi and Ostertag 2005) presented the relation of the amount of reactivity observed vs. the time. Mainly they present the relation as a linear relationship which is the case here too. The kinetics of the reaction are constant whereas the kinetics of expansion changes due to the cracking and thus the microstructural disorder induced.

The great advantage of this approach is the possibility for the quantitative description of the gel formation process using the laws of chemical thermodynamics. This possibility will be used in this work for the theoretical calculation and experimental determination of the activation energy parameter.

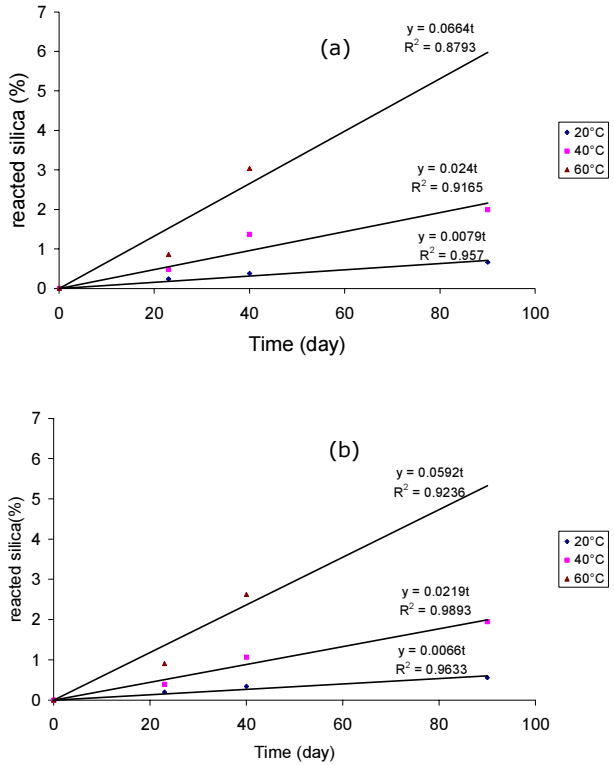

Figure 10: figure reacted silica plotted against time for (a) Aggregate A, (b) Aggregate C for alkalinity 1.2% Na_2O_{eq}

Figure 10 represent the evolution of the reaction degree and the gel sites evolution for three temperatures: 20, 40 and 60°C. Aggregates of maximum size 3.15 mm was used for the mortars in these experiments. The alkalinity parameter was 1.2% Na_2O_{eq} for both mixes. The aggregates did not contain a large amount of fine particles which, like a pozzolana, are immediately dissolved. Therefore, for the percentage of reacted silica calculations, we considered that initial aggregate quantity is the reference for our calculations. This does not affect the activation energy calculation.

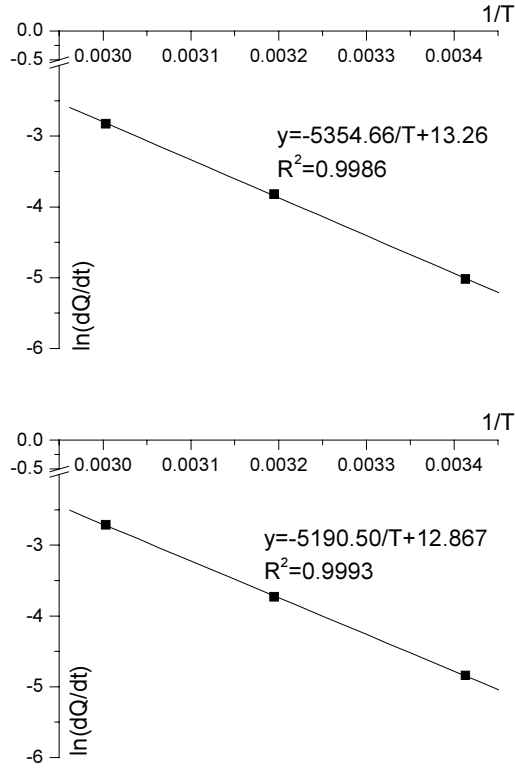

Figure 11: Kinetics of reacted silica against the inverse of temperature for both aggregates A(in the top) and C (in above)

We define:

$$Q(t) = \frac{reac\,agg}{Init\,agg}$$

Where

$reac\,agg$ is the quantified amount of reactive sites using SEM-IA presented in the previous chapter.

And

$Init\,agg$ is the initial quantity of aggregates used for the mix of mortars.

$$Q(t) = k_i(t)e^{-\frac{E_a}{RT}}$$

k_i is function of time and depends on the nature and the quantity of reactive particles in the aggregates.

E_a is the activation energy for ASR.

R is the gas constant

T is the temperature of the reaction.

From the previous equation we can calculate the derivative of time

$$\frac{dQ}{dt} = \frac{dk_i}{dt}e^{-\frac{E_a}{RT}}$$

Applying the logarithm, we obtain

$$\ln(\frac{dQ}{dt}) = -\frac{E_a}{RT} + \ln(\frac{dk_i}{dt})$$

Figure 10 shows reaction rate for larger time. Using the Arrhenius law, we find activation energy of 44kJ mol^{-1} (Figure 10). This value is close to the value of activation energy obtained from the expansion curves which can confirm the relation between the mechanical and the chemical process.

The parameters in the ASR model are dependent on the material behaviour and its test results. Nevertheless comparing our results and the results of other groups (Larive C 1998; Larive C 2000a) the activation energy could be considered equal to 43 KJ.mol-1. The standard deviation for different measurements in all aggregates is equal or below 2 kJ mol−1. This magnitude could be considered as the activation energy of the ASR and used for structural modeling at lower temperatures.

The activation energy calculated from the degree of reaction is in agreement with the value calculated from the expansion measurements for both aggregates in mortars and concrete. This is an additional proof of validity of the method and of the uniqueness of the expansion phenomenon observed in the samples.

Table 7: Summary of activation energy

Method	Mortar A	Mortar C	Concrete A	Concrete C
Expansion 0.8%	41	40	41	41
Expansion 1.2%	41	41	41	43
Microscopy	43	44		
Average Energy	42.3	42.4	41.2	42.0

As it is shown the different values got from the different experiments are similar in both concretes and mortars

5.5. Effect of alkali content on expansion

In literature, no intrinsic expansion rate data related to alkali content have been measured, so no (appropriate) verification was made that alkali content limitations were absent. The low alkali content however, suggests that the data presented in these studies were not limited by this factor.

Many researchers(Grattan-Bellew 1992a; Grattan-Bellew 1992b; Berube, Duchesne et al. 1995; Bérubé 2000)indicated that a low alkali level could be sufficient to stop expansive reactions for certain types of aggregates, whereas it could be too restrictive for other varieties of aggregates(Ramachandran 1998). In our case expansion occurred even in the presence of low alkali cement.

A very useful method to deduce the rate law of reactions is the initial rate method. The general principle is very simple (Lasaga 1998) : if the overall rate is sufficiently low, then no extensive chemical change will occur to vary the concentration of reactants or products over the regime of measurement. In this case we can vary the initial amount of one reactant or product and find the relation between the rate and that particular reactant. So it was decided to vary the alkali content of the mix and to link it to expansion, which is supposed to be proportional to reaction product in the initial stage.

Assume that the initial rate law in our reaction is written:

$$\frac{\partial \varepsilon}{\partial t} = k'[alk]^{\alpha} \qquad (3)$$

Where $[alk]$ refers to the initial concentration of the alkaline solution and k' is considered to be a constant at a given temperature. Therefore, if the initial

amount of alkalis is varied keeping other parameters constant, the coefficient α, can be deduced. The usual procedure is to take the logarithm of both sides of equation. The slope of the plot of log rate versus log alkalis gives α.

$$\ln\left(\frac{\partial \varepsilon}{\partial t}\right) = \ln\left(k'\right) + \alpha \ln\left(\left[alk\right]\right) \quad (4)$$

The obtained results show that the expansion rate of concrete due to ASR and thus to gel formation depends on alkali content, and the range of storage temperatures of the samples.

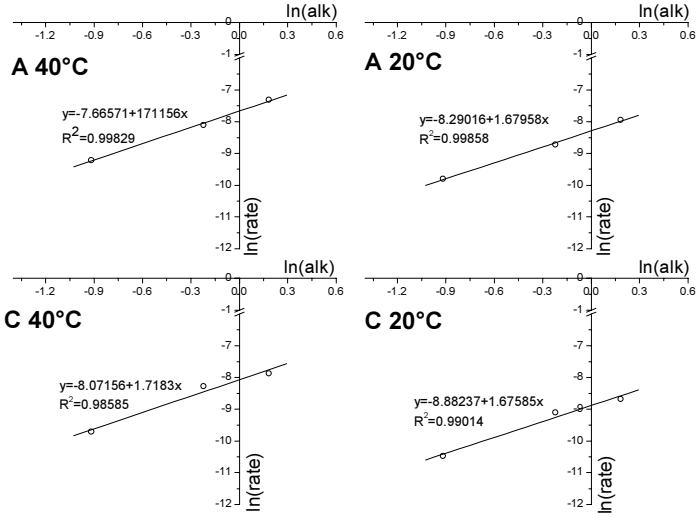

Figure 12: effect of alkali content on the rate of expansion of concrete A and C at different temperatures

Referring to Figure12, with changing the alkaline level at a constant temperature, the increase of the alkalinity increases the rate of expansion factor.

In the experiments, the use of the total alkalinity instead of ion concentration makes the analysis of the results much easier.

Based on the observations presented above, kinetic regime can safely be assumed approximately equal to 1.7 at all temperatures for both aggregates A

and C. A complete kinetic modelling of the reaction is therefore undertaken for these experiments.

6. Aggregate size effect on expansion

6.1. Experimental observations

In order to study the behaviour of the effect of particle size of aggregate on the kinetics of expansion, the mortar and concrete aggregates were exposed to the different alkaline level maintaining the same level for both composites was compared for the samples stored at different temperatures.

From the rate of expansion and knowing the activation energies we tried to calculate the pre exponential factor in the Arrhenius law k. its values are given in the table 8 for all the temperatures, reactive aggregates and mixes.

Table 8: pre-exponential factor of Arrhenius law

Temperature(°C)	Mortar A	concrete A	Mortar C	concrete C
20	7895.32	3893.76	8290.79	4170.02
40	8067.95	4187.86	7997.95	3620.71
60	8065.09	4007.53	7852.60	3816.54
Mean value	8009.45	4029.72	8047.11	3869.09

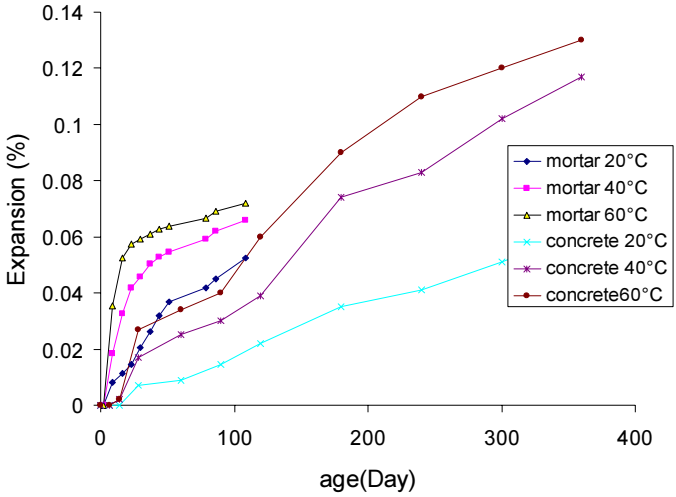

Figure13: difference in the rate of expansion between mortars and concrete with the same alkaline level

Figure 13 shows the experimental results of the expansion due to ASR for mortar and concrete with 0.8 Na_2O_{eq}. It can be seen that the value of initial expansion rate for all of size fractions is consistently bigger in mortars than in concretes for all compositions.

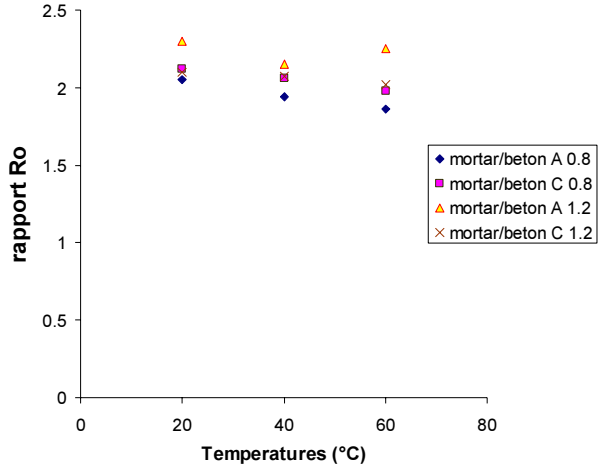

Figure 14: ratio of kinetics of expansion between mortar and concrete at different temperatures and for different compositions

From the results obtained, it is possible to evaluate the extent of the structural modifications of the substrate due to the aggregate size. The changes in the values of the expansion ratio coefficient k at different temperatures show this evolution (Figure 14). At the selected alkaline level, a constant coefficient, approximately equal to 2.12, has been observed between the kinetics of expansion at the start of the reaction. This ratio reflects the different times for diffusion of alkali into the aggregates between mortars and concrete.

In all the cases, the mortar samples show higher rates of expansion than the concretes indicating faster diffusion into aggregates in mortar samples. Therefore, we can conclude that the smaller the aggregate, the faster is the reaction.

Moreover, the aggregate distribution produces an increase in the rate showing an increase of the observed reactivity of mortars. In that case, the concrete sample shows the lower expansion rate constant showing that decrease of the size produces a mixture less resistant to the alkaline penetration and thus more accessible to ASR.

6.2. Diffusion as parameter

From the microscopical study it was found that the reaction takes place inside the aggregates. This implies that the alkali diffused into the aggregate. In order to investigate this factor we tried to calculate the theoretical difference in diffusion rate between mortars and concrete. This value was compared to the difference in expansion rate between the two composite.

Table 9: Mix proportions

Aggregate size	Mortar	Concrete
0/3	100%	42%
3/8.	0	33%
8/15.	0	25%

From the mix proportion and if we normalise everything relative to the rate of diffusion in aggregate size (0/3) range we can estimates the difference in the diffusion time between mortar and concrete. The diffusion time is considered to be proportional to $\frac{1}{r^2}$ where r is the average radius of the aggregates

The calculation for the mean diffusion actor is used with weighting the different aggregate size present in the mix. So that for concrete

$$td_{conc} = 0.42td_{0/3} + 0.33td_{3/8} + 0.25td_{8/15}$$

Table 10: relative diffusion rate of each aggregate size

median diameter	relative diffusion
1.2	1.00
4.5	0.07
10	0.01

Table 10 gives the relative diffusion of each aggregate site range compared to the (0/3) range.

Table 11: relative diffusion rate of mortar and concrete

Mortar relative diffusion	1.00
Concrete relative diffusion	0.45
Diffusion Ratio	2.24

The calculation gave a ratio 2.24 times (Table 11) faster in mortar than in concrete this value compares very well to the experimental ratio of 2.12 to the experimental value obtained from the expansion rate values. The aspect of diffusion into aggregates is developed in appendix 2.

7. Simulation of the expansion of a dam

To verify the relation given by Arrhenius law and the alkali level relation,

$$\varepsilon = R_0 \, Exp(-\frac{E_a}{RT})(alk)^{\alpha} F(t)$$

We tried a simple simulation of the expansion observed in dams. For this simulation we took the following hypothesis:

- An alkali content equal to 0.8 % weight in cement.
- A dam concrete temperature of 5°C and 10°C.
- Use of the activation energy given by the laboratory concrete and mortar.
- The rate of expansion observed in lab concrete is the same as in the dam concrete.
- No comparison to Dam data was performed. The dam data in hand were in mm and not in (mm/m).
- The time step chosen were equal to 1 year. No data concerning the temperature fluctuation in the dam was in hand.

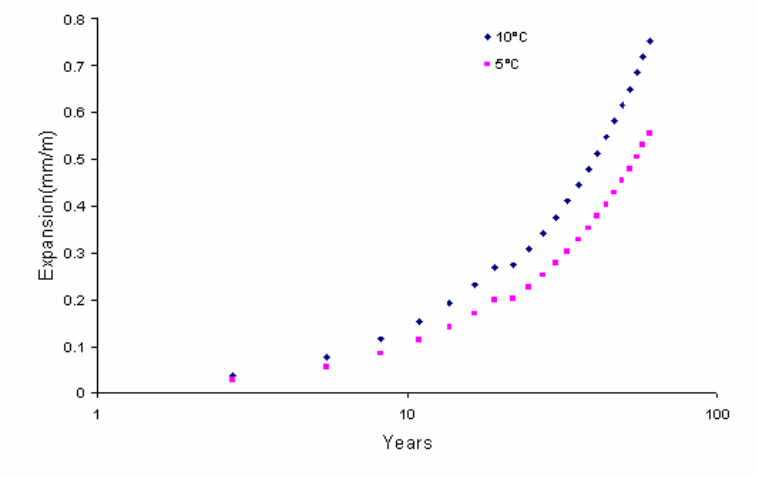

Figure 15: use of Arrhenius law to recreate the expansion in a dam

As observed in the figure 15 the simulation reproduced fairly the movement of the dam in a free expansion. However once we have in hand more data concerning the temperature the fluctuation could be better observed. This simulation can also overestimated the dam deformation. So a more mechanical model is needed to integrate the stress effect on expansion.

8. Development of microstructural disorder due to ASR

The growth of cracks in aggregate due to ASR gel formation was studied in SEM images for various ages (Figure 16). Figure 16 shows typical images of aggregates particles in the mortar sample with aggregate A, 1.2% alkali at 60°C at the ages of 7, 23, 60 and 180 ages.

In the image from the sample at 7 days some cracks can be observed of this early age these are not the result of ASR but-pre existing cracks in the aggregates.

In the sample at 23 days, gel has started to form in small areas but as yet no cracks propagate from these reactive sites.

In the sample at 60 days, a few cracks start to propagate from the reactive sites, however the cracks are not too wide.

In the sample at 180 days the cracks formed a network sometimes with large cracks.

The rate of expansion is important when the samples have no cracking process occurring in the aggregates. It must be noted that the principal axes of the cracks should be basically perpendicular to the direction of expansion due to gel formation, at least around the reactive sites. Nevertheless there are numerous locations where marked differences occur in the crack distribution.

A second important observation is the fact that most of the cracking related to the gel formation process localises in a region around the reactive site on the large aggregates. Although there exist strain concentration domains outside this small region on or close to the aggregates surface in the cement matrix, these deformations are insufficient to cause crack formation so that no cracks in matrix are observed neither macroscopic crack is observed in the specimen as demonstrated in chapter 6. A micromechanical study indicates that the aggregates are in tension n and the matrix is in compression

7 days

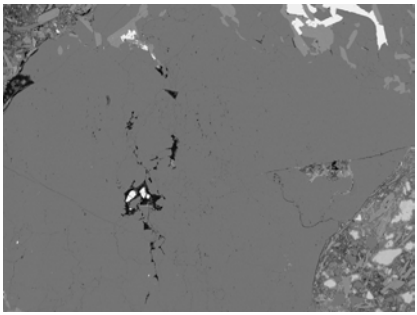

23 days

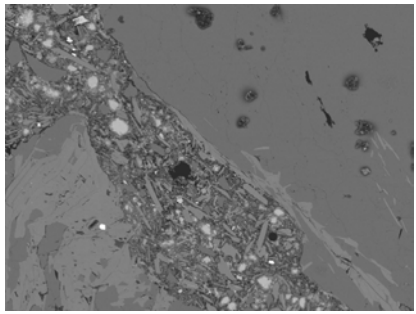

60 days

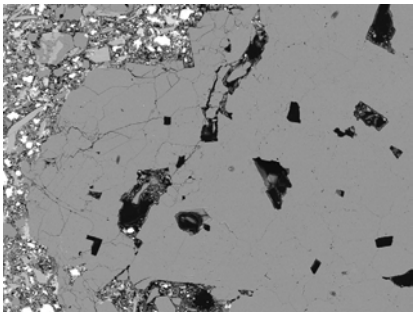

180 days

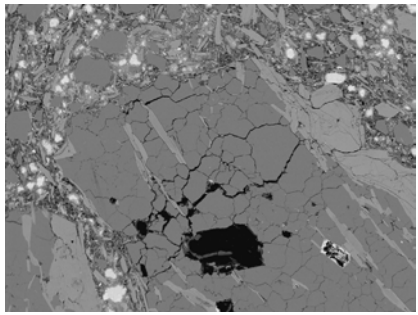

Figure 16: The growth of crack network in the aggregates of mortar A due to ASR gel (BSE-images at different ages 7, 23, 60 and 180 days)

Finally, we assume that an energy release is a factor determinant once localisation has occurred but does not significantly affect the behaviour prior to crack interaction. Stresses in the cement matrix are then allowed to relax and dilate adjacent to an affected aggregate. This reduces the local confining stress that allows the apparent confined strength to be reduced to the uniaxial minimum. This local confinement reduction leads to enhanced crack propagation as well when the aggregate concentration is reduced.

9. Cracking severity of mortars and concrete

9.1. Graphic observations: Cracking of concrete

Figure 17 shows the cracking severity in mortars and concrete at the same reaction degree.

From Figure 17, it can be seen that the cracking of concrete became significant when the exposure temperatures were higher than 20°C and alkaline level higher than 0.4%Na2Oeq, which is in good agreement with some previous reported observations (Hobbs 1988; Berube, Duchesne et al. 1995; Bérubé 2000). The crack patterns in the aggregates, though quite similar, were less severe than those observed in the aggregates of the microbar specimens. From the progress of cracking as observed in the pictures at different stages of the reaction, it is evident that the cracks propagated to the cement paste of the concrete specimen after initiating in the aggregates. However a few isolated cracks were observed in the cement possibly caused due to shrinkage.

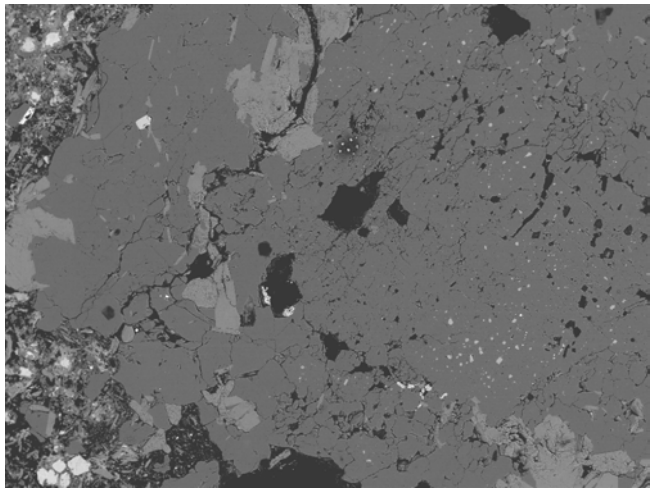

Figure 17 a: Cracking of mortars at degree of reactivity of 2% (alkaline level 1.2% and temperature 60°C)

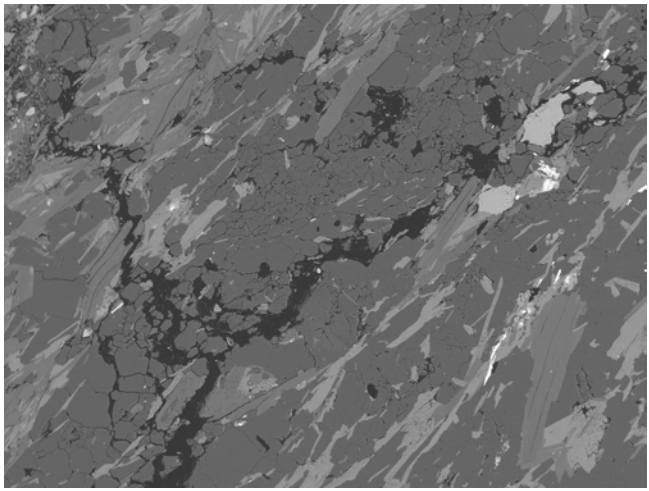

Figure 17 b: Cracking of concrete samples at the degree of reactivity of 2% (alkaline level 1.2% and temperature 60°C)

The cracking was observed to be more severe in the mortars compared to the corresponding concrete specimens due to the absence of aggregates that would otherwise act as global alkali consumers. Cracks were more apparent in mortars aggregates at less expansive state and shorter time of exposure.

9.2. Influence of aggregate size on cracking

The crack patterns of concretes and mortars made with different alkali contents were quite distinguishable from one sample to the other. Several days after exposure to 60°C, concrete exhibited several major cracks in big aggregates. For mortars however, a network of minor cracks was observed at the same degree of reaction. The crack widths and lengths became smaller when the aggregate content was decreased. Similar observations to dam concrete were found in concretes, where the influence of aggregate size could be easily noticed (Figure 10).

It appears that the presence of aggregates generates barriers that restrain the propagation of cracking into the matrix. The most severe cracking was observed in pure microbars, which have the least amount of aggregate. At the same amount of aggregates, the influence of size became increasingly

significant, which infers that the aggregate plays a major role in alleviating cracking. Thus, an appropriate grading of aggregates in concrete is an effective method for improving its resistance to cracking upon exposure to alkaline environment.

9.3. Influence of cracking on residual mechanical properties

The degree of cracking appeared to have more influence on the tensile strength than on the compressive strength. When the exposure temperature was 20°C, an increase in compressive strength was observed even when there was a drop in the tensile strength of concrete. This might be due to the insensitivity of compressive strength to minor cracks. Storage at 20°C generated a relatively small amount of cracking, which did not cause any immediate loss of the concrete capacity in compression. However, the cracking affected the tensile strength of concrete. For samples at 40°C and 60°C, the residual compressive strength also dropped slightly below the original values with further crack development. The tensile strength further deteriorated to about 25% of its original value.

This observation was consistent with the experimental results on expansion. It can be explained that cracks in aggregates due to ASR shortened the paths of larger cracks allowing them to pass through the concrete slices. Presence of cracks appeared to cause greater reductions in Young's moduli and tensile strengths in concretes with higher aggregate density at the same observed reactivity, especially in cases where the maximum exposure temperature was 60°C. For instance, the mortar series showed a rapid nonlinear decreasing rate of tensile strength but a constant quasi-linear increasing rate of crack density. The mortars showed a severe reduction in flexural strength. This might be due to the mortars tendency to develop a network of shorter but wider cracks when exposed to higher temperatures.

9.4. Summary

Small cracks were observed for concrete and mortar specimens stored at 20°C. After exposure to 40°C and 60°C, the cracking of aggregates in concrete was more significant. The crack density increased almost linearly with the

exposure time. Significant increase in cracking was observed between 40 and 60°C.

Cracking patterns varied when different C/A ratio were used in concretes. The concrete with the lowest ratio (1/6) exhibited several major cracks. With increasing of C/A ratio, a fine network of cracks was observed. Higher C/A ratio contents led to more evenly distributed cracks.

Lower C/A ratios resulted in fewer major cracks. However, the cracks density was higher in comparison with the cracks in specimens made with higher C/A ratios.

10. Summary

The results presented in this chapter demonstrate that there is direct connection between the progress of the ASR as measured by microscopy and the macroscopic expansion.

This relationship depends only on the formulation of the cementitious material- cement to aggregate ratio, aggregate size etc, and not on the kinetics of the reaction i.e. it is general to all temperatures alkali levels and aggregate types for a given formulation.

It is shown that the kinetics of the reaction depend on the temperature according to the Arrhenius equation and alkali according to a power law.

These finding of the potential to extrapolate the kinetics in laboratory concrete to field structures.

Microscopic examination shows that the sites of ASR in the aggregates studied are within the aggregates and there is no evidence of a "rim" of reaction at the aggregate surface.

This is almost certainly related to the complex mineralogy of the aggregates with small region of reactive minerals embedded in a non reactive aggregate matrix.

It is observed that the gel forms at the reaction sites and then cracks the aggregates due to the pressure generated. It is likely that this mechanism of pressure generation with aggregates explains the general relationship between

the degree of reaction and expansion. This hypothesis will be developed in more detail in the chapter 6.

11. references

Bérubé , F., J. Pedneault, A. Rivest (2000). "laboratory assessment of the potential rate of ASR expansion of field concrete." 11th international conference on alkali aggregate reaction: pp821-830.

Bérubé , F., J. Pedneault, A. Rivest (2000). laboratory assessment of the potential rate of ASR expansion of field concrete. 11th international conference on alkali aggregate reaction: pp821-830.

Berube, M. A., J. Duchesne, et al. (1995). "Why the Accelerated Mortar Bar Method Astm-C-1260 Is Reliable for Evaluating the Effectiveness of Supplementary Cementing Materials in Suppressing Expansion Due to Alkali-Silica Reactivity." Cement Concrete and Aggregates 17(1): 26-34.

D. Bulteel, E. G.-D., C. Vernet and H. Zanni (2002). "Alkali–silica reaction: A method to quantify the reaction degree." Cement and Concrete Research Volume 32(Issue 8).

Dent Glasser, L. S. and N. Kataoka (1981). The chemistry of alkali-aggregate reaction. Cement and Concrete Research. 11: 1-9.

Gillott, J. E. (1995). "Review of Expansive Alkali-Aggregate Reactions in Concrete." Journal of Materials in Civil Engineering 7(4): 278-282.

Grattan-Bellew, P. E. (1992a). "Chemistry of the alkali-aggregate reaction-Canadian experience, in: the alkali aggregate reaction in concrete." Ed. R.N Swamy,Blackie, Van nostrand Reinhold,: pp30-53.

Grattan-Bellew, P. E., Danay. A (1992b). "comparison of laboratory and field evaluation of AAR in large dams." proceedings of the international conference on concrete AAR in hydroelectric plants and dams(CEA, Fredericton, Canada): 23 Pages.

Hobbs, D. W. (1988). "Alcali-silica reaction in concrete." Thomas Telford, London: 183pages.

Jensen, A. D., Chatterji S, Christensen P. Thaulow N and Gudmundsson H (1982). "Studies of alkali aggregate reactions part1 . a comparison of two test methods,." Cement and Concrete Research 12: pp641-647.

Jones, T. N. (1988). "a new interpretation of alkali-silica reaction and expansion mechanisms in concrete." Chemistry and industry: pp40-44.

Larive C (1998). "apports combinés de l'expérimentation et de la modélisation à la compréhension de l'alcali réaction et de ses effets mécaniques." LCPC thèse: 395pages.

Larive C, T. F., Joly, Laplaud, Derkx, Merliot (2000a). "Structural effects of ASR in France on real and laboratory structures." 11th international conference on alkali aggregate reaction: pp979-988.

Lasaga (1998). Kinetic theory in earth sciences. Princeton university press: 811.

Pleau r, B. M. A., Pigeon M, Fournier, Raphael S (1989). "mechanical behaviour of concrete affected by ASR." 8th international conference on alkali aggregate reaction: pp721-726.

Ramachandran, V. S. (1998). "Alkali-aggregate expansion inhibiting admixtures." Cement & Concrete Composites 20(2-3): 149-161.

Salomon M., G. J.-L. a. C. J. (1993). "alcalis réactions: mise au point d'un essai d'autoclavage rapide et fiable par lacaractérisation des granulats." Rceherches CEBTP-LCPC sur l'alcalis-réactions : techniques de mesures N 512(annales de l'institut technique du bâtiment et des travaux publics).

Swamy R.N, a. A.-A. M. M. (1986). "influence of Alkali silica reaction on the engineering properties of concrete." Alkalis in concrete, ASTM STP 930, Ed, V.H. Dodson, American society for testinfg and materials Journal, Philadelphia: pp69-86.

Yi, C. K. and C. P. Ostertag (2005). Mechanical approach in mitigating alkali-silica reaction. Cement and Concrete Research. 35: 67-75.

Chapter 5: Changes in mechanical properties

1. Introduction

In this chapter, the results of the changes in mechanical properties due to the alkali-silica reactions for the different mortar and concrete compositions are presented. It was shown in the previous chapter that the aggregates A and C show reactivity while the expansion of mortar and concrete using the aggregates B was small. The results presented here concern the aggregates A, B and C. The results of aggregate B can be considered as a reference for a non reactive sample.

2. Mortar results

2.1. Effect of ASR on compressive strength

Figure 1 (a, b and c) shows the results of compressive stress tests on mortar made with the 3 aggregates up to 90 days. Tests were not made beyond this period also due to the limited number of samples available for destructive testing. However a threshold of the expansion due probably to lack in alkalis due to leaching or consumption in the reaction was also observed in mortar samples.

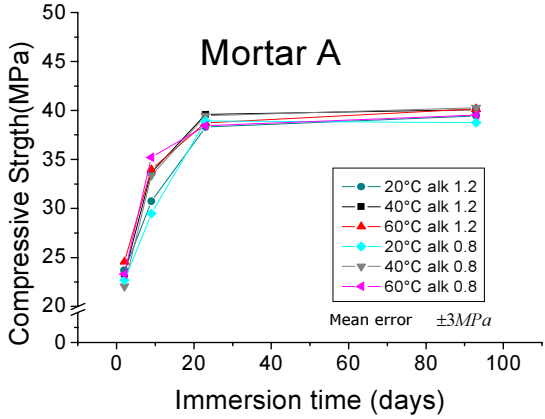

Figure 1a: mortar bars compressive strength vs. time (reactive aggregate A) 3 temperatures 2 alkaline content levels

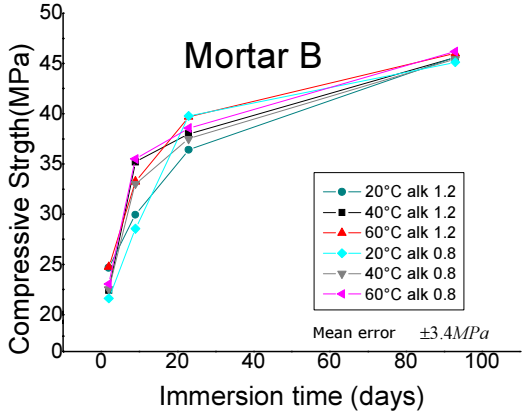

Figure 1 b: mortar bars compressive strength vs. time (non reactive aggregate B) 3 temperatures 2 alkaline content levels

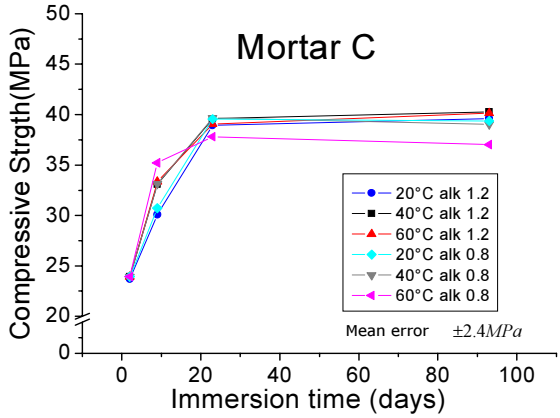

Figure 1c: mortar bars compressive strength vs. time (reactive aggregate C) 3 temperatures 2 alkaline content levels

In general the reactive aggregates A and C showed a compressive strength that remains stable or that drops slightly from 28 to 90 days for the samples with fatstest reaction kinetics. However compared with the strength of the samples with aggregate B it can be seen that the reaction has a negative effect on the compressive strength (a reduction of 10% compared to the non reactive sample is observed).

The results confirmed the previous findings presented in the chapter 2. the compressive strength is less affected by ASR than the other properties). However compressive strength is often not the main concern when assessing the mechanical strength of Mortars affected by ASR.

2.2. Effect of ASR on flexural strength

Figure 2(a, b and c) shows the evolution of flexural strength in mortars samples up to 90 days. Here again the numbers of samples available for destructive testing was limited. Therefore flexural strength tests were performed in every time the expansion showed significant difference.

The curves of flexural strength (Figure 2) show an increase followed by a decrease depending on the temperature.

The ASR effect is identified from comparisons of results from the mortars stored at 20°C to results from the higher temperatures, which does not have ASR effect at the early ages. Because of the slow reactivity even after a long term immersion, the results of the 20°C remain higher than those of highest temperatures. However, in comparison with the non reactive samples, the flexural strengths of reactive samples decrease significantly.

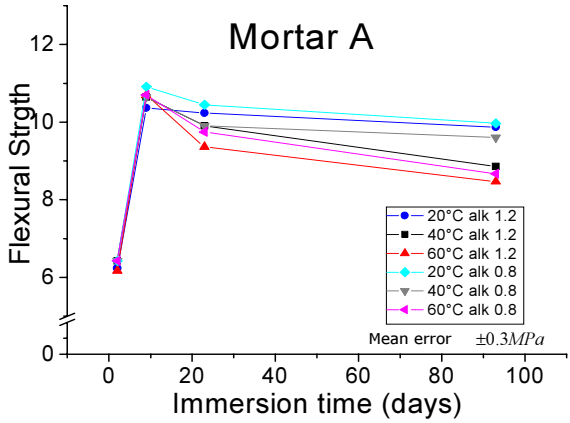

Figure 2a: mortar bars flexural strength vs. time (reactive aggregate A) 3 temperatures 2 alkaline content levels

This delay was caused by both, the kinetics of the reaction condition and the cracking process induced by the reaction. In the mortar with high alkaline addition, the leaching process is observed less in the long term immersion. The temperature in the mortars exerted a similar effect on both aggregates. The flexural strength decrease in the mortar at low temperatures is much smaller than the mortar at 40°C and 60°C. These differences depict the temperature effect on ASR in case of reactive aggregates and could be related to the cracking process observed (detailed in the previous chapter).

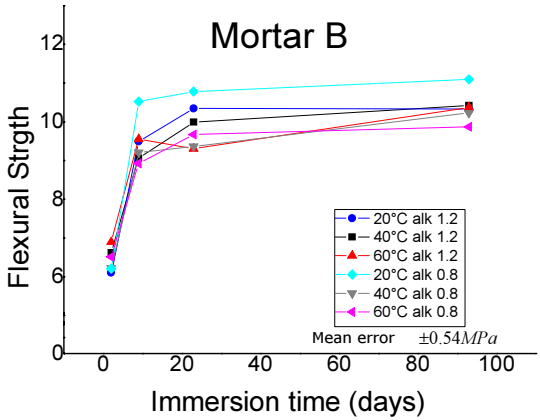

Figure 2b: mortar bars flexural strength vs. time (non reactive aggregate B) 3 temperatures 2 alkaline content levels

At the end of the three first months, the flexural strength was reduced by about 19%. Similar effect is also shown in aggregate A, wherein the alkaline content and temperature has a much greater effect on ASR effect. These changes in flexural strength caused by ASR will further affect other mechanical parameters of the mortars as its toughness.

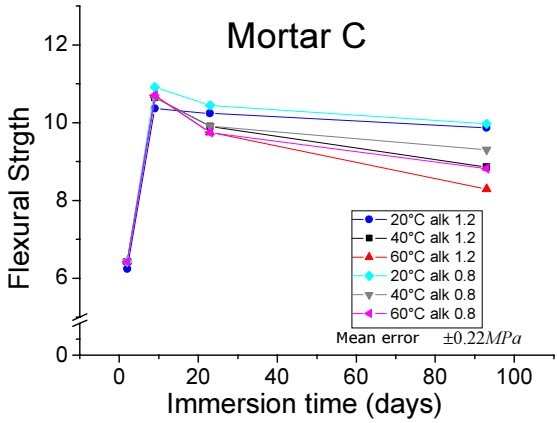

Figure 2c: mortar bars flexural strength vs. time (reactive aggregate C) 3 temperatures 2 alkaline content levels

The ASR effect on flexural strength for these aggregates was elucidated. And clearly, flexural strength variation was confirming the literature results for both aggregates A and C with different temperatures in two alkaline content compositions of mortars.

2.3. Effect of ASR on Young modulus of mortars

The figure 3 presented the variation of the Young's modulus of mortar of reactive aggregates A and that are compared to the variation of the non reactive one B.

The observed Young modulus average given in the graphics was obtained from the average of 7 observations.

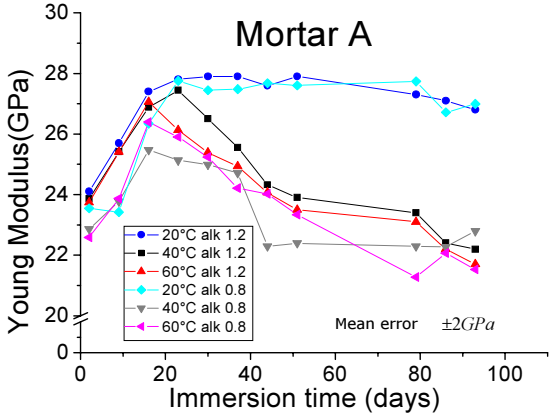

Figure 3 a: mortar Young modulus vs. time (reactive aggregate A) 3 temperatures 2 alkaline content levels

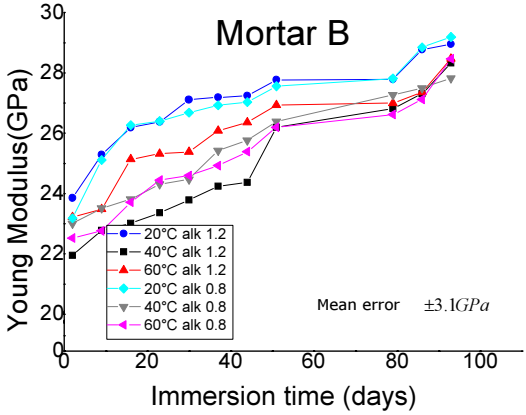

Figure 3 b: mortar Young modulus vs. time (non reactive aggregate B) 3 temperatures 2 alkaline content level

In both results of reactive aggregates A and C, the curves are showing an increase in the beginning and then the Young modulus decreases from the 28 days following changes in lengths for mortars stored at 40 and 60°C. The decrease shows cracking process propagation at microstructural level indeed the Young's modulus is sensitive to the cracking process and thus a decrease is equivalent to the cracking into the aggregates.

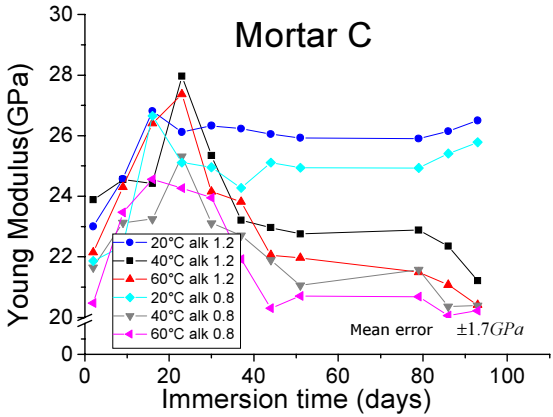

Figure 3c: mortar Young modulus vs. time (reactive aggregate C) 3 temperatures 2 alkaline content levels

The difference between the results at 40°C and 60°C shows the effect of temperature in ASR affected mortars on elastic properties. Because of the temperature effects and high alkaline level used for the tests on ASR kinetics, length variations can result in spatial heterogeneity in crack distributions and, subsequently, decrease in Young modulus. It was thus important to evaluate the significance of such heterogeneity and its effect on mechanical properties. Indeed in the following chapter an analytical modelling tries to link this cracking process to the expansion and the Young modulus.

3. Results from concrete bars

3.1. Effect of ASR on compressive strength

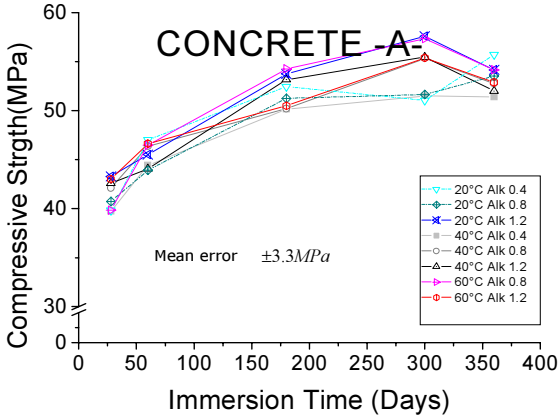

Figure 4a: compressive strength vs. time (reactive aggregate A) 3 temperatures 3 alkaline content levels

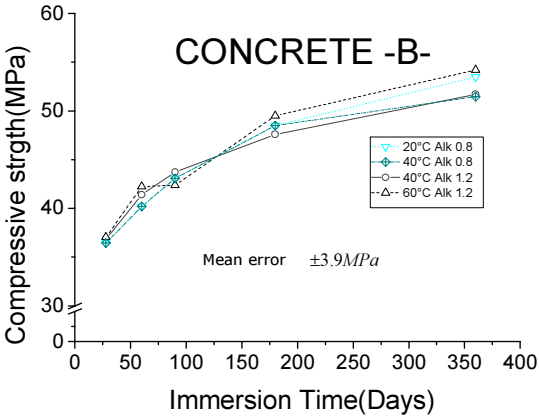

Figure 4b: compressive strength vs. time (reactive aggregate B) 3 temperatures 3 alkaline content levels

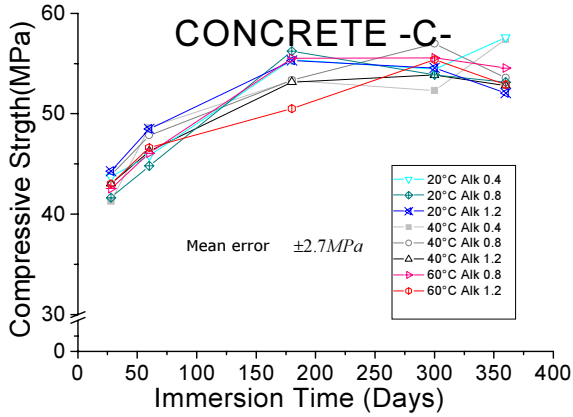

Figure 4c: compressive strength vs. time (reactive aggregate C) 3 temperatures 3 alkaline content levels

The figure 4(a, b) shows the evolution of compressive strength in reactive concrete A and C. an important result shown is the increase of this property in the first steps of the reaction up to 180 to 240 days depending on the temperature and the alkaline level followed by a decrease in this property. However, reactivity in concrete did not result in a very large reduction in the compressive strength. The reduction is about 10 % of the maximum value observed.

The main reduction with respect to the high alkali content was obtained at 300 days and the differences remained somewhat similar afterwards, i.e., up to 360 days (Figure) at the different temperatures. The two reactive concretes nevertheless showed continuous increase in compressive strength during the 360-days testing period (Figure) at low alkali content. These results confirm the previous obtained from the mortar tests.

3.2. Effect of ASR on tensile strength

The figure 5(a, b, c) shows the evolution of tensile strength under ASR conditions for the 2 reactive aggregates A and C. it gives also how the tensile strength varies when a non reactive aggregate (aggregate B) was used.

Despite some scatter in the test results (stochastic process of cracking), the addition of alkalis to the concrete mixture resulted in reduction in the tensile strength from 5% to 25% over the 360-day testing period (Figure).

A decrease in the tensile strength of different alkali content concrete specimens containing reactive aggregates was noted after 8 weeks of exposure. In the specimens containing the highest alkaline level, the tensile strength decreased up to 25 % in the specimens prepared with the reactive aggregates. It can also be shown that the reduction increases when the temperature increases. No big apparent loss in the tensile strength was noted in the specimens prepared with reactive aggregates and placed at 20°C nevertheless the tensile strength did not show any increase as it should be observed in non reactive concrete .This small decrease can be explained by the high variability of tensile strength values of concrete

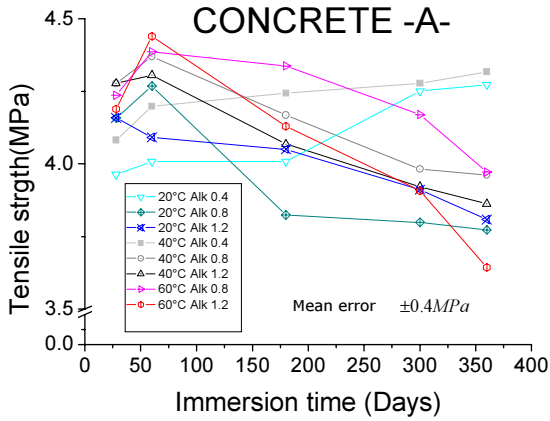

Figure 5a: Tensile strength vs. time (reactive aggregate A)
3 temperatures 3 alkaline content level

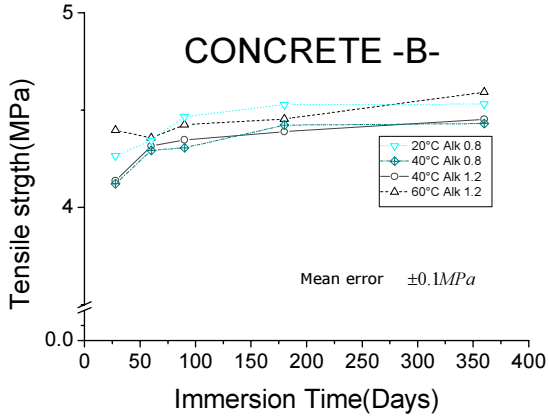

Figure 5b: Tensile strength vs. time (reactive aggregate B) 3 temperatures 3 alkaline content level

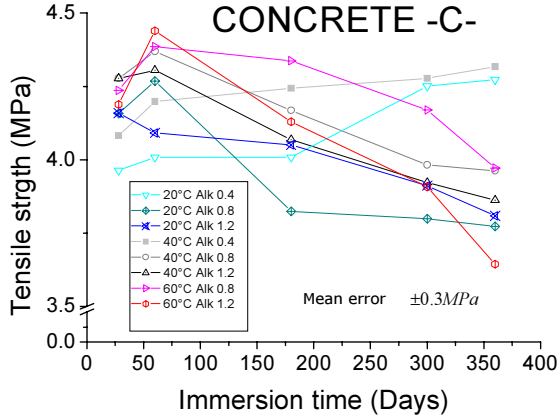

Figure 5c: Tensile strength vs. time (reactive aggregate C) 3 temperatures 3 alkaline content levels

As observed previously in other studies, the long term immersion of concrete and thus the high reactivity level observed in concrete resulted in a noticeable

reduction in the tensile strength (Figure 5). Again, the main reduction was observed in high level alkali content concrete at the highest temperatures.

3.3. Effect of ASR on Young modulus of concrete

The figure 6 (a, b, c) shows the results of Young's modulus on concrete made with the 2 reactive aggregates and the non reactive one up to 360 days.

A decrease in the Young's moduli of different alkali content concrete specimens containing reactive aggregates was noted after 8 weeks of exposure. In the specimens containing the highest alkaline level, the tensile strength decreased more than 20 % in the specimens with the high alkali content.

It can also be shown that the reduction increases as the temperature increases. Only a small loss in the Young's modulus strength was noted in the specimens prepared with reactive aggregates and placed at 20°C.The evolution of Young modulus here shows the cracking within the samples. The Young modulus drops significantly due to ASR immediately after cracking.

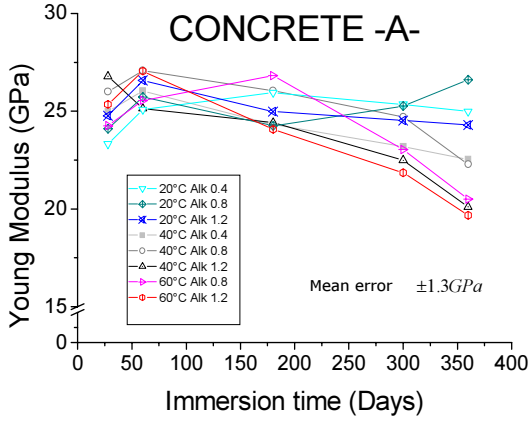

Figure 6 a: Young modulus vs. time (reactive aggregate A) 3 temperatures 3 alkaline content levels

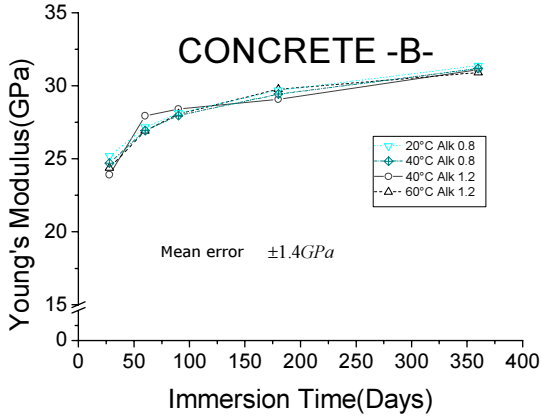

Figure 6 b: Young modulus vs. time (reactive aggregate B) 3 temperatures 3 alkaline content levels

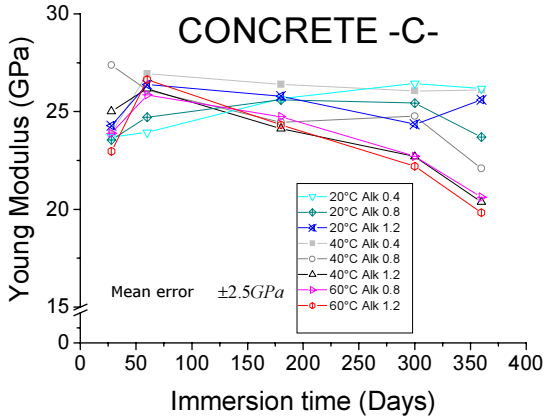

Figure 6 C: Young modulus vs. time (reactive aggregate C) 3 temperatures 3 alkaline content levels

In this situation, damage can be reasonably interpreted and quantified as a reduction in stiffness. The degradation of Young's modulus may be regarded as damage indicator.

For high alkaline content concrete prisms at high temperatures the decrease in Young moduli can be used as an attempt to detect and evaluate damage by determining constitutive elastic parameters. Knowing that concrete is a non-linear, non-elastic material; it does not display a unique or constant value of elastic modulus as shown in Figure 6, and sustains permanent deformation on removal of load. When subjected to an internal stress, concrete strains increase with time.

4. Relation of reactivity to mechanical properties

As concrete strengths vary with aggregate content and aggregate size used in different mortars and concrete, separated studies of each type of concrete were adopted to analyse the experimental results.

As shown in Figure 7 (a, b), the peak strength of compressive strength of each Mortar was observed at low degree of reaction. However, all specimens showed some small losses in compressive strength. No correlation between compressive strength and reactive degrees could be observed.

An insignificant effect on the specimens at all temperature was observed with only about 6 % loss in strength after 3% reactivity, possibly due to the un-cracked matrix. It was derived from microscopic observations that the cracking occurred essentially in the aggregates. Since the cement matrix did not crack no significant loss in compressive strength was observed in any of the mixtures (Figure 7).

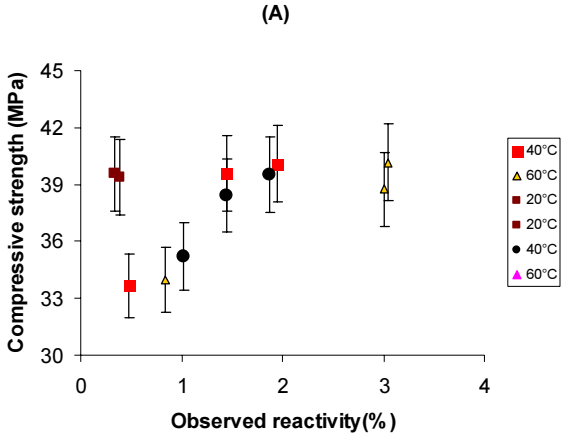

Figure 7a: Mortar A compressive strength vs. observed reactivity (different temperatures and both alkaline level 0.8% and 1.2% Na_2O_{eq})

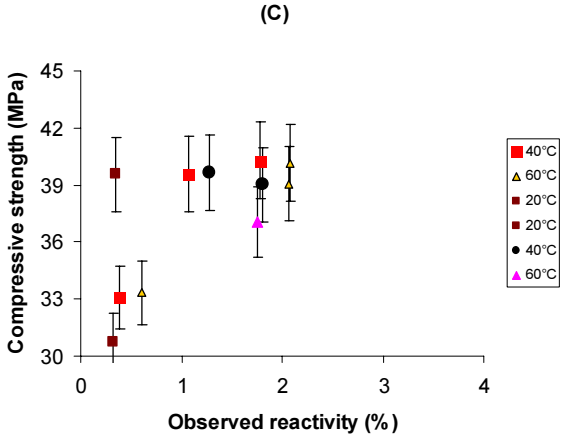

Figure 7b: Mortar C compressive strength vs. observed reactivity (different temperatures and both alkaline level 0.8% and 1.2% Na_2O_{eq}

Figure 8 shows the mechanical properties (flexural and young modulus) of mortars. The data points present the mean strengths or moduli for each sample against their observed reactivities.

The flexural strength and Young's modulus of mortar were affected significantly by the increase in reaction and thus the crack propagation. The greatest values for these two parameters occurred at an observed degree of reaction of 0.3% when the gel formation is not accompanied by crack formation, indicating that a little presence of gel (<0.3%) improves the interaction of cement matrix and swelled aggregates.

After certain time of exposure and from certain level of reactivity 0.3% losses were observed in mainly tensile strengths of concretes and flexural strengths of mortars. Mortars suffered big losses in both Young's modulus and tensile strengths almost 20% and 24% respectively. The modelling of the losses in Young's modulus were treated in the chapter 6.

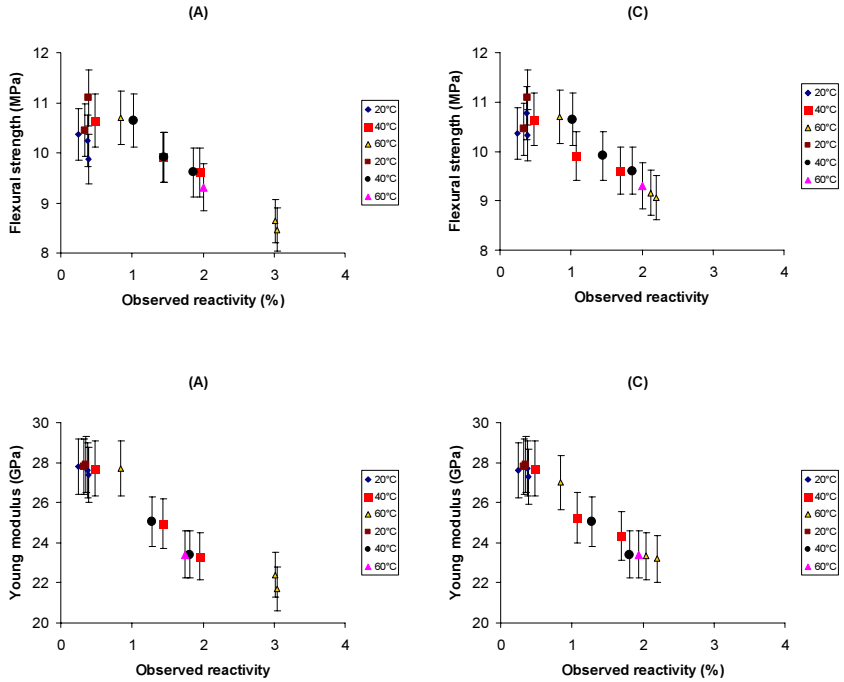

Figure 8: Residual Mortar Flexural strength vs. observed reactivity and Young's modulus vs. observed reactivity (different temperatures and both alkaline level 0.8% and 1.2% Na_2O_{eq})

The figure 9 presented the variation of the tensile strength of concrete vs. the reactive degrees.

A similar correspondence to the results of flexural strength and young's modulus in mortar was observed in the tensile strengths of concrete specimens. When the observed reactivity did not exceed 0.3%, the gels did not weaken the concrete or mortars.

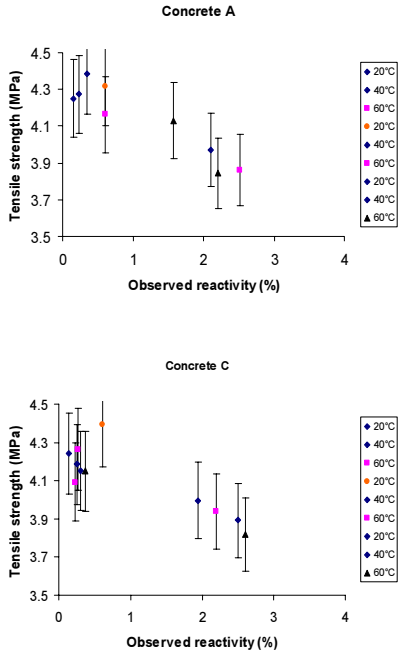

Figure 9: Residual Concrete tensile strength vs. observed reactivity (different temperatures and all alkaline level 0.4, 0.8% and 1.2% Na_2O_{eq})

At increased reaction degrees, reactive concretes A and C exhibited a reduction in tensile strength.

Thus while ASR had little effect on compressive strength, the effect was more severe on the other mechanical properties.

5. Summary

In general, the effect of ASR on the mechanical properties of concrete and mortars can be summarised as follows. Concrete and mortars specimens containing high amount of alkaline solution exposed at different temperatures showed small reduction in compressive strength, but showed high reduction in the modulus of elasticity. For similar specimens containing the moderate alkaline content, the reduction in the mechanical properties was much less.

Concrete and mortar specimens containing reactive aggregate with low alkaline content showed a much smaller reduction in modulus of elasticity than mortars and concrete containing high alkali content. This is attributed to the kinetics of the reaction that increases with the increase of alkaline content. Moreover, the lack of alkali in some cases reduces the mobility of aggressive agents. In addition, the secondary alkaline addition, provided to the mix by the NaOH, chemically brings the alkalis that otherwise may be available to initiate ASR. The following specific conclusions can be derived from the experimental investigations:

- The effects of ASR on the mechanical properties of low alkali concrete were minimal nevertheless some expansion was observed. The superior performance of low alkali content concrete can be explained by the lack of alkalis and may be a leaching process happening when placed into water solution so a micro-structure poor in alkali that resulted from the dissolution reaction in the cement paste
- In general, mortar bar specimens containing highly alkali content experienced a greater loss of mechanical properties than did mortar bars containing less alkali content.
- The tensile strength at high temperature of concrete containing the highly alkali content decreased by 20% while the modulus of elasticity decreased by 25%. For concrete containing the less alkali content, the ultimate tensile strength remained almost constant (5% of lost), while a decrease in modulus of elasticity of 7% was recorded.
- The flexural strength of both mortars containing the high alkali content was found to be very sensitive to the effects of ASR. The flexural strength of the both mortars containing the highly and lower alkali content 1.2% and 0.8% Na_2O_{eq} respectively decreased by 24%, and 18%, respectively .
- It has been shown in the previous researches Swamy (Swamy R.N 1986; Al-Asali 1988; Hobbs 1988; Ono K 1990; Swamy R.N 1992; Monette L.J 2000)that the effect of ASR on the compressive strength of concrete is a function of time. Nevertheless it has been found that the compressive strength decreases slowly as damage due to the reaction increases at the micro-structural level. Many researchers reported that the loss in compressive

strength is not that significant for low reactive aggregates and the reduction observed is less than 20 % being likely to occur for expansions found in practice. The losses in compressive strength from each experiment depended greatly on several parameters, such as mix design, aggregate type, and storage conditions; none of which have been duplicated in the earlier studies. However, the general trends observed are applicable. The effect of ASR on the compressive strength of concrete specimens was negligible. The compressive strength of specimens containing the high alkali content at high temperatures experienced a small decrease.

6. References

Al-Asali, S. a. (1988). "Engineering properties of concrete affected by alkali silica reactions." ACI materials Journal: pp367-374.

Hobbs, D. W. (1988). "Alcali-silica reaction in concrete." Thomas Telford, London: 183pages.

Monette L.J, G. N. J., Grattan-Bellew P.E, (2000). "Structural effects of the alkali aggregate reactions on non-loaded and loaded reinforced concrete beams." 11th international conference on alkali aggregate reaction: pp999-1008.

Ono K (1990). "strength and stiffness of alkali silica reaction concrete and concrete members." structural engineering review **2**: pp121-125.

Swamy R.N (1992). "testing for alkali-silica reaction in concrete." the alkali silica reaction in concrete ed R N Swamy , Blackie, Van Nostrand Reinhold: pp54-95.

Swamy R.N, a. A.-A. M. M. (1986). "influence of Alkali silica reaction on the engineering properties of concrete." Alkalis in concrete, ASTM STP 930, Ed, V.H. Dodson, American society for testinfg and materials Journal, Philadelphia: pp69-86.

Chapter 6: Modelling of ASR

1. Introduction

Models are very useful to reproduce and predict long-period behaviour of concrete under ASR conditions. The problem is very complex, influenced by many factors. This makes it impossible to make realistic predictions solely by intuitive reasoning based on the present qualitative knowledge of the ASR chemistry. The factors that are important under various circumstances, and those that are not, cannot be sorted out without a comprehensive mathematical model. Such a model seems to be unavailable at present. Its simplified formulation was taken as the objective of this study.

In order to built a comprehensive model, two basic problems treated in the modelling were proposed here

- The modelling of the mechanical damage to concrete, using micromechanical model to understand the effect of aggregate content on reactivity and expansion curves presented in this chapter.
- The modelling of the kinetics of the chemical and diffusion processes involved using a basic diffusion model presented in appendix 2

In this chapter we present a literature survey of the different theory of existing modelling followed by the proposed micromechanical approach and its details. The details of the literature survey of modelling and the constitutive equations are given in the appendix 1 Literature survey of modelling approaches

2. Literature survey of modelling

2.1. Introduction

ASR is complex problem involving physical, chemical and mechanical aspects of long term behaviour of cementituous material. Many approaches coupling the chemistry to the mechanics derived either from chemistry, physics or mathematical ways have been used to better understand the ASR mechanism.

Macroscopic modelling of ASR has been studied by a lot of authors and different approaches are reported (Moranville M 1997; Lemarchand 2002).

To describe the AAR modelling of concrete, we will try to divide them in groups of chemical modelling, micromechanical modelling and macromechanical modelling.

2.2. The chemical modelling

These models try to predict the kinetics of the reaction and the expansion. It concerns mainly:

- Reaction mechanisms: diffusion of alkalis and permeation of gel.
- Approaches with a R.V.E (Representative Volume Element) in a spherical form
- Mechanical aspects simplified

In these models we can include the following models: Sellier, Xi, Bazant, Umoto, Suwito, here we present the basics of this approach.

2.2.1. Sellier model

The modelling suggested by Sellier (Sellier. 1995) consists of two parts. The first models the mechanisms of the reaction (chemical reactions and diffusion of the species), the second describes the mechanical effects induced by expansion of gel. These two parts use probabilistic concepts.

The various assumptions are as follows:

- The aggregates are supposed to be spherical, homogeneous and all of the same diameter;
- The ions Na+ and K+ are supposed to have the same effect, they are interchangeable in the model;
- The attack is uniform on the surface of the aggregates.

Gel is formed at the surface contact of the reactive aggregate; it can then migrate in the connected porosity of the cement paste surrounding the aggregate. The pressure generated is supposed to open and to propagate cracks in mode I. The cracks created constitute a new place for expansion for gel. The author modelled the porous distribution by a lognormal statistical distribution which it fixed according to experimental values. That enables him to connect the pressure in the gel to the concerned pore radius.

2.2.2. Uomoto model

The model suggested by Uomoto et al. (Uomoto, Furusawa et al. 1992) allows the kinetics and the amplitude of the swellings generated by the reaction alkali-silica to be predicted. The reactional mechanisms retained for this model are:

- Diffusion of alkaline in the reactive aggregates;
- Reactive silica reacts with alkaline ions;
- Formation of products around the aggregates.

The constitutive assumptions of the model are:

- The aggregates are spherical and entirely consist of reactive silica;
- Existence of a porous zone surrounding the aggregates in which the products are formed;
- The layer of gel surrounding the aggregates is fine compared to the diameter of the aggregates and its thickness is uniform;
- The diffusion of alkalis in the aggregates is the limiting stage of the process.

2.2.3. Model of Suwito and Suwito, Xi

Suwito (Suwito A. 2002) presented a model which characterises the effects of various influential parameters on the pessimum size effect of ASR expansion. As in chemoelasticity, the model emphasises the coupling of the chemistry and the mechanical behaviour in the expansion process the chemical part of the model includes two opposing diffusion processes, one is the diffusion of the ions from the pore solution into the aggregate and the other is the permeation of ASR gel from the aggregate surface into the surrounding cement matrix. The mechanical part is developed based on a modified version of the self-consistent theory. The ASR gel is divided in two parts:the gel directly deposited in the interface pores and the gel directly permeated into the surrounding paste. The amount and the rate of the permeation depends on the aggregate size and the porosity of the cement paste.

Xi and Suwito proposed a two stage diffusion model. First there is ion diffusion from the cement paste into the aggregate governed by where ion concentration present in the pore inside aggregate, the diffusivity and ion permeability of the aggregate are the most important factors, the gel

concentration around the aggregate, depends on the concrete porosity. ASR is assumed to initiate when the concentration in ions reaches a critical concentration, the corresponding volume of reacted aggregates is then determined, and the corresponding amount of gel is finally obtained from the reaction level reached

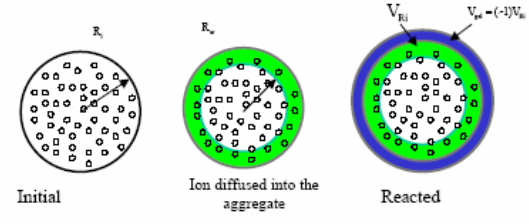

Figure 1. Ion diffusion from cement to aggregate

In a second phase, the gel permeates from the aggregate into the cement paste. First it fills up the interface zone (ITZ) of the aggregate. When the pores are filled, a pressure will be exerted on the cement paste resulting in an interfacial pressure governed by gel permeation, concentration and viscosity.

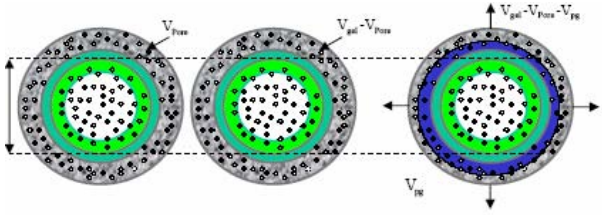

Figure 2 : Gel diffusion into cement matrix

In general and according to the authors the isotropic expansion caused by ASR can be simulated by the thermal expansion of an inclusion in a composite. Thus the total expansive strain of concrete can be determined using the models developed for effective thermal expansion of composites such as the thermoelastic model developed by Levin (Levin V M. 1967)which needs the effective bulk modulus developed by Hashin (Hashin Z. 1962).

The basic material is a composite spherical material with one constituent phase associated with another. The central phase is the aggregate and the outside layer is the cement paste. the same idea was used by Herve (Herve E. 1993) and Xi (Xi Y. 1997)

The configuration of the basic elements can also be used to model heterogeneous multiphase composite materials. Which means that there could be multiple layers outside of the center sphere as reported(Herve E. 1993; Xi Y. 1997).

The thickness of the gel layer formed at the aggregate surface is constant and not proportional to the size of the aggregate. This means if they consider the gel as a different phase they will have different fractions of the gel phase for different aggregate sizes.

The element can be considered equivalent to a 3 phase layers element.

In this model the concrete and all constituents are treated as elastic materials. That means that this model can be only applied for predicting the behaviour with moderate expansion due to ASR.

2.2.4. Bazant model

Bazant (Bazant Z. P. 2000) investigated the mathematical modelling of the kinetics of the alkali-silica reaction. The two basic problems that the model was designed to solve are:

- The modelling of the kinetics of the chemical of diffusional processes
- The modelling of the mechanical damage of the concrete which calls for fracture mechanics.

The mathematical model for diffusion of alkali is based to the assumption of similarity of diffusion between alkali and all the other processes of diffusion, e.g. moisture.

The process of micro-diffusion is described by Fick's law.

The ASR process takes place within the surface layer of each aggregate particle, when ionic concentrations reach a certain concentration level.

The mathematical equation describing the peremation of ASR gel is taken in account

Then the diffusion of the gel is conducted and characterised by a Darcy's law for a viscous flow.

Because the gel is expelled into the pores the geometry of diffusion is no longer spherical

It is difficult to choose any particular idealized geometry of the diffusion flow of water that should be analysed

2.3. Micromechanical modelling

These models try to link the kinetics to 2 levels micro and meso levels. It consists in the superposing the particles solid and fluid

Hypo: mean pressure in the samples

Effect of the microstructure through the porosity

The chemical effect are almost ignored

It uses the chemo-poro-mechanics

In this part we found some models like the one of lemarchand, dormieux Ulm and Coussy, Nielsen

Here a presentation of some of these models

2.3.1. Nielsen Model

This model (Nielsen, Gottfredsen et al. 1993) proposes to calculate the stresses and the strains induced by the expansion of a single spherical reactive aggregate in a representative elementary volume. Expansion is due to ions and water diffusion into aggregate (Chatterji (1989),), that generates cracks in the mortar and thus the expansion of the concrete. The cracks are supposed to be radial. The kinetics of swelling are the input datum of the model.

The influence of the external loading is taken into account. This model does not predict the internal expansion generated by the reaction, but the macroscopic consequence of this internal expansion. This last is an entry of the model and not a result. Expansion is directly connected to the relative humidity in the pores. The calculation of the constraints and the deformations is thus coupled with a hydrous calculation. The model makes it possible to highlight the great importance of the hydrous transfers expansion and the constraints generated by the reaction. It takes into account one reactive aggregate.

2.3.2. The chemo-elastic modelling

In order to account for the local information due to the ASR, Ulm (Lemarchand 2002) proposed a micromechanical interpretation of these deleterious phenomena. The analysis focuses on the mechanical consequences in macroscopic stress free situation. They showed that the macroscopic strain is related to the gel mass increase, i.e. the volume of gel exceeds the initial connected pore space through a chemo-elastic coefficient which takes the gel

into account. Analytical solutions for the chemo-elastic coefficient are made for both mechanisms.

In their model, a uniform distribution of the gel due to the consideration of other researchers is assumed. Indeed the gel diffuses from the reaction site at the aggregate pore solution interface through the connected porosity suggesting a poromechanical approach. An elastic behaviour of the solid matrix is assumed.

They considered incompressible and compressible gel. The gel was considered incompressible, the gel pressure the swelling strain are linear functions of the non dimensional gel mass increase.

From a micromechanical point of view, concrete is a composite material in which aggregates and cracks that develop in the contact of the aggregates are embedded in a connected cement paste matrix. It is assumed that the gel does not invade the porosity of the cement paste but is trapped in cracks.

In a first morphological approximation mesocracks and aggregates are regarded as distinct elements. The mesocracks are modelled as oblate spheroids. The approach is restricted to the situation of gel saturing the available porosity. The filling process is addressed by other researches (Lemarchand 2001; Lemarchand Submitted)) as given by the authors.

The equations of the volume of mesocracks and macroscopic strain in the gel yield a linear relation between the macroscopic strain and the relative gel mass increase, which also takes a pressure exerted by the fluid saturating the connected porosity of the cement paste

In summary, the micromechanical approach provides an estimate of the chemoelastic coupling tensor for the considered process in one crack family. Combining the pressure state equation and the uniform distribution of the gel through the porosity yields to a linear relation between the stress-free macroscopic strain and the gel relative mass increase

2.3.3. Chemo-plasticity modelling

Multiple models have been proposed to model the ASR induced concrete swelling at material level(Moranville M 1997), a thermo-chemo-elastic modelling was proposed by Larive (Larive C 1996)and applied to a calculation of concrete gravity dam with the concrete as a reactive porous medium subjected to an internal Chemical-mechanical coupling (Li K. and O. Coussy 2002).

Li and Coussy (Li K. and O. Coussy 2002) presented a new approach to link the micro and macro-modelling using a chemo-elasto-plastic model.

Supposing the concrete as a closed reactive elastic media, the AAR is simplified by a reaction $A \rightarrow B$. The thermodynamics of the system permits to identify a normalised irreversible reaction as its chemical state variable.

The state variable of this chemical-mechanical system are the material strain, an external variable and a global reaction expansion extent, an internal variable.

The materials irreversible strain is supposed to be only induced only by autogeneous tension.

The above chemo-elastic model can be extended to a chemo-plastic by introducing a local irreversible strain.

By three-dimensional application of this modelling it is proved that the observed stress induced anisotropy of ASR is well induced according to Li and Coussy (Li K. and O. Coussy 2002)due to the coupling between the plastic porosity and the chemical swelling (Peterson M G. 2000).

2.4. Macromechanical modelling

This modelling presents only the mechanical consequences due to ASR. It relates the expansion due to ASR to humidity temperature and stresses, etc..

Here we can also introduce the elsatoplastic models and chemoplastic ones and the damage models. We found some models as Léger, Coussy, Ulm and Capra.

2.4.1. Capra model

Other researchers investigated the modelling of the induced mechanical effects of AAR(Capra B. 1998), (Capra B. 2002). In this kind of modelling and due to the complexity of AAR modelling (random distribution of reactive sites and imperfect knowledge of the chemistry of the reaction), a new approach using fracture mechanics and probabilities to describe the swelling of the structure subjected to ASR is used, the coupling between AAR and mechanics makes it possible to simulate tests carried out on concrete specimens.

The authors first identify moisture, temperature, stress, and reaction kinetics as the major parameters controlling ASR evolution. A probabilistic model is adopted for the crack opening which is related to concrete damage. All of this results in an orthotropic decreasing of the elastic properties of concrete and the

residual swelling under the combined effects of AAR and mechanical load. An orthotropic damage theory is adopted for concrete in terms of a damage parameter "d" defined as the ratio between the surface of the discontinuities (voids, cracks) and the total specimen surface.

The volume of the cracks occupied by AAR, is supposed to be proportional to the total volume of cracked concrete, On the other hand the volume of pores accessible is assumed to be proportional to the initial porosity.

The approach used to describe the concrete behaviour is based on a phenomenological approach that is based on the a physical description of deterioration of concrete by creation of surface area discontinuities. Numerous theoretical approaches are proposed further to model cracking, the most widely accepted being probably damage mechanics (Fichant S. 1997)and (Mazars J. 1990), fracture mechanics(Tandon S. 1995; Bazant Z. P. 1998)and plasticity (Feenstra P. H. 1995).

The model used in this study can be classified within the general framework of anisotropy damage mechanics with reproduction of inelastic strains. The cracks are assumed to initiate and to propagate in Mode I and consequently bulk collapse and crack propagation in mode II or III are not described. The elastic part of the behaviour law of concrete is based on damage theory as described by Lemaitre (Lemaitre J. 1988)

The inelastic crack opening due to AAR evolves in an asymptotic way when cracking becomes significant.

2.5. Discussions

The models present in the literature can be separate in 2 distinct classes. "chemical" models and "phenomenologic" models. The first are based on probable reactional mechanisms to predict the evolution of the ionic species in material and the advancement of the reaction. They characterize the reaction at the local level (microscopic) and expansion on the level of material.

The seconds base themselves on physical phenomena observed in experiments to describe the evolution of expansion (or of the generated stresses) induced by the reaction according to observable data (loading, temperature, relative humidity...) without knowing the origin of it. They are coupled with models of behaviour and have the role the evaluation of the structural effects of the reaction on real works.

The "chemical" models are reduced all to the study of a V.E.R. by means of adequate assumptions (spherical aggregates, homogeneity and isotropy of materials and reaction, statistically homogeneous distribution of the aggregates). The reactional mechanisms described in these models are very similar. These reactional mechanisms are based on experiments performed on opal and highly reactive aggregates. These aggregates are not of common use in structures. The reaction products of ASR are hydrous gels whose chemical composition includes silica from the reactive aggregates. The damage in concrete is associated with expansion and cracking that occurs when the reaction products absorb water and swell.

The reaction may occur at the paste-aggregate interface. This is true in case of very reactive aggregates, waste glasses for example. However, the mineralogy of slow reacting aggregates is usually complex. The reactive parts are embedded in non-reactive phases. This morphology leads to the formation of swelling gel in a rigid matrix which causes the expansion and the fracture of the aggregates.

Microstructural modification of concrete materials is the most important cause of changes in their strength. The widely used technique is the homogenisation.

The mechanical properties of alkali aggregate affected concrete composites are impaired. In particular, Young's moduli and flexural strength of the material are significantly decreased with the advancement of ASR. Especially, aggregates that are the main constituent of concrete have relatively poor mechanical properties over the time of the ASR process.

These observations are consistent with the formation of cracks in the aggregates. In this chapter a simple micromechanical model is presented based on aggregates concentration and characteristics. The connection between cracked aggregates and matrix make the geometrical modelling of cementitious composites very difficult. The situation is even worse for stress analyses and/or damage modelling. Very few studies have been reported on modelling of damaged and cracked aggregate, and, as a result, the failure mechanisms of concrete due to the cracking process of this component are still not well understood.

A purely macroscopic approach cannot provide answers to these problems. However, the physical mechanisms at the origin of the non-linear relation between reaction degree and expansion can be integrated in a micro-mechanical

approach. The soundness of the basic physical mechanisms introduced in the modelling can be evaluated with respect to experimental results. Moreover, the theory suggests experimental routes to be explored.

In this work, we explore the hypothesis that the non-linear response of the concrete is entirely due to the existence of a network of micro-cracks in the aggregate phase. The progressive opening of cracks generated by the ASR gel expansion is viewed to control the material non-linearity. The discussion is mainly focused on the existence and propagation of these cracks and on the consequences of such a generation on expansion.

Because of the highly complexity of the phenomenon and cracking process induced, their mechanical properties are very difficult to characterise either experimentally or analytically. This necessitates approximations and simplifications of various kinds in their modelling.

3. Aggregate content effect on ASR expansion

3.1. Aggregate characterisation

Table 1 presents the mechanical properties (tensile strength and the modulus of elasticity) of the various non-immersed (immersion time=0) aggregates in two orthogonal directions. Aggregate A presents a strong anisotropy (factor of 8 and 5 respectively for the modulus and the strength) whereas the aggregates B and C can be regarded as being isotropic.

Table 1: Mechanical properties of aggregates

	Aggregate A		Aggregate B		Aggregate C	
	LD	TD	LD	TD	LD	TD
σ_c (MPa)	10	1.2	11.2	10.9	11.2	10.3
E (GPa)	59.7	11	67.9	64.5	61.9	58.9

LD: longitudinal direction, TD: transverse section.

The fracture characteristics of the aggregate are given in the appendix 3

3.2. Experimental observations

Besides alkaline content and temperature, it was shown in the chapter 4 that the mix design of the concrete also strongly affects the expansion level of the mortar or concrete. Considering the high cost of cement compared to

aggregates, it is of general interest in structures like dams to keep the amount of cement used in concrete to a minimum without compromising the development of mechanical properties.

It is of considerable interest to be able to identify the effect of aggregate content on the expansion in order to extrapolate from laboratory samples to field concrete. In this section this effect is examined in more detail from the micromechanical viewpoint. In order to compare the expansion with different aggregate content, the expansions of concrete and mortar specimens were measured, and it was found that the specimens with the lower aggregate content have a faster rate of the expansion and a lower level of expansion for the same observed reactivity (degree of reaction) relative to the aggregate.

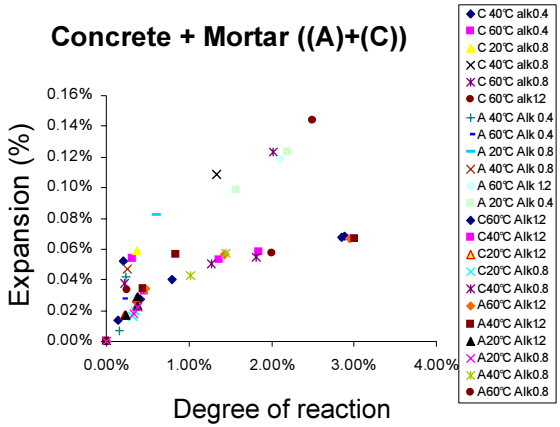

Figure 3: Difference of pattern and reaction level between mortar and concrete

The differences in the pattern of expansion level in mortar and concrete are illustrated in Figure 3. The expansion curves represent the response of the two mixtures to the reaction in the aggregates up to 3% degree of reaction. The data clearly shows higher expansion in the concrete than in the mortar samples. In the curves of expansion vs. time presented in the chapter 4, a higher rate of expansion in the mortars was noted, even at lower alkaline contents, due to the smaller size of aggregate present in the mixture.

The most significant feature is that though the rate of expansion in concretes was lower than mortars, the final expansions were higher. The lower rate of expansion is attributed to the diffusion of into the aggregates (appendix 2).

Such a process has been already reported in previous studies (Diamond and Thaulow 1974; D. W. Hobbs and Gutteridge 1979; Zhang, Wang et al. 1999)but not satisfactorily explained. The explanation proposed here is that differences in aggregate contents, coupled with differences in particle size distribution, lead to differences in diffusivity of alkaline products in aggregates. Needless to say such diffusion process is expected to be faster in small aggregates than in large ones, explaining thus the difference in the rates.

A micromechanical approach can explain the differences observed in the expansion level with the assumption that the expansion takes place only in the aggregates.

3.3. Micromechanical approach

3.3.1. Introduction

Micromechanics have the potential to solve many of the deficiencies of constitutive equations developed for particulate continua by incorporating information obtained from particle-scale measurements. The outstanding problem in applying micromechanics to particulate media is the projection scheme that relates the continuum variables to the particle scale variables which are subject to direct observation.

The influence of the aggregate volume concentration is proposed by Hobbs to illustrate and correlate the external deformation to the internal ones. The approach is based on an application of different parameters and the corresponding calculations are performed according analytically. Thus the model has as an objective to relate the different parameters as follows:

$$\langle \varepsilon \rangle = f(C_a, E_a, E_m, \langle \varepsilon_a \rangle, \langle \varepsilon_m \rangle)$$

Where E_m and E_a are respectively the young's modulus of the the matrix and the aggregates.

$\langle \varepsilon_m \rangle$ and $\langle \varepsilon_a \rangle$ are respectively the expansion of the matrix and the aggregates.

C_a is the volumetric concentration of aggregate present in the composite.

3.3.2. Hypothesis of Hobbs approach

In previous research (Hashin Z. 1962; Levin V M. 1967; Hobbs 1969; Hobbs 1971), expressions were derived for the bulk modulus, shrinkage, thermal contraction and thermal expansion of a two phase materials consisting of aggregates dispersed in a matrix , the expression for the overall bulk moduli:

$$k = k_m \left[1 + \frac{2C_a(k_a - k_m)}{(k_a + k_m) - C_a(k_a - k_m)} \right]$$

Where k , k_m and k_a are respectively the bulk modulus of the composite, the matrix and the aggregates.

It is assumed that the matrix and inclusions (aggregates in case of concrete) are homogeneous isotropic and behave in elastic manner, that the two phases fit perfectly and that the dispersion of aggregate in the matrix is uniform.

If an external stress is applied on the composite, and if the bulk moduli of the two phases present are not the same, a change in the stress distribution is introduced by the aggregate particles. The volumetric strain values are different for the aggregates and the matrix. It is assumed that the volume strain changes at the interface matrix-aggregate are the same for both matrix and aggregates.

$$V_m + dV_m = V_a + dV_a$$

Where $V_m + dV_m$ corresponds to the volumetric strain induced in the matrix and $V_a + dV_a$ is the volumetric strain induced in the aggregate.

The bulk moduli of the matrix, aggregate and composite can be expressed in terms of their Young's moduli and Poisson's ratios as follows:

$$k_m = \frac{E_m}{3(1-2\upsilon_m)} \text{ , } k_a = \frac{E_a}{3(1-2\upsilon_a)} \text{ and } k = \frac{E}{3(1-2\upsilon)}$$

E , E_m and E_a are respectively the young's modulus of the composite, the matrix and the aggregates.

υ , υ_m and υ_a are respectively the Poisson ratio of the composite, the matrix and the aggregates.

If we assume $\upsilon = \upsilon_m = \upsilon_a = 0.2$ which is the case generally of concrete, we obtain the simple model of Hashin (Hashin Z. 1962):

$$E = E_m \left[1 + \frac{2C_a(E_a - E_m)}{(E_a + E_m) - C_a(E_a - E_m)} \right]$$

If the volumetric strain expansion of the aggregate is greater than that of the matrix, then compressive stresses are induced in the matrix and tensile stresses in the aggregates.

In the case of thermal expansion the expression of the overall coefficient of thermal expansion of the composite is:

$$\alpha = \alpha_m - \frac{(\alpha_m - \alpha_a) C_a 2k_a}{k_m + k_a + C_a(k_a - k_m)}$$

And the induced stresses are:

$$\langle \sigma_m \rangle = \frac{3C_a k_m k_a (\alpha_m - \alpha_a)\tau}{k_m + k_a + C_a(k_a - k_m)}$$

and

$$\langle \sigma_a \rangle = \frac{3(C_a - 1) k_m k_a (\alpha_m - \alpha_a)\tau}{k_m + k_a + C_a(k_a - k_m)}$$

α , α_m and α_a are respectively the coefficient of thermal expansion of the composite, matrix and aggregates.

3.3.3. Application to ASR

$\langle \sigma_m \rangle$ is the average induced stress in the matrix and $\langle \sigma_a \rangle$ the stress induced in the aggregate particles. In free expansion and in the case of ASR balancing the stresses gives:

$$(1 - C_a)\langle \sigma_m \rangle + C_a \langle \sigma_a \rangle = 0$$

The averaged measured strain in the composite is given by the following expression:

$$\langle \varepsilon \rangle = \frac{\langle \sigma_m \rangle (1 - C_a)}{k_m} + \frac{\langle \sigma_a \rangle C_a}{k_a}$$

Where $\langle \varepsilon \rangle$ is the observed expansion.

An additional assumption is that the bulk moduli are independent of the volumetric expansion if no cracks occur in the samples, which is supposed up to an observed reactivity of 0.3%.

The induced stresses in the matrix and aggregates obtained from the equations given before are:

$$\langle \sigma_m \rangle = \frac{3C_a k_m k_a (\langle \varepsilon_m \rangle - \langle \varepsilon_a \rangle)}{k_m + k_a + C_a(k_a - k_m)}$$

and

$$\langle \sigma_a \rangle = \frac{3(C_a - 1)k_m k_a(\langle \varepsilon_m \rangle - \langle \varepsilon_a \rangle)}{k_m + k_a + C_a(k_a - k_m)}$$

The expansion of the composite per unit of volume then equals:

$$\langle \varepsilon \rangle = \langle \varepsilon_m \rangle - \frac{(\langle \varepsilon_m \rangle - \langle \varepsilon_a \rangle)C_a 2k_a}{k_m + k_a + C_a(k_a - k_m)}$$

Since it is known that $\langle \varepsilon_m \rangle = 0$ and ASR occurs only in aggregates, the observed expansion can be related to the expansion of aggregates due to alkali silica reactions by the relation:

$$\langle \varepsilon \rangle = \langle \varepsilon_a \rangle \frac{C_a 2k_a}{k_m + k_a + C_a(k_a - k_m)}$$

When we assume that the Poisson ratios of the composite and constituents are equal i.e. $\upsilon = \upsilon_m = \upsilon_a$, the following expression of the expansion which is function of the aggregate expansion and the Young's moduli is obtained:

$$\langle \varepsilon \rangle = \langle \varepsilon_a \rangle \frac{C_a 2E_a}{E_m + E_a + C_a(E_a - E_m)}$$

Therefore we can assume that the expansion is proportional to the aggregate volume C_a.

The values of the stresses show tensile stresses in the aggregates and compressive stresses on the matrix. It explains the observation" cracks are only observed in the aggregates in the first steps of the reactions, no cracks were observed in the matrix".

3.3.4. Model validation

The case of coupling between gel growth kinetics and mechanical response of the mortars and concrete can be modelled as follows:

Dispersed spherical gel growing by replacement of aggregate in a hydrostatically stressed elastic rock;

The formed gel is incompressible ($k_g = \infty$). Thus the volume of cracks product is related to the volume deformation of aggregates through this formula:

$$\langle \varepsilon_a \rangle_{vol} = \beta . \frac{V_{reac}}{V_a}$$

Where $\langle \varepsilon_a \rangle_{vol}$ is the volumetric deformation of the aggregate.

Where V_{reac} is the observed degree of damage (reaction) and V_a is the total volume of aggregates.

And β is a factor of filling of cracks and pores with created gel.

From that assumption the linear deformation is equal the to

$$\langle \varepsilon_a \rangle = \frac{1}{3} \beta \frac{V_{reac}}{V_a}$$

Where $\frac{V_{reac}}{V_a}$ corresponds to the reaction degree observed by microscopy.

This together with additional assumptions or knowledge about elastic properties of the aggregates and the matrix before cracking, provides refined estimates of the behaviour of a macroscopic volume element.

3.3.5. Application in the case of elasticity

Before cracking occurs we assume the elasticity case. All the pores created are filled with the gel. Thus the factor β is equal to 1. The linear deformation is thus equal to :

$$\langle \varepsilon_a \rangle = \frac{1}{3} \frac{V_{reac}}{V_a}$$

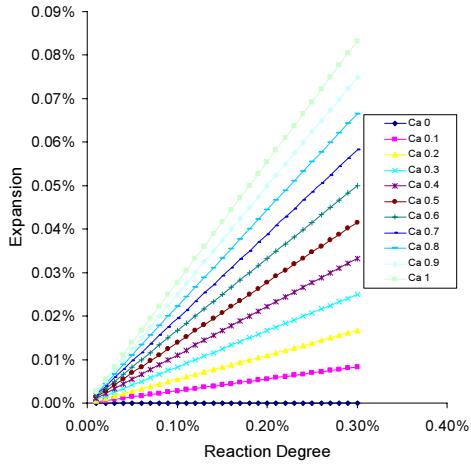

Figure 4: difference in expansion depending on different aggregate concentration C_a

Figure 4 shows in analytical way how the aggregate concentration influences the expansion. The assumptions taken for the calculation were:
A cement matrix of 14 GPa and aggregate Modulus of 60 GPa. We varied the concentration and we tried to evaluate the expansion depending on the aggregate concentration C_a

3.3.6. Application to our case of study

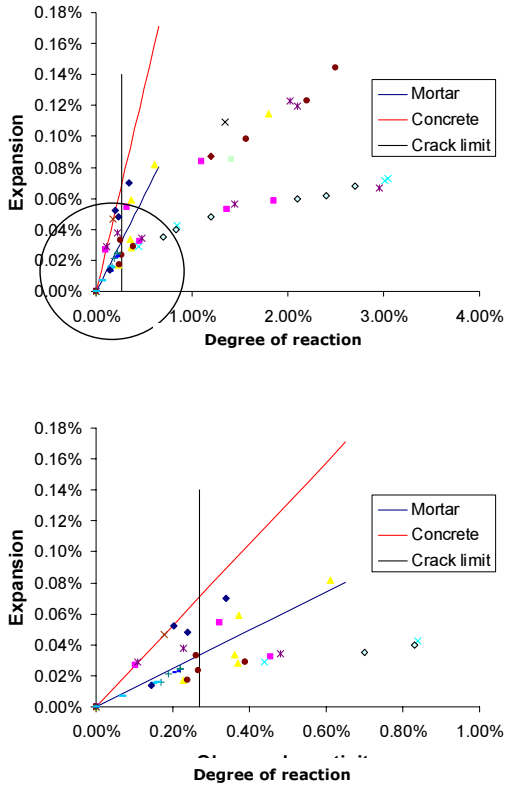

Figure 5: validation of the model in elasticity (up: all the data, down: zoom on the first part)

The Figure 5 shows the experimental and model results for the mortars and concrete subjected to ASR. The results show that the approach predicts well the expansion behaviour of the composite before cracking while it overpredicts the expansion from a certain point that corresponds to the appearance of cracks. This is consistent with hypothesis of elasticity of the model.

Thus, the model compares well quantitatively with the experimental data before crack occurs.

The integration of definition of damage in the model is required to further solidify and understand our findings. The integration of changes in Young's modulus during cracking in the composites and the overall consistency of their behaviour with analytical models would give better idea of the expansion behaviour of concrete and mortars after cracking.

3.3.7. Evaluation of young modulus of aggregates

The correlation between the expansion in aggregates and the global expansion measured depends on the Young's modulus of both aggregates and matrix. The Young's modulus after cracking has an important influence on expansion behaviour. So it is necessary to determine how it changes during crack propagation. We will try to estimate the Young's modulus of aggregates from the measurements obtained on the matrix using a Hashin-Hobbs approach. This approach allows the global characteristics of the aggregates inside the volume of concrete to be estimated and takes into account the variations of the randomly distributed crack density induced by the expansion.

If we suppose that crack orientation and size distribution are random with the size distribution being independent of orientation. From Hobbs approach we know that:

$$E = E_m\left[1+\frac{2C_a(E_a-E_m)}{(E_a+E_m)-C_a(E_a-E_m)}\right]$$

Where E is the measured Young's modulus of the composite.

E_m is the Young's modulus of the matrix: knowing that no cracks occurs within the matrix, this can be assumed constant as a first approximation.

C_a and E_a are the aggregate volume and the aggregate Young's modulus respectively.

From the previous expression we obtain

$$E_a = \frac{(1+C_a)E-(1-C_a)E_m}{(1+C_a)-(1-C_a)\dfrac{E}{E_m}}$$

Thus, given the Young's moduli of the composite vs. the observed reactivity, obtained using SEM-IA presented in chapter 5, the aggregate Young's modulus can be calculated.

3.3.8. Aggregate expansion in non-elasticity

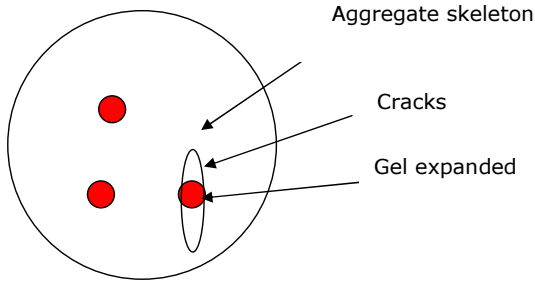

Figure 6: Expanded aggregate scheme

We assume that the expansion happens within the aggregates, but it is the formation of gel that expands the aggregates. The volume of gel is referred by the factor given before β.

The aggregate expansion is equal then to

$$\langle \varepsilon_a \rangle = \frac{1}{3}\beta \frac{V_{reac}}{V_a}$$

If we apply the same approach given before for the matrix and aggregates we can obtain the relation between the gel "expansion" and aggregate expansion,

The expansion is equal to:

$$\langle \varepsilon \rangle = \frac{1}{3}\beta \frac{V_{reac}}{V_a} \frac{C_a 2E_a}{E_m + E_a + C_a(E_a - E_m)}$$

We should notice here that $\beta \frac{V_{reac}}{V_a} \geq 0.3\%$, the limit of cracking found before.

Therefore we can assume that the expansion of the aggregates is related to the gel concentration volume C_{gel}.

3.3.9. Comparison of aggregate expansion

Experimentally obtained expansion data, for all mixes of mortars and concrete, was compared with calculations based on relations discussed above. Two different curves are observed for mortars and concretes. The curves first show a phase of accumulation of ASR products followed by the initiation of cracking. The expansion of the composites due to ASR products can be observed in Figure 7.a

As can be seen in Figure 7.b, the expansion related to the aggregate volume C_a using the micromechanical approach developed previously fits well the curve obtained using the experimental data sets on Mortars and concrete. The values obtained for the parameter C_a were used with the assumption that the Young's moduli of matrix remains constant (no cracks are observed in the matrix) and those of aggregates are calculated from the measured values on the composites at different degree of reactivity starting form the cracking point. For instance, though the values of gel pressures are not available, the relative expansion can be related to the expansion in aggregates due to the ASR gel product.

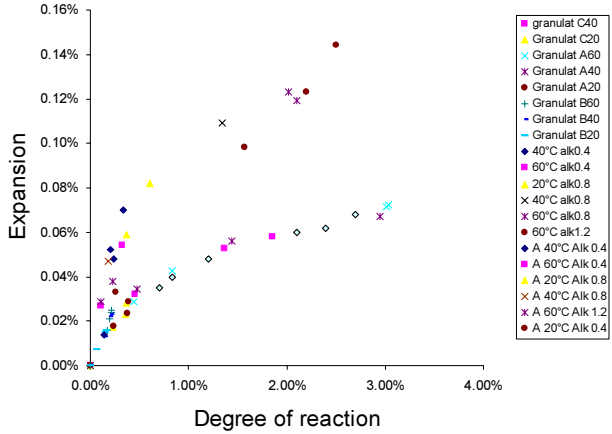

(a)

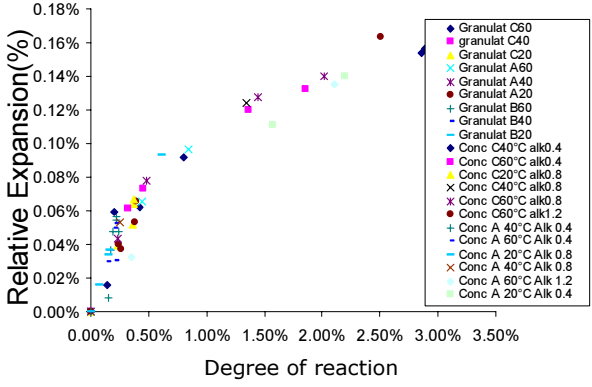

(b)

Figure 7: measured expansion (a) and relative expansion (b) (expansion in aggregates) vs. observed reactivity for all mixes (concrete and mortars with different alkalinity and at different temperatures

It can be seen in Figure 7.b that it was possible to obtain a good fit for the 2 different types of mixtures with the simple use of the parameter C_a. As mentioned above, this parameter is related to aggregate content of the mixtures. Thus, as the conditions of temperature and concentration only influence the kinetics of the reaction. The same reactivity in aggregate produces a predictable expansion of the composite. This strongly supports the hypotheses that the reaction happens within the aggregates. it should be also noted that as the reaction increases, the aggregate concentration C_a remains the same; the only thing that changes is the Young's moduli of aggregates which can be related, by simple homogenisation techniques, to the cracking process.

Another relevant result is the change in expansion observed at a reactivity of 0.3% corresponding to an expansion of 0.05-0.06 % in the aggregate that could be considered as the limit of elasticity of the aggregates. This agrees with the typical values given in the literature (Van Mier Jan G 1997).

3.3.10. Discussion

In the model presented here we deduce that the expansion in aggregates is the same in both mortars and concrete. The only difference lies in the final level of expansion measured for mortars and concrete with respect to the observed reactivity is related to the aggregate concentration C_a: the volume of aggregate present in the mix. The final relation is:

$$\langle \varepsilon \rangle = \langle \varepsilon_a \rangle \frac{2C_a k_a}{k_m + k_a + C_a(k_a - k_m)}$$

Where $\langle \varepsilon \rangle$ and $\langle \varepsilon_a \rangle$ are the global expansion measured on the samples and the aggregate expansion respectively. The k_m and k_a are the bulk moduli of the matrix and the aggregate respectively

It is shown that this equation is in good agreement with the results obtained from SEM-IA and expansion data. Examinations of the curves showed that the aggregate content has considerable influence on the expansion of the material. The stresses induced in the matrix and the aggregate confirm the localisation of cracking observed within the aggregates. This would be expected since, the cracking occurring mainly inside the aggregates, aggregate content influences the bulk moduli of the composite.

3.4. estimation of the effective moduli of aggregates

3.4.1. Principle of Averaging of a cracked poro-elastic medium

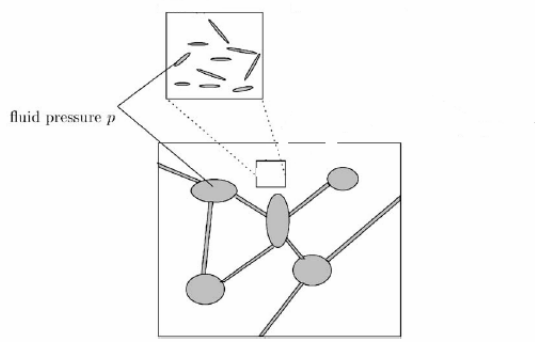

Figure 8 : Schematic view of a cracked aggregate with ASR gel filled microcracks

Different interpretations of the behaviour of fluid saturated elastic bodies have been proposed in the literature. A possible origin of non-linearity is based on the existence of microcracks in the solid phase. Indeed, suppose, in general, the porous phase is made up of a set of cracks and a network of connected pores. The total porosity c is the sum of the volume fractions of pores c_p and cracks c_c.

In rocks under ASR, the contribution of cracks to the total porosity is significant in the latest stages of reaction. Their effect on the overall response is more significant.

While the evolution of the state of cracks is an important factor in this model, the modifications of shape and volume fraction c_p of pores are very small for the range of mechanical loadings considered here; therefore these variations are neglected.

3.4.2. Evaluation of the effective Young moduli

2 cases are presented in this part which are: the case of dry cracks and the case of saturated cracks

Case of dry cracks

For the estimation of the effective moduli the approach given by Budiansky(Budiansky and O'connell 1976) is used as a basis.

Under the simplifying assumption that all the cracks are elliptic and have the same aspect ratio b/a, the different effective parameter are correlated from the initial parameter through these relation

$$\frac{\overline{K}}{K} = 1 - \frac{8\pi N \langle ab^2 \rangle (1-\overline{\nu}^2)}{9(1-2\overline{\nu})E(k)}$$

But note that the area A of a crack is πab, and its perimeter is $P = 4aE(k)$, so that the expression of the bulk moduli can be rewritten in its final form:

$$\frac{\overline{K}}{K} = 1 - \frac{16}{9}\left(\frac{1-\overline{\nu}^2}{1-2\overline{\nu}}\right)c$$

where the crack density parameter c is defined by

$$c = \frac{2N}{\pi}\left\langle \frac{A^2}{P} \right\rangle$$

With this choice for c the result of the ratio between the bulk moduli does not depend explicitly on b/a; also c reduces simply to $c = N\langle a^3 \rangle$ in the case of circular cracks (penny shape cracks). Further, it is clear that the result, with the definition of the crack density parameter, continues to hold for bodies containing elliptical cracks of various b/a, as long as their size and aspect-ratio are uncorrelated.

The crack density factor can be reduced in the case of plan observation (microscopic observation using image analysis) to $c' = N\langle a^2 \rangle$

The ratio of Young's moduls is given by

$$\frac{\overline{E}}{E} = 1 - \frac{16(1-\overline{\nu}^2)}{45}\left[3 + T(b/a, \overline{\nu})\right]c$$

For a given value of ν, the relation between $\overline{\nu}$ and c is determined by

$$c = \frac{45}{8}\frac{\nu - \overline{\nu}}{(1-\overline{\nu}^2)\left[2(1+3\nu) - (1-2\nu)T\right]}$$

Then, the variations of $\frac{\overline{K}}{K}$ and $\frac{\overline{E}}{E}$ with c follow directly from previous equations. It is useful to note that $\overline{\nu}$ is a decreasing function of c; that $T(b/a,0)=2$,

This vanishing of the moduli can be interpreted as a loss of coherence of the material that is produced by an intersecting crack network at the critical value of the crack density parameter.

Again for the penny shape case we have $b/a=1$, $T=4/(2-\overline{\nu})$ and as was said before the $c=N\langle a^3\rangle$

Then

$$\frac{\overline{E}}{E}=1-\frac{16}{45}(1+\overline{\nu})(5-4\overline{\nu})c$$

$$\frac{\overline{G}}{G}=1-\frac{32}{45}\frac{(1-\overline{\nu})(5-\overline{\nu})}{(2-\overline{\nu})}c$$

And

$$c=\frac{45}{8}\frac{(\nu-\overline{\nu})(2-\overline{\nu})}{(1-\overline{\nu}^2)\left[10\nu-\overline{\nu}(1+3\overline{\nu})\right]}$$

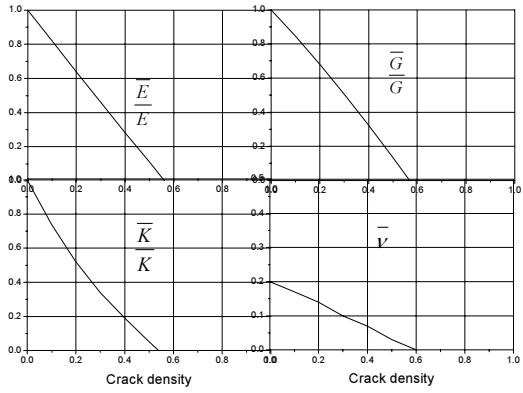

Figure 9a: Effective moduli dry penny shape cracks.

Case of saturated cracks

Cracks are fluid saturated. They sustain the same pressure p as pores. Therefore the micro-cracked matrix itself can be considered as a porous medium in which the porous phase is identified with the network of connected cracks. The geometry of cracks evolves during loading. It can be recalled that for non-connected cracks, the average stress σ in the homogenised matrix was assumed to be solely function of the strain ε :

For the estimation of the effective moduli the approach given by Budiansky(Budiansky and O'connell 1976) is used as a basis. The assumptions are the following:

We suppose the thin cracks contain a fluid. The mathematical assumption of a zero-thickness crack can no longer be assumed as easily as it was in the case of empty cracks. It is important to note here that a basic assumption in the calculations that follow is that the fluid in each crack is considered to be isolated. That is, the moduli to be calculated are appropriate for stress changes that occur with sufficient rapidity to prevent communication of pressure between cracks. This is the situation corresponds to elastic waves of sufficiently high frequency and is in contrast to other treatments that assume homogeneous fluid pressure throughout the body. To do the calculation, it is only necessary to modify the expression for the crack energy.

To simplify the expression of the solution of Budiansky (Budiansky and O'connell 1976) we suppose elliptic shapes of the cracks and those we can estimate

$$D = \left[1 + \frac{4}{3\pi} \left(\frac{K}{\overline{K}} \right) \left(\frac{1-\overline{\nu}^2}{1-2\overline{\nu}} \right) \omega \right]^{-1}$$

Where

$$\frac{\overline{K}}{K} = 1 - \frac{16}{9} \left(\frac{1-\overline{\nu}^2}{1-2\overline{\nu}} \right) Dc$$

$$\frac{\overline{E}}{E} = 1 - \frac{16(1-\overline{\nu}^2)}{45} \left[3D + T \right] c$$

And

$$\frac{\overline{G}}{G} = 1 - \frac{32}{45}(1-\overline{\nu})\left[D + \frac{3}{4}T\right]c$$

With fully saturated cracks we have $\omega = \infty$ thus $D = 0$

From the crack expression which is equal to

$$c = \frac{45}{8}\frac{\nu - \overline{\nu}}{(1-\overline{\nu}^2)\left[2D(1+3\nu) - (1-2\nu)T\right]}$$

So the expression will be just simplified to

$$c = -\frac{45}{8}\frac{\nu - \overline{\nu}}{(1-\overline{\nu}^2)(1-2\nu)T}$$

We can express T function of the crack c and the Poisson ratio ν

$$T = -\frac{45}{8}\frac{\nu - \overline{\nu}}{(1-\overline{\nu}^2)(1-2\nu)c}$$

The derivation of these results was approximate in the sense that the crack opening was imagined to be so small that the response of the material to pressure on the crack surface was assumed to be the same as that for perfectly flat cracks. In addition, no account was taken in the energy balance of the small strain energy associated with the solid material missing from the crack cavity.

Although the critical filled-cracks c are not too far apart from each other, they differ substantially from those for dry empty crack. This is not inconsistent with the view that cracks saturated with a "hard" "fluid gel" ($\omega = \infty$) should permit a larger crack density prior to loss of elastic coherence, Note also that for fluid filled cracks (with $\omega = \infty$) Poisson's ratio always increases to the limiting value $\overline{\nu} = 0.5$.

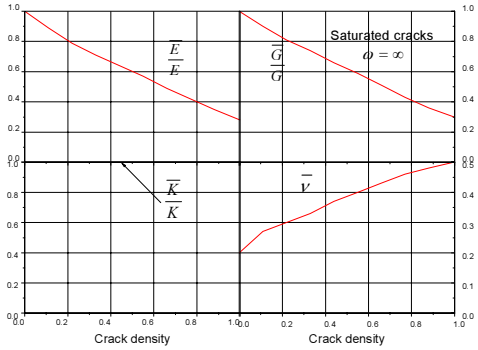

Figure 9b: Effective moduli; circular cracks saturated with "hard" fluid

3.5. Comparison of observed elastic moduli and calculated ones

In this part, the results of micromechanical the model are studied and compared with the observed data from the microscopical study and measured elastic moduli. With the model proposed by Budiansky (Budiansky and O'connell 1976) coupled to the approach proposed by Hobbs and applied for the calculation of the overall moduli of the material at different degrees of reaction, it is possible to study the behaviour of the material and compare it with a simple approach. The expansion is also related to the crack growth in the material.

As mentioned in the chapter 5, the dynamic method was selected to monitor the elastic moduli of the concrete and mortar. The corresponding moduli linked to each reactive degree were given in the previous chapter (Chapter 5).

It is observed that a large decrease in the Young's moduli occur in the mortar and concrete samples after a cracking within the aggregates. In Figure 10 and 11, the experimental Elastic moduli of the mortars are compared with those calculated by the micromechanical approach,. Based on the results, the elastic moduli for the aggregates at low crack density are very close to the simulated one given by the micromechanical approach.

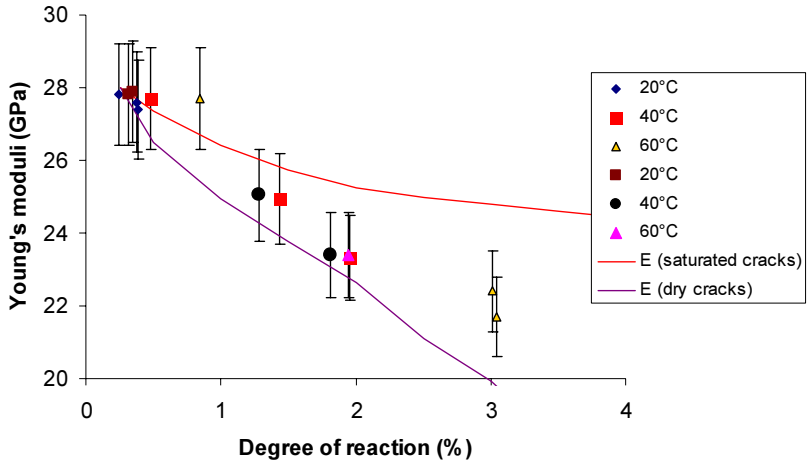

Figure 10: Comparison of observed elastic moduli and calculated ones based on the micromechanical approach applied to mortar A

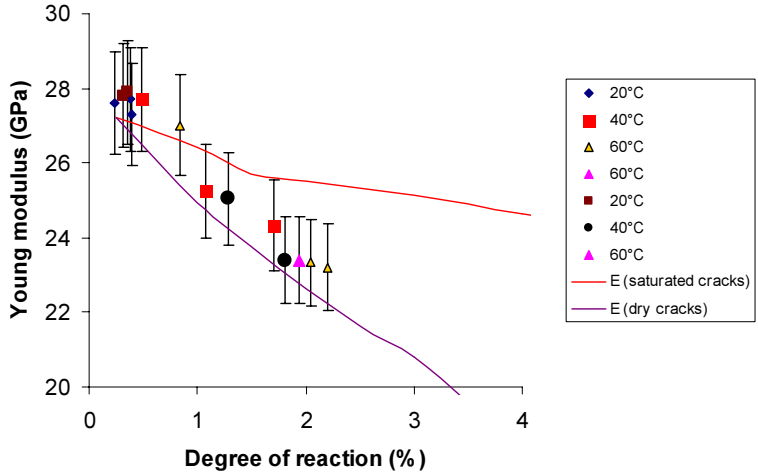

Figure 11: Comparison of observed elastic moduli and calculated ones based on the micromechanical approach applied to mortar C

Based on the obtained results, the micromechanical model can appropriately approximate the Young's moduli at starts of expansion and cracking. In this regard, the calculated Young's moduli in both mortars are around 26.5 GPa, which is very close to the observed one in. In addition, maximum values of Young's moduli are close to the simulated ones in comparison with non cracked case. The model overestimates the Young's moduli at higher observed reactivities however the errors remains less than 10% for both mortars.

The application of the Hashin-Hobbs model with dry cracks results in an underestimation of the elastic modulus. As seen, the values observed from the experiments are localized between the saturated and dry values which confirm that the experiments lie in the non-saturated zone. Though it can be concluded that for the prediction of the expansion, the degree of saturation β should be determined in order to obtain better prognosis of the expansion values, this approach needs further investigation. This degree of saturation will also affect the effective moduli of the cracked aggregates which will help to improve the modeling of ASR expansion effect.

3.6. Expansion of microbars

The observed expansion in the microbars can be compared to values calculated from the gel expansion values. It was seen in the experimental part that the values obtained for gel concentration were the same for the different aggregate concentrations. Using these experimental values, the aggregate expansion from one set of experiments was calculated (the C/A ratio = 2). This was then used to estimate the values of the expansion at lower aggregate density.

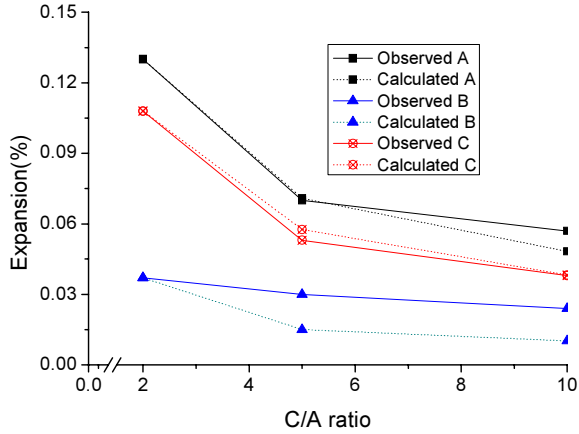

Figure 12: Comparison of observed expansion and calculated ones based on the micromechanical approach applied to microbars

As it is shown in the Figure 12, the micromechanical calculation reproduces well the expansion at the lower C/A ratios for both reactive aggregates. So the approach is applicable even for the lowest aggregate concentration. The non reactive aggregate B is underestimated in Figure 12. This is due mainly to the density of cracks and gel that differs from lower aggregate density to the highest one.

3.7. Discussion

The proposed model presents certain simplifications: The most obvious simplification is the assumption of homogeneous elastic parameters and porosity assigned to the matrix and aggregates (in reality the elastic properties would vary depending on physical discontinuities (e.g. crack density), and the porosity would depend on gel pressure).

The assumption of gel incompressibility can also be argued against, since preferential paths of fluid migration are present in aggregate porosity. Furthermore, the same values of expansion at different C/A ratio were assigned as expansion parameters for the different aggregate concentration. This

assumption does not seem to be a critical one since, even in an elastically layered medium, the displacement field must be continuous across layer boundaries and, in any case, the moduli depends on the crack density. Accordingly, it seems plausible that a suitable average rigidity can be employed to compute the deformation due to the ASR cracking process.

Accordingly, the observed expansion of the reactive system in microbars that happens within a short time can be plausibly triggered by high pressure of the gel formed within the aggregates. However, the possibility of some viscous behaviour of the cement matrix, leading to the shrinkage of the matrix, cannot be ruled out.

The poro-elastic expansion of the alkali silica reaction as the driving mechanism for the expansion within concrete has previously been suggested (Li K. and O. Coussy 2002), where the peculiar time history of the deformation field was reproduced for concretes at different temperatures. The present study shows that at early ages the microbar observations are also compatible with such an interpretation (elastic body) with a link to the microstructural disorder.

4. Cracks and their origins

4.1. Origin of the cracks in the aggregates

The reactive aggregates are unstable in cement environment conditions and in contact with alkalis and moisture they undergo an alteration. This chemical phenomenon results in the formation of gel which reacts with water to expand. The deterioration of the aggregates due to the expansion is irreversible. It leads to the formation of a microcracked zone around the gel clusters. These microscopic tension cracks are due to the increase in the volume of inclusion because of the expansion phenomena of the gel phases. These microcracks then develop under the coupled effect of the axial tensile stress within the aggregates and of gel production from the aggregates. The expansion rate of the ASR itself is linked to the evolution of the microcracked zone. Indeed, the local increase in porosity around gel inclusions promotes additional space for gel percolation and thus induces the deceleration of the process of expansion. These microcracks propagate by taking support on the coarsest grains, by changing direction or by dividing into new cracks. Their length can become very significant compared to the size of the inclusion that generates them and these cracks can reach the free

edges of the sample. It follows that a network of connected cracks can form in the areas where gel clusters exist. This phenomenon and the confined structure of normal aggregates "reactive particles embedded in non reactive ones" explain why we do not observe the same cracks on the highly reactive aggregates.

The induced stresses in the matrix and aggregates obtained from the equations given before are:

$$\langle \sigma_m \rangle = \frac{3D_a k_m k_a (\langle \varepsilon_m \rangle - \langle \varepsilon_a \rangle)}{k_m + k_a + D_a (k_a - k_m)}$$

And

$$\langle \sigma_a \rangle = \frac{3(D_a - 1) k_m k_a (\langle \varepsilon_m \rangle - \langle \varepsilon_a \rangle)}{k_m + k_a + D_a (k_a - k_m)}$$

The differences of the mechanical properties between the cementituous matrix and the aggregates induce significant concentrations and stress deviations that are probably at the origin of the damage. This damage results in a local increase in volume of the aggregates. The pressure of the newly formed phases produced by the ASR then leads to the propagation of a tensile fracture and, at the same time, the axial compressive stress on the matrix. This simple model showing the effect of aggregate density shows that, under the mechanical action of ASR gel expansion the induced stresses in the aggregates are tensile and in the matrix are of compressive nature.

Before the stress peak, there is a deterioration of the elastic properties related to the damage of the sample and since the rupture emerges through the formation of fractures, it would perhaps be necessary to establish a model based on a local approach of cracking. In any case, the principal interest of the models lies rather in their capacity to reproduce real behaviours, observed in situ.

Elastic and elastoplastic laws can be utilized to model the mechanical effects of the cementitious systems. However, it should be recalled that our goal is not to fit laws of behaviour on experimental curves. The laws used here remain well too simple to claim that we achieved this goal. Furthermore, we disregarded the bedded structure aggregates (the homogenisation technique is too simple and gives a mean of stress in matrix and aggregates and not at singular points). The tests performed here do not make it possible to measure mechanical parameters such as the gel pressure which could be directly integrated in a

phenomenological model. The obtained results must be interpreted by taking into account the sample's modest geometrical dimensions and the weak aggregate disorder to which it is subjected during the test. These two factors partly account for the evolution towards rupture on relatively low stress levels.

4.2. Origin of cracks in the surface

The storage or the exposure of the cementitious matrix to water was seen to suppress the pH by reducing the hydroxide content and thus alkaline content (Xu and Hooton 1993; Marc-André Bérubé 2002). Mass transport and release of hydroxide ions were decreased due to the consumption of hydroxide ions during the water transport of these ions outside of the structures or the samples. Within the structure two different zones appear one with normal concentrations of hydroxide and alkali ions and second that shows a decrease in ions content due to the dissolution during leaching.

Sufficient alkaline content provides a satisfactory medium for ASR with the presence of reactive aggregates. Occasionally, however, a combination of circumstances causes changes in the alkaline content, and as said before, leaching becomes the major factor affecting this content. Thus, the generated swelling is sometimes of such different magnitude that it, in turn, causes differential movements in a building, sometimes with disastrous results. This statement describes some of the common causes of concrete volume change and discusses the results that could take place due to volume change.

The physical dimensions, or volume, of coarse-aggregates in internal concrete are governed solely by internal loading stresses and external loads. In contrast to this and due to the lack of alkalis, the volume of aggregates on the surface does not govern internal stresses (ASR can not take place) but only by external stresses.

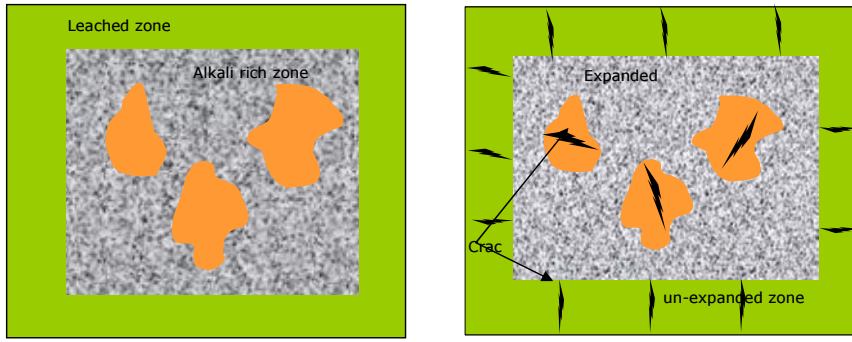

Figure 13: origin of the cracks in the surface of structures and samples

The internal stresses arise from physico-chemical forces which increase as the gel formation increases. A surface concrete which has long existed in an environment where abundant moisture has been available, will have small internal stresses and has little tendency to form gel. Aggregate expansion however, may induce internal stresses much greater than the stresses applied by external environment!

In humid areas concrete with lack of alkali contents and which have not previously been subjected to ASR gel formation will tend to shrink on loading more than they will tend to swell. Under other conditions, concrete that have been subjected to ASR conditions (abundance of alkalis) or previously subjected to higher gel formation may tend to swell greatly when allowed access to water under light loading. Their rate of swelling is governed by the rate at which alkali reaction can propagate into the aggregates, i.e., the permeability and diffusivity of the aggregate to water and alkalis. Because of small pore size and thus their low permeability; aggregates of concrete structures may take years to reach stress equilibrium conditions. This can explain the long dormancy period observed in concrete structures under loading.

The magnitude of expansion or shrinkage is dependent on the amount and type of aggregate minerals present, the previous stress history of the structure, the magnitude of expansion change from initial to final ASR conditions, and the thickness of the concrete affected in addition to elapsed time. Although concrete is a complex material, susceptible mixes can be identified and rates and

magnitude of volume change that can introduce cracking in the un-expanded region can be predicted.

5. Conclusion

In recent years, concrete has been treated as a two-phase composite material in the literature. Experimental studies and mechanical modelling have been conducted to evaluate the effect of each phase on the mechanical behaviour of the two-phase concrete. To understand the ASR expansion mechanism, a three-phase model is proposed in this paper. Despite simplifications between the proposed model and real concrete, it gives valuable insights into the real problem. The preliminary calculation results show that the proposed model can consider the elastic properties and cracks interactions between different volume fractions of each phase as expected. Based on the calculation results, the following conclusions are obtained:

- The aggregate phase has significant effects on the mechanical properties of affected concrete.
- In practice, coarse aggregate phase is one of the most important design variables. It was shown in that increasing the elastic modulus; enhancing volume fraction, decreasing the maximum grain size, and adopting fine reactive aggregates could have positive results with rapid consumption of the alkalis by fine as observed in diffusion part (Appendix 2).
- Although the theoretical analysis by the present model is qualitatively supported by a preliminary experimental study on cement composite, further and systematic experimental studies are needed in order for the proposed model to be applicable in practice.

6. References

Bazant Z. P., A. S. (2000). "Mathematical model for kinetics of alkali-silica reaction in concrete." Cement and concrete research 30: pp 419-428.

Bazant Z. P., P. J. (1998). "Fracture and size effect in concrete and otheer quasibrittle Materials." CRC Press.

Budiansky, B. and R. J. O'connell (1976). "Elastic moduli of a cracked solid." International Journal of Solids and Structures 12(2): 81-97.

Capra B., B. J.-P. (1998). "modelling of induced mechanical effects of alkali aggregate reactions." Cement and concrete research Vol 28(N°2): pp251-260.

Capra B., S. A. (2002). "modelling of alkali aggregate reaction:orthopic behaviour and numerical simulation." concrete science and engineering Vol 4(March 2002): pp56-70.

Chatterji ((1989),). "Mechanisms of alkali–silica reaction and expansion. ." In: K. Okada, S. Nishibayashi and M. Kawamura, Editors, Proceedings of the 8th International Conference on Alkali–Aggregate Reaction in Concrete, Kyoto (Japan): pp. 101–105.

D. W. Hobbs and W. A. Gutteridge (1979). particle size of aggregate and its influence upon the expansion caused by the alkali silica reaction. magazine of concrete research. Vol 31: 235-242.

Diamond, S. and N. Thaulow (1974). A study of expansion due to alkali -- silica reaction as conditioned by the grain size of the reactive aggregate. Cement and Concrete Research. 4: 591-607.

Feenstra P. H., D. B. R. (1995). "plasticity model and algorithm for model-I cracking in concrete." international journal for numerical methods in engineering 38 (15): pp2509-2529.

Fichant S., P.-C. G., and La Borderie C. (1997). "continuum damage modelling : approximation of crack induced anisotropy." mechanics research communications 24 (2): pp109-114.

Hashin Z. (1962). "the elastic moduli of heterogeneous materials." Journal of applied mechanics Transaction of ASME(March 1963): pp143-150.

Herve E., Z. A. (1993). "n-layered inclusion-based micromechanical modelling." international journal of engineering sciences 31(1): pp1-10.

Hobbs, D. W. (1969). Bulk modulus, shrinkage and thermal expansion of two phase material. Nature, Lond. Vol 222: 849-851.

Hobbs, D. W. (1971). the dependance of the bulk modulus, Young's Modulus, Creep, Shrinkage and Thermal expansion of concrete upon aggregate volume concentration. matériaux et constructions. Vol. 4: 107-114.

Larive C, C. O. (1996). "behaviour of AAR-affected concrete modelling." Proc 10th AAR Int conf Québec: pp662-669.

Lemaitre J., a. C. J. L. (1988). "mécanique des matériaux solides." Dunod Paris.

Lemarchand , D. L., Ulm F-J. (Submitted). "micromechanics of expansive reactions." Roy. Soc. Of London.

Lemarchand, E. (2001). "contribution de la micromécanique à l'étude des phénomènes de transport et de couplage poromécanique dans les grains poreux: application aux phénomènes de gonflement dans les géomatériaux." Ph D thesis Ecole nationale des ponts et chaussées.

Lemarchand, L. D. a. F., -J. Ulm (2002). "Elements of micromechanics of ASR-induced swelling in concrete structures." concrete science and engineering Vol 4(March 2002): pp12-22.

Levin V M. (1967). "thermal expansion coefficients of hetergeneous materials." mechanics of solids 2(1): pp58-61.

Li K. and O. Coussy (2002). "Concrete ASR degradation: from material modelling to structure assessment." concrete science and engineering Vol 4.(March 2002): pp35-46.

Marc-André Bérubé, J. D., J. F. Dorion and M. Rivest (2002). "Laboratory assessment of alkali contribution by aggregates to concrete and application to concrete structures affected by alkali–silica reactivity." Cement and Concrete Research Volume 32(Issue 8): pp1215-1227.

Mazars J., B. Y., and Ramtani (1990). "the unilateral behaviour of damaged concrete." Engineering Fracture Mechanics 35 (4): pp1669-1673.

Moranville M (1997). "modelling of expansion induced by ASR: new approaches." Cement and Concrete Composites 19: pp415-425.

Nielsen, A., F. Gottfredsen, et al. (1993). "Development of stresses in concrete structures with alkali-silica reactions." Materials and Structures, . Vol. 26,: pp. 152-158.

Peterson M G., a. U. F.-J. (2000). "chemoplasticity of the Alkali silica reaction in concrete: modelling of stress induced anisotropy." CEE report , R00-02, Massachusetts Institute of Technology, Boston.

Sellier., A. (1995). "Modélisations probabilistes du comportement de matériaux et de structures en génie civil." hèse de doctorat de l'Ecole Normale Supérieure de Cachan,: 150p.

Suwito A., J. W., Xi Y., Meyer C (2002). "a mathematical model for the pessimum size effect of ASR in concrete." cioncrete science and engineering Vol 4(March 2002): pp23-34.

Tandon S., F. K., bazant Z.P., Li Yuan (1995). "coehesive crack modelling of influence of sudden changes in loading rate on concrete fracture." Engineering Fracture Mechanics 52 (6): pp987-997.

Uomoto, T., Y. Furusawa, et al. (1992). " A simple kinetics based model for predicting alkali-silica reaction,." Proceedings of the 9th International Conference on Alkali-Aggregate Reaction in concrete London, England,: pp. 1077-1084,.

Van Mier Jan G (1997). "Fracture Processes of concrete." assessment of material parameters for fracture models(CRC Press): 448.

Xi Y., J. H. (1997). "shrinkage of cement paste and concrete modelled by a multiscale effective homogeneous theory." material structures 30: pp329-339.

Xu, Z. Z. and R. D. Hooton (1993). "Migration of Alkali Ions in Mortar Due to Several Mechanisms." Cement and Concrete Research 23(4): 951-961.

Zhang, C., A. Wang, et al. (1999). Influence of aggregate size and aggregate size grading on ASR expansion. Cement and Concrete Research. 29: 1393-1396.

Chapter 7: Conclusions and Perspectives

1. Conclusions

In this study a series of test was carried out on three different aggregates, of which two appeared reactive. Microbar tests at 150 °C as well as tests of free swelling on mortar bars and concrete were carried out at various temperatures (20, 40, 60 °C) with various alkalinities (0.4, 0.8, 1.2 %). Tests of strengths (compression, Flexure, direct tensile) and of modulus of elasticity were carried out for the various formulations. The main results obtained from this research were the following:

- The most significant outcome of this research was the establishment of the relation between aggregate reaction and observed expansion. This would be explained by micromechanical modelling. Despite various alkaline compositions and the different temperatures used during the study, the plotted curve of expansion vs. amount of reactive product was unique.
- A new method for quantitative measurement of the reaction degrees of ASR was proposed. The microscopic study showed the formation of silica gel inside the aggregates. This is due to the alkaline diffusion through the porosity of the aggregate to reactive sites. This method allows the active sites due to dissolution of reactive particles to be identified.
- From a simple micromechanical modelling, It was shown that the only difference in expansion level observed is due to the aggregate concentration used in the mix and that the expansion in the first stage can be related to the expansion in the aggregates. Thus, as the conditions (temperature and concentration) were the only variables that influence the kinetics of the reaction, no variation should be expected for the same reactivity in aggregate expansion. Low aggregate content with small aggregate size may result in less

expansion in the composite material. This can be used as proof for evidence to support the observation that the expansion happens within the aggregates. Note also that as the time increases, the only parameter that changes is the Young's modulus of aggregates which can be expressed in terms of cracking density through micromechanical modelling.

- Using this modelling we related the apparent expansion to the degree of reaction, more than to the reaction product properties "appearance of gel corresponds to aggregate expansion". ASR Gel formation causes significant expansion in the first steps of the reaction. All the later expansions can be predicted by changes due to gel formation and appearance of microcracks into the aggregates.
- The kinetics of ASR were affected by temperature and alkali content. The use of the expansion data and the data from SEM-IA technique allowed these dependences to be determined. The effect of temperature was described by the Arrhenius law. Simple regression models were sufficient to explain the variation in expansion with the temperature. The activation energy is equal to 42 $kJ.mol^{-1}$.
- The dependence of the expansion rate on the alkaline content exhibits a linear relation on a logarithmic scale. All the points at both temperature 20 and 40°C are located on parallel lines. The approximation by the least-square method has allowed a factor of 1.67 as slope of the linear curve to be obtained.
- The effect of ASR on the mechanical properties confirmed the losses in mechanical properties of reactive mortar and concrete (compressive, tensile and flexural strength as well as Young's modulus) corresponding with previously published research.
- It was demonstrated that the cracking process affected the Young modulus and the flexural strength of mortars. However, it is also interesting to determine whether the reactivity parameters are related to the bulk mechanical properties of the composite, such as its toughness, or friability/brittle fracture tendency. Based on this information, one could potentially make predictions on the reaction amounts, depending on the elastic properties of aggregates, which will impart favourable characteristics to mortars or concretes.

2. Future work

In the light of the results obtained and observations given above it is of primary importance to look further into the investigations; to be able on the one hand to verify the hypotheses put forth in this study, and on the other hand to explain the difference in certain experimental results with those obtained by other groups of research, also the application of the quantitative approach developed on cores taken on the existing dams.

2.1. Methodology verification

The applicability of the results obtained with the aggregates of this study to a wide range of other aggregates should be undertaken as a starting point for the future study. The application of this methodology to the cores obtained from dam construction is also an important point to be studied.

2.2. Stress effect

The existing studies relate only the influence of the axial compressive stress on the expansion. It is generally assumed that the stress does not influence directly the kinetics of the chemical reaction (there is decoupling).

The influence of the loading level (triaxial in the ideal case) on the degree of transfer (total or partial) and also on the microstructure (localisation and nature of the products) remains an open field of investigation at the same time on both samples in laboratories and dam cores.

2.3. Start and quantification of cracking

Cracking, intimately related to the microstructure, has an important effect that is on the level of the kinetics of the reaction (through the parameters of diffusion) or on the level of the mechanical behaviour.

Concerning the start of cracking process, opinions are divided between the appearance of micro cracking from the start of expansion or later, after a certain threshold of critical deformation. The determination of the starting point of cracking as well as the evolution of the crack density, the orientation of the cracks in terms of the advance of the reaction and apparent swelling would be of a great utility in the interpretation of the mechanical results.

2.4. Aggregate size effect

The influence of the aggregates is very important for the alkali-silica reaction. The expansion generated, the kinetics and the amplitude depend on their reactivity. The size of the aggregates has a great influence; it seems that the expansion obtained increases with the diameter of the reactive aggregates. However, contradictory results were obtained with opal (for which the expansion increases when the diameter decreases) and from the waste glass aggregates.

The granular distribution is important also. The extension of aggregate distribution to fines or the reactive fine addition makes possible the decrease of the expansion. Moreover, it appears that when two aggregate size ranges are mixed, resulting swelling is lower than the sum of their unit swellings. Tests on concretes of larger maximum diameter are necessary from the point of view of the application of methodology for the dam's concrete to validate the possible modelling.

2.5. ASR modelling

A first approach of modelling, relating the free expansion to the degree of the reaction (or the reactivity) and to the parameters of the composite materials was developed, through the micromechanical solution (chimico-poro-mechanics) of a problem of micro cracked inclusion, undergoing a pressure or an intrinsic deformation of chemical origin.

Results from the tests of concretes in the laboratory as of others taken in the literature will be used for the validation of the model. Parametric studies could then be carried out in order to study the influence of modelling with respect to the various parameters incorporated in the model in optics to optimise.

As a next step, and if the first validations of the model prove to be profitable, the mathematical model will be integrated in the numerical model which makes it possible to take into account the aggregate distribution, the sample size, a random microcracking and especially the interactions between inclusions and the microscopic cracks. In end, the consideration of a case study on the scale of the structure while based on the data which will be obtained in from dam concrete will be of a great help for the applicability of this study.

ASR Modelling: literature review

1. Introduction

ASR is complex problem involving physical, chemical and mechanical aspects of long term behaviour of cementituous material. Many mechanics approach coupling the chemistry to the mechanics are used to better understand the ASR mechanism. The modelling approaches are derived either from chemistry or physics or mathematical way.

Macroscopic modelling of ASR ahs been studied by a lot of authors (Charlwood R.G. 1992; Léger P. 1995)

To describe the AAR modelling of concrete, we will try to divide them in groups of mathematical modelling chemistry modelling and mechanical modelling.

2. The chemoelastic modelling

In order to account the local information due to the ASR, ((Lemarchand 2002) propose a micromechanical interpretation of these deleterious phenomena. The analysis focuses on the mechanical consequences of both the classical through solution and the topochemical mechanisms, in macroscopic stress free situation. They showed that the macroscopic strain is related to the gel mass increase, i.e. the volume of gel exceeds the initial connected pore space through a chemeoelastic coefficient which takes the gel into account. Analytical solutions for the chemeoelastic coefficient are e for both mechanisms.

In their model, they assumed an uniform distribution of the gel due to the consideration of other researchers. Indeed the gel diffuses from the reaction site at the aggregate pore solution interface through the connected porosity. So that distribution suggests a poromechanical approach. Assuming an elastic behaviour of the solid matrix, the poroelastic state equation:

$$\Sigma = \mathbb{C}^{hom} : E - p^g B \qquad (1)$$

$$p^g = M(-B : E + \Phi - \Phi_0) \qquad (2)$$

$$\frac{1}{M} = \delta : \mathbb{S}^s : (B - \Phi_0 \delta) \text{ where } \mathbb{S}^s = \mathbb{C}^{-1} \qquad (3)$$

where $\mathbb{C}^{hom}$ and B are the tensor homogenised elasticity in drained conditions and the tensorial Biot coefficient respectively. δ is the unit tensor of the second order. for an isotropic behaviour of both the solid matrix and the r.e.v(3) takes the classical form.

$$\begin{cases} p^g\left[\frac{p^g}{K^g}+1\right]\left[\frac{1}{M}+B:\mathbb{S}^{hom}:B\right]+\Phi_0\frac{p^g}{K^g}=\mu^g \\ \mu^g=\left\langle\frac{m^g}{\rho_0^g}-\Phi_0\right\rangle \end{cases} \quad (4)$$

If the gel was incompressible, the gel pressure p^g then and the swelling strain are a linear functions of the non dimensional gel mass increase μ^g.

In the other hand if the gel is compressible the following expression of the gel is obtained from (4)

$$p^g=\frac{K^g}{2}\left(\sqrt{\left(1+\frac{\Phi_0}{k}\right)^2+4\frac{\mu^g}{k}}\right)-\left(1+\frac{\Phi_0}{k}\right) \quad (5)$$

where $k=K^g\left[\frac{1}{M}+B:\mathbb{S}^{hom}:B\right]$

From a micromechanical point of view, concrete materials are composite materials in which aggregates and cracks that develop in the vicinity of the aggregates are embedded in a connected cement paste matrix. In their models they assumed that the gel does not invade the porosity of the cement paste but is trapped in cracks.

In a first morphological approximation mesocracks and aggregates are regarded as distinct element. For a pupose of simplicity , the compressibility of the gel was neglected. The mesocracks are modelled as oblate spheroids. The approach is restricted to the situation of gel saturing the available porosity. The filling process is addressed by(Lemarchand 2001) and ((Lemarchand , Submitted #3) as given by the authors of the article.

The volume fraction of a mesocracks or the Lagrangian is given by

$f_c=\frac{4}{3}\pi\omega\varepsilon$ where $\varepsilon=Na^3$ and N is the crack density (6)

the boundary conditions on $\partial\Omega$ of the Hashin type

$\xi(\underline{x})=E.\underline{x}$ (7)

This boundary condition ensures that both macroscopic strain and microscopic strain are kinematically compatible. Therefore the macroscopic strain is the volume average of the microscopic strain fields:

$$E=\langle\varepsilon(\underline{x})\rangle_\Omega=\frac{1}{\Omega}\int_\Omega\varepsilon(\underline{x})dV \quad (8)$$

the average $\langle A^D\rangle_i$ of the strain concentration tensor A over Ω_i can be estimated by(Zaoui A. 1997)

$$\left\langle A^D \right\rangle_i = \left(I + P_i : (\mathbb{C}^i - \mathbb{C}^0)\right)^{-1} \qquad (9)$$

the local strain (11) is then derived from (9) and (10) expressed by the following equations:

$$\varepsilon_i = \left\langle A^D \right\rangle_i : \left[E_0 - P_i : (\sigma_i^p - \sigma_0^p)\right] \text{ with } P_i = \mathbb{S}_i : \mathbb{S}^0 \qquad (10)$$

$$\begin{cases} \varepsilon_c = \left\langle A^D \right\rangle_c : \left[B : E + \left(f_c B : T_c - \mathbb{S}_c\right) : \mathbb{S}^m : \left(pb^m - p^g \delta\right)\right] \\ \varepsilon_m = B : \left[E + f_c T_c : \mathbb{S}^m : \left(pb^m - p^g \delta\right)\right] \text{with} \left\langle A^D \right\rangle_m = I \\ \varepsilon_I = \left\langle A^D \right\rangle_I : \left[B : E + \left(f_c B : T_c - \mathbb{S}_c\right) : \mathbb{S}^m : \left(pb^m - p^g \delta\right) - P_I : b^m\right] = 0 \end{cases} \qquad (11)$$

the equations of the volume of mesocracks and macroscopic strain in the gel yield a linear relation between the macroscopic strain and the relative gel mass increase , which also takes a pressure exerted by the fluid saturing the connected porosity of the cement paste

$$E^g = T^c \left[\mu_c^g + p\left(\frac{1}{N_c} - \beta_c : \mathbb{S}^{hom} : B\right)\right] + p\mathbb{S}^{hom} : B \qquad (12)$$

where T^c is the chemoelastic coupling tensor:

$$T_c = \left[\beta_c : \mathbb{S}^{hom} : B_c + \frac{1}{M_c}\right]^{-1} \mathbb{S}^{hom} : B_c \qquad (13)$$

In summary, the micromechanical approach provides an estimate of the chemoelastic coupling tensor T_c for the considered process in one crack family with the only knowledge of Elshelby's tensor $\mathbb{S}_c$ for ellipsoidal inclusions embedded in an elastic matrix.

Due to the connectivity between the two pore families (mesocracks and the whole connected porosity), the gel pressure is uniformly distributed in the whole porosity introducing this relation the macroscopic strain is then

$$\begin{cases} E^g = p^g \mathbb{S}^{hom} : \left(B_c + B\right) \\ f_c \, tr\varepsilon_c = \beta_c : E^g + \left(\frac{1}{M_c} + \frac{1}{N_c}\right) p^g \end{cases} \qquad (14)$$

combining the pressure state equation and the uniform distribution of the gel through the porosity yields to alinear relation between the stress-free macroscopic strain E^g and the relative mass increase μ_p^g :

$$E^g = T^p \mu_p^g \qquad (15)$$

where T^p is the free swelling chemoelastic coefficient associated with the pressurization of the gel saturing the whole connected porosity of the concrete.

3. Chemo-plasticity modelling

Multiple models have been proposed to model the ASR induced concrete swelling at material level(Moranville M 1997), a thermo-chemo-elastic modelling was proposed (Larive C 1996) and applied to a calculation of concrete gravity dam(Ulm F-J. 2000) with the concrete as a reactive porous medium subjected to an internal Chemical-mechanical coupling (Coussy O, 1995 #73.

(Li K. and O. Coussy 2002) presented a new approach to link between the micro and macro-modelling using a chemo-elasto-plastic model.

Supposing the concrete as a closed reactive elastic media, the AAR is simplified by a reaction $A \to B$. The thermodynamics of the system permits to identify a normalised irreversible reaction as its chemical state variable(Coussy O 1995).

The state variable of thischemical-mechanical system are the material strain ε, an external one and a global reaction expansion extent ξ an internal one. The system free energy Ψ thus reads

$$\Psi(\varepsilon,\xi) = \frac{1}{2}E_s(\varepsilon - \kappa\xi)^2 + \frac{1}{2}E_m\varepsilon^2 + \frac{1}{2}A_0(1-\xi)^2$$

according the state equations read

$$\begin{cases} \sigma = \dfrac{\partial\Psi}{\partial\varepsilon} = E(\varepsilon - \beta\xi) \\ A = -\dfrac{\partial\Psi}{\partial\xi} = \beta\sigma + A_0(1-\xi) \end{cases}$$

with

$$E = E_s + E_m,\ \beta = \kappa\frac{E_s}{E_s + E_m}$$

Following the mechanism, if the material irreversible strain is supposed to be only induced only by autogeneous tension σ_u the above chemo-elastic model can be extended to a chemo-plastic by introducing a local irreversible strain γ_p

To convert the model , the equivalence can be readily proved by the following relations:

$$\begin{cases} \bar{\beta} = \kappa\dfrac{E_m}{E_s + E_m} \\ E_h = \dfrac{E_s}{E_m}(E_s + E_m), K_m = k_m\dfrac{E_s + E_m}{E_m} \end{cases}$$

the coupled Chemo-plasticity is basically given by the relation if $E_s \ll E_m$ then $\beta\xi \to 0$

in such chemical-mechanical system, the material plasticity concerns its irreversible strain ε_p and χ its internal hardening variable. It is an isothermal process with the states variables $(\varepsilon, \varepsilon_p, \chi, \xi)$, the free energy reads

$\Psi\left[\left(\varepsilon-\varepsilon_p\right),\chi,\xi\right]=\frac{1}{2}\left[\mathrm{E}\left(\varepsilon-\varepsilon_p\right)^2+\mathrm{E_h}\left(\overline{\beta\xi}-\chi\right)^2\right]+\frac{1}{2}\mathrm{A}_0\left(1-\xi\right)^2$ accordingly the state equations read

$$\begin{cases}\sigma=\dfrac{\partial\Psi}{\partial\varepsilon}=-\dfrac{\partial\psi}{\partial\varepsilon_p}=\mathrm{E}\left(\varepsilon-\varepsilon_p\right)\\ \mathrm{p_s}=-\dfrac{\partial\Psi}{\partial\chi}=\mathrm{E_h}\left(\overline{\beta\xi}-\chi\right)\\ \mathrm{A}=-\dfrac{\partial\Psi}{\partial\xi}=\mathrm{A}_0\left(1-\xi\right)\end{cases}$$

By tridimensional application of this modelling it is proved that the observed stress induced anisotropy of ASR is well induced according to (Li K. and O. Coussy 2002)

Due to the coupling between the plastic porosity and the chemical swelling(Peterson M G. 2000).

4. modelling of the mechanical effects

Some other authors investigated in the modelling of the induced mechanical effects of AAR(Capra B. 1998), (Capra B. 2002). In that kind of modelling and due to the complexity of AAR modelling(random distribution of reactive sites and imperfect knowledge of the chemistry of the reaction), a new approach using fracture mechanics and probabilities to describe the swelling of the structure subjected to ASR is used, the coupling between AAR and mechanics makes it possible to simulate tests carried out on concrete specimens.

The approach used to describe the concrete behaviour is based on the a phenomenological approach that is based on the a physical description of deterioration of concrete by creation of surface area discontinuities. Numerous theoretical approach are proposed further to model cracking the most widely accepted are probably damage mechanics (Fichant S. 1997) and (Mazars J. 1990), Fracture mechanics(Bazant Z. P. 1998), (Tandon S. 1995) and plasticity (Feenstra P. H. 1995)

The model used in this study can be classified within general framework of anisotropy damage mechanics with reproduction of inelastic strains. The cracks are assumed to initiate and to propagate in Mode I and consequently bulk

collapses and crack propagation in mode II or III are not described. The elastic part of the behaviour law of concrete is based on damage theory as described by Lemaitre (Lemaitre J. 1988)

The partition of stresses and strains is carried out clasiicaly according to the sign of the eigenvalues of the apparent stress tensor:

$$\begin{cases} \varepsilon_i^e = \dfrac{1}{E_i^+}\sigma_{effi}^+ + \dfrac{1}{E_0}\sigma_{effi}^- - \dfrac{\upsilon_0}{E_0}\left(\sigma_{effj} + \sigma_{effk}\right) \\ \text{with } \dfrac{1}{E_i^+} = \dfrac{1}{E_0}\left(P_i + \left(1-P_i\right)\left(\dfrac{1-d_i^+}{1-d_i^{*+}}\right)\right) \\ \sigma_{appi} = \sigma_{effi}^+\left(1-d_i^+\right) + \sigma_{effi}^-\left(1-d_i^-\right) \end{cases}$$

the cracking state of the concrete is represented by two second-order tensor of probability of cracking due to a mechanical loading of tension $\left(Pf_i^t\right)$or compression $\left(Pf_i^c\right)$. The tensile stress has a direct effect on the opening of the crack in the loading direction. In the other hand the compressive strength can generate self-stresses of traction that are able to create a crack perpendicular to the loading direction.

It is obviously assumed that a Weibull's law (Weibull A. 1936) can globally describe the damage evolution in concrete:

$$Pf_i^t = 1 - \exp\left(-\frac{1}{m^+}\left(\frac{\langle\sigma_i\rangle^+}{\sigma_i^{ut}}\right)^{m+}\right)$$

$$Pf_i^c = 1 - \exp\left(-\frac{1}{m^-}\left(\frac{\left\langle\sigma_i + \sqrt{\left(C^-\right)^2\left(\left(\langle\sigma_i\rangle^-\right)^2 + \left(\langle\sigma_k\rangle^-\right)^2\right)}\right\rangle^+}{\sigma_i^{uc}}\right)^{-m}\right)$$ The total strain is assumed to be

the sum of the elastic strain ε_i^e the mechanical inelastic strains ε_i^{pl} (without AAR) and of the strains due to the AAR ε_i^{AAR}

$$\varepsilon_i = \varepsilon_i^e + \varepsilon_i^{pl} + \varepsilon_i^{AAR}$$

the self stress generated by the AAR in the direction "i" on uncracked concrete must balance the pressures generated in the cracks filled with product of the reactions. Let P_g be the average pressure exerted by those products on a part α of the cementitious matrix, the effective strength exerted is equal to:

$$\sigma_{gi} = -\frac{\alpha P_g}{\left(1-Pf_{aari}\right)}$$

the gel pressure is assumed to be proportional to the volume of the gel created. The volume of the cracks created by the AAR is assumed to be proportional to the total volume of cracks

the pressure due to the gel is given by the expression

$$P_g = \left\langle \frac{KV_g}{1+KV_g\left(K_c tr\varepsilon + K_p P_0\right)} \right\rangle$$

where K, K_p, K_c are respectively, the pseudo bulk modulus of AAR products, the initial porosity and the total volume of the created cracks.

The anelastic crack opening due to AAR evolves in an asymptotic way when cracking becomes significant. This phenomenon is modelled by the following equation

$$\varepsilon_i^{AAR} = \varepsilon_0^{AAR} \frac{Pf_i^{AAR}}{1-Pf_i^{AAR}}$$

where ε_0^{AAR} is a material parameter to be determined. Therefore we can link between the AAR swelling and the tension damage

$$\varepsilon_i^{AAR} = \varepsilon_0^{AAR} \frac{d_i^+}{1-d_i^+}$$

Experimental results (Larive C 1998)(engineers(ISE), 1992 #69) show a decrease in the mechanical characteristics of concrete according to the swelling rate.

5. The mathematical modelling

though the literature on the chemistry of the alkali-silica reaction (ASR) in concrete has become, a comprehensive mathematical model allowing quantitative predictions seems lacking.

In the mathematical models normaly we try to characterize the various effects of the influential parameters in the ASR.

(Suwito A. 2002) presented a model which characterises the effects of various influential parameters on the pessimum size effect of ASR expansion. As in the chemoelasticity, the model emphasises the coupling of the chemistry and the mechanical behaviour in the expansion process the chemical part of the model includes two opposing diffusion processes, one is the diffusion of the ions from the pore solution into the aggregate and the other is the permeation of ASR gel from the aggregate surface into the surrounding cement matrix. The mechanical part is developed based on a modified version of the self-consistent theory. The

ASR gel is divided in two parts:the gel directly deposited in the interface pores and the gel directly permeated into the surrounding paste. The amount and the rate of the permeation is depending on the aggregate size and the porosity of the cement paste.

In general and according to the authors the isotropic expansion caused by ASR can be simulated by the thermal expansion of an inclusion in a composite. Thus the total expansive strain of concrete can be determined using the models developed for effective thermal expansion of composites such as the thermoelastic model developed by (levin V M. 1967)which needs the effecticve bulk modulus developed by (Hashin Z. 1962)

The basic material is a composite spherical material with one constituent phase associated with another. The central phase is the aggregate and the outside layer is the cement paste. the same idea was used by (Herve E. 1993) and (Xi Y. 1997)

The configuration of the basic elements can also be used to model heterogeneous multiphase composite materials., which means that there could be multiple layers outside of the center sphere as reported by (Xi Y. 1997) and(Herve E. 1993).

The thickness of the gel layer formed at the aggregate surface is constant and not proportional to the size of the aggregate. This means if they consider the gel as a different phase they will have different fractions of the gel phase for different aggregate sizes.

The elemnt can be considered equivalent to a 3 phase layers element. Applying the elasticity theory to the problem for any single phase that expands, the equilibrium equation in spherical coordinates is

$$\frac{\partial^2 U_i}{\partial r^2}+\frac{2}{r}\frac{\partial U_i}{\partial r}-\frac{2}{r^2}U_i-\frac{1+\upsilon_i}{1-\upsilon_i}\alpha_{i,r}=0$$

where U_i is the displacement of the phase i in the radial direction, r the radial location coordinate. When all the phases expand, but each with its own coefficient of expansion the solution of the equation neglecting $\alpha_{i,r}$ is

$U_i = C_i r + \frac{D_i}{r^2}$ where

$$\sigma_i = 3K_i C_i - 4G_i \frac{D_i}{r^3} - 3K_i \alpha_i$$

where σ_i is the stress of phase i in the radial direction K_i, G_i are the bulk modulus and shear modulus of phase i respectively

in the case of concrete, the aggregate is the constituent phase that expands during ASR and the cement paste matrix does not expand therefore

$$\alpha_{eff} = \frac{K_1 V_1 (3K_2 + 4G_2)}{K_2 (3K_1 + 4G_2) - 4V_1 G_2 (K_2 - K_1)} \alpha_1$$

the final step is the derivation to find the interface pressure between the aggregate and the matrix. By using the stress equation the interface pressure is obtained

$$P_{int} = -\sigma(R_1) = \frac{12K_1 K_2 G_2 (1 - V_1)}{4V_1 G_1 (K_1 - K_2) + K_2 (3K_1 + 4G_2)} \alpha_1$$

in this model the concrete and all constituents are treated as elastic materials. That means that this model can be only applied for predicting the behaviour with moderate expansion due to ASR.

The mathematical model for diffusion of alkali is based to the assumption of similarity of diffusion between alkali and all the others processes of diffusion like moisture.

The process of micro-diffusion is described by Fick's law

$$B_{ion} = \frac{\partial C_{ion}}{\partial t} = \nabla (D_{ion} \nabla C_{ion})$$

in which C_{ion} is the free concentration of the pore solution inside the aggregate which could be hydroxide ions, calcium ions sodium ions etc..

the solution of the Fick equation in a polar coordinate is

$$C_{ion}(r, t) = C_0 + \frac{2R_i C_0}{\pi r} \sum_{i=1}^{\infty} \frac{(-1)^n}{n} \exp\left(\frac{-\kappa_{ion} n^2 \pi^2 t}{R_i^2}\right) \sin\frac{n\pi r}{R_i}$$

in which $\kappa_{ion} = \frac{D_{ion}}{B_{ion}}$

The ASR process takes place within the surface layer of each aggregate particle, where C_{ion} reaches a certain concentration level.

The mathematical equation describing the peremation of ASR gel is based and described by this equation:

$$V_{gel,eff}^{R_i} = \left\langle V_{gel}^{R_i} - V_{pore}^{R_i} \right\rangle_+$$

then the diffusion analysis is conducted and characterised by a Darcy's law for a viscous flow:

$$\frac{\partial C_{gel}}{\partial t} = \nabla\left(\frac{\kappa_{gel}}{\eta_{gel}}\nabla P_{gel}\right)$$

which C_{gel} and η_{gel} are the concentration and viscosity of the gel respectively, κ_{gel} is the gel permeability of the porous cement paste .

the resolution of this differential equation gives the solution of the concentration of the gel thus the distribution and the diffusion of the gel.

(Bazant Z. P. 2000) investigated their research on the mathematical modelling of the kinetics of the alkali-silica reaction.

The two basic problems that the model was fitted to solve are :

- The modelling of the kinetics of the chemical of diffusional processes
- The modelling of the mechanical damage of the concrete which calls for fracture mechanics.

Unfortunately this problem is very comples, inluences by many factors. This makes it impossible to make realistic predictions solely by intuitive reasoning based on the present quantitative knowledge of the ASR chemistry.

In their study, (Bazant Z. P. 2000) consider a relatively high concentrations for which a better idealisation seems to be a periodically repetitive cubic cell of concrete of side s containing only one reactive particle of initial diameter D obviously

$\rho_s \xi_{ss} s^3 = \frac{\pi D^3}{6}$ where ρ_s is the mass density of the reactive silica and ξ_{ss} is the silica concentration

the diffusion may be assumed to be governed by a Fick's law. Thus the radial flux of water

$J_w = a_s \bar{\nabla} \xi_w$ where ξ_w is the water concentration within layer of ASR gel and a_s the permeability of ASR gel to water.

Mass conservation of the gel requires that

$\dot{\xi}_s = -\mathrm{div} J_w = a_s \Delta \xi_s$ respect to time

the front can advance from an element dx to the next only after enough water has been supplied to combine all the silica within this element (P.Bazant, 1975 #11)

consequently the radial profile of ξ_w may be expected to be almost the same as steady-state diffusion equation

$$\frac{1}{x^2}\frac{\partial\left(x^2\,\partial\xi_w/\partial x\right)}{\partial x}=0$$

the solution yields to profile

$$\xi_w = w_s F\left(\bar{x}\right), F\left(\bar{x}\right)=\frac{1-\frac{2z}{D\bar{x}}}{1-\frac{2z}{D}}, \bar{x}=\frac{2x}{D}$$

the velocity of the reaction front is then obtain by differentiation of the preceding equation

$$\dot{z}=-\frac{2w_s DF'\left(\bar{x}\right)}{r\rho_s\tau_w}$$ with $\tau_w=\frac{D^2}{a_s}$ represents the half time of diffusion

The relation between the amount of water and silica involved is

$$r=\frac{\xi_w}{\xi_s}=\frac{2m_w}{m_s}$$

the next assumption taken in their model is the solid form of the ASR product in the absence of water according to Powers and Steinour(T.C Powers 1955)as reported by (Zdenek P.Bazant, 2000 #10) . the swelling is typical propriety of colloidal systems such as the reactions product gel, and is explained by electrical double layer repulsion known from surface chemistry (Prezzi M. 1997)

denoting by w_i the mass of water imbibed by the basic gel the volume increase of gel is

$$\Delta V=\frac{w_i}{\rho_w}$$

since the gel is constrained in the concrete, this increase in volume produces pressure in the gel which depends on the gel compressibility κ_g

$$P=\kappa_g\Delta V$$

because the gel is expelled into the pores the geometry of diffusion is no longer spherical and it appears difficult to choose any particular idealized geometry of the diffusion flow of water that should be analysed. It is reasonable to assume that

$$\dot{w}_i=\frac{A_i}{\tau_i}$$

where A_i characterises the thermodynamic affinity in terms of a concentration difference. The chemical potential of the water imbibed by the gel may be considered approximately proportional to $n(p)m(h)\xi_g$. So that

$$A_i = n(p)m(h)\xi_g - w_i$$

the fact that the water w_i in the cell will govern the imbibition rate . an approximation rate equation is given as follow for the water imbibition:

$$w_i = \left\| \left[\min\left\{ 1, \left| \left(\frac{D + 2\delta_c}{S^3} \right)^3 \right| \right\} - \left(\frac{D}{S} \right)^3 \right] \right\|$$

6. References

Lemarchand, E. (2001). "contribution de la micromécanique à l'étude des phénomènes de transport et de couplage poromécanique dans les grains poreux: application aux phénomènes de gonflement dans les géomatériaux." Ph D thesis Ecole nationale des ponts et chaussées.

Lemarchand, L. D. a. F., -J. Ulm (2002). "Elements of micromechanics of ASR-induced swelling in concrete structures." concrete science and engineering Vol 4(March 2002): pp12-22.

levin V M. (1967). "thermal expansion coefficients of hetergeneous materials." mechanics of solids 2(1): pp58-61.

Li K. and O. Coussy (2002). "Concrete ASR degradation: from material modelling to structure assessment." concrete science and engineering Vol 4.(March 2002): pp35-46.

Marc-André Bérubé, J. D., J. F. Dorion and M. Rivest (2002). "Laboratory assessment of alkali contribution by aggregates to concrete and application to concrete structures affected by alkali–silica reactivity." Cement and Concrete Research Volume 32(Issue 8): pp1215-1227.

Mazars J., B. Y., and Ramtani (1990). "the unilateral behaviour of damaged concrete." Engineering Fracture Mechanics 35 (4): pp1669-1673.

Monette L.J, G. N. J., Grattan-Bellew P.E, (2000). "Structural effects of the alkali aggregate reactions on non-loaded and loaded reinforced concrete beams." 11th international conference on alkali aggregate reaction: pp999-1008.

Moranville, J. P. B. a. M. (1997). "Durability of concrete: the crossroad between chemistry and mechanics." Cement and Concrete Research Volume 27(Issue 10): pp1543-1552.

Moranville M (1997). "modelling of expansion induced by ASR: new approaches." Cement and Concrete Composites 19: pp415-425.

Natesayier K, a. H. K. C. (1988). "in situ identification of ASR products in concrete." Cement and Concrete Research 18: pp455-463.

Nielsen A (2000). "alkali aggregate reactions strengthening or total collapse? the different effects of AAR on concrete structures." 11th international conference on alkali aggregate reaction: pp1009-1018.

Ono K (1990). "strength and stiffness of alkali silica reaction concrete and concrete members." structural engineering review 2: pp121-125.

P. Léger, P. C. a. R. T. (1996). "Finite element analysis of concrete swelling due to alkali-aggregate reactions in dams." Computers & Structures Volume 60(Issue 4): pp601-611.

Pantazopoulou S.J, T. M. D. A. (2000). "mechanical behaviour of AAR damaged R.C members." 11th international conference on alkali aggregate reaction: pp1019-1028.

Patrice Rivard, J.-P. O. a. G. B. (2002). "Characterization of the ASR rim: Application to the Potsdam sandstone." Cement and Concrete Research Volume 32(Issue 8): pp1259-1267.

Pérez, D. G. d. A. a. B. C. (2001). "Diagnosis of the alkali-silica reactivity potential by means of digital image analysis of aggregate thin sections." Cement and Concrete Research Volume 31(Issue 10): pp1449-1454.

Peterson M G., a. U. F.-J. (2000). "chemoplasticity of the Alkali silica reaction in concrete: modelling of stress induced anisotropy." CEE report , R00-02, Massachusetts Institute of Technology, Boston.

Pleau r, B. M. A., Pigeon M, Fournier, Raphael S (1989). "mechanical behaviour of concrete affected by ASR." 8th international conference on alkali aggregate reaction: pp721-726.

Poole, A. B. (1992). "introduction to alkali aggregate reaction in concrete, in the alkali-silica reaction in concrete." Ed. R. N. Swamy, Blackie Van Nostrand Reinhold.

Prezzi M., M. P. J. M., Sposito (1997). "The alkali aggregate reaction:Part I. Use double layer theory to explain the behavior of recations product gel." ACI Materials Journal 123: pp10-11.

Rivard P, F., Ballivy (2000). "Quantitative assessment of concrete damage due to alkali-silica reactions(ASR) by petrographic analysis." 11th international conference on alkali aggregate reaction: pp889-898.

Rotter H (1996). "The impact of alkali aggregate reactions on the fracture mechanics of concrete." Ph-D thesis(T-U Vienna Austria,).

Salomon M., G. J.-L. a. C. J. (1993). "alcalis réactions: mise au point d'un essai d'autoclavage rapide et fiable par lacaractérisation des granulats." Rceherches CEBTP-LCPC sur l'alcalis-réactions : techniques de mesures N 512(annales de l'institut technique du bâtiment et des travaux publics).

Shayan A, R. E. W., Anthony Moulds (2000). "Diagnosis of AAR in canning dam, characterisation of the affected concrete and rehabilitation of the structure." 11th international conference on alkali aggregate reaction: pp 1383-1392.

Shrimer, F. H. (2000). "application and use of damage rating index in assessment of AAR affected concrete - selected case studies." 11th international conference on alkali aggregate reaction: pp899-908.

Siemes T, V. J. (2000). "Low tensile strength in older concrete structures with alkali-silica reactions." 11th international conference on alkali aggregate reaction: pp1029-1038.

Suwito A., J. W., Xi Y., Meyer C (2002). "a mathematical model for the pessimum size effect of ASR in concrete." cioncrete science and engineering Vol 4(March 2002): pp23-34.

Swamy R.N (1992). "testing for alkali-silica reaction in concrete." the alkali silica reaction in concrete ed R N Swamy , Blackie, Van Nostrand Reinhold: pp54-95.

Swamy R.N, a. A.-A. M. M. (1986). "influence of Alkali silica reaction on the engineering properties of concrete." Alkalis in concrete, ASTM STP 930, Ed, V.H. Dodson, American society for testinfg and materials Journal, Philadelphia: pp69-86.

T.C Powers, H. H. S. (1955). Jour Am Concrete inst (Proc) 55: pp497-516 and pp781-808.

Tandon S., F. K., bazant Z.P., Li Yuan (1995). "coehesive crack modelling of influence of sudden changes in loading rate on concrete fracture." Engineering Fracture Mechanics 52 (6): pp987-997.

Ulm F-J., C. O., Li K., and Larice C. (2000). "Thermo-Chemo-mechanics of ASR expansion in concrete structures." Journal of engineering mechanics 126(3): pp233-242.

Weibull A. (1936). "Statistical theory of the sterngth of material." Proceed royal Swedish inst. for engineering research: pp139-151.

Xi Y., J. H. (1997). "shrinkage of cement paste and concrete modelled by a multiscale effective homogeneous theory." material structures 30: pp329-339.

Zaoui A. (1997). "Structural morphology and constitutive behaviour of microheterogeneous materials, continuum micromecahnics." CISM courses and lectures N°377(edited by P. Suquet).

Diffusion model

1. Experimental method

A double reservoir diffusion cell apparatus was designed as shown in the figure below. The maximum capacity of the apparatus when connected is approximately 1 l. a disk of aggregate is placed in between of the two cells.

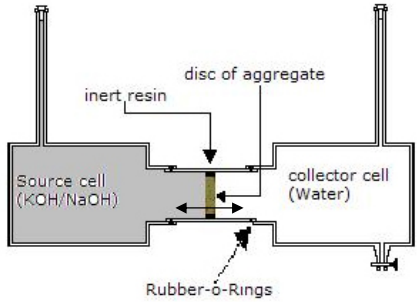

Fig1: diagram of the diffusion test

Core samples of aggregate were taken from a massive rock. Once the samples were cut , they were soaked with de-ionised water. The mass conservation with the system was ensured with alkali measurements of diffusion cells no detectable sources of alkali were noted within the experimental apparatus. The experiment was conduct in a closed system. Thus it is not possible to the alkali to leave the confines of the diffusion cell during the experiment.

Mass conservation within the system was ensured with fluoride measurements of blank diffusion cells measurements were made on alkaline solutions added to fully- equipped diffusion cells. No detectable sources or sinks of alkaline were noted within the experimental apparatus itself. No post-experiment mass conservation checks were conducted because of the difficulties in re-extracting and measuring the mass of alkali sorbed on the aggregates. the mean value of diffusivity coefficient obtained was equal to 5.0 $10^{-14}m^2/s$.

2. Model principles

The models consist on a 2D section of aggregates in a cement paste matrix. Aggregates and matrix arrangement were considered taken from images of the mortars these include a range of aggregate size.

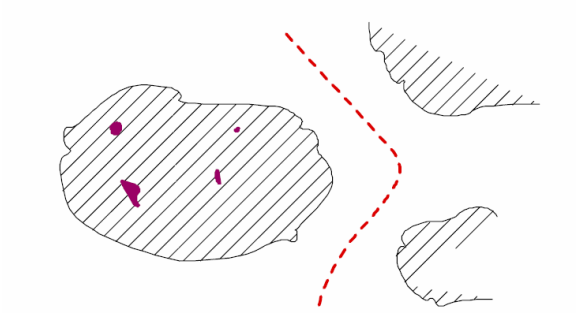

Figure 3: Distribution in fields and position of the limits of the modelled areas (purple: reactive sites, hatched: aggregate, white: paste cement, red line: limit of the area)

The areas modelled were selected so that the limits correspond to a symmetry plane from the point of view of the diffusion, i.e. they always pass halfway between the closest aggregates. The areas thus defined were divided into three fields: One of the fields represented the paste cement.

The second field represented the aggregates and the third the reactive sites. On the other hand, in the reactive sites alkalis can react with the aggregate. The differentiation in two fields was thus done for two reasons. The first was to be able to follow more exactly the concentration in the reactive sites and to be able to make statistics of reactive sites exceeding a certain alkali concentration (considered to be reacted) over the time. The second reason was that if the sites started to react before the diffusion is complete, a term of alkali consumption can be introduced.

The principal assumptions that were considered to develop this modelling were:

- The aggregates are assumed to contain a number of reactive sites whose distribution and density is approximated from observations of reacted mortars. In a real reacted mortar only sites close to the surface of the coarse aggregates were apparent. So the distribution was completed by addition of further sites in the centre of aggregates with a similar spatial density.
- Within porous media such as concrete or aggregate, diffusion cannot proceed as rapidly as it can in free solution due to physical, electrical and chemical factors. Chemical mechanisms may influence diffusion through complicated

reactions which may alter electrical properties or a size of migrations species [1]. These factors are combined in a single coefficient as they are not mutually independent and so cannot be easily separated [2]. So a single coefficient of diffusion calculated from the tests performed at 20°C in the laboratory was applied.

- At the start, the alkali level is considered to be uniform and equal to the level of alkali introduced to the mix. The cement matrix had consequently an initial concentration of 1.2 % Na_2O_{eq} and a coefficient of alkali diffusion equal to 7.5 $10^{-12}m^2/s$. The diffusion coefficient (5.0 $10^{-14}m^2/s$) and the initial concentration (0 % Na_2O_{eq}) are the same in the aggregates and the reactive sites. To have a criterion to consider the reaction happening within a reactive site, we choose a concentration criterion so that if the concentration in the reactive sites exceeds 0.5 % $Na_2O_{eq,}$ it is considered as reacted.
- The pore water acts as the necessary transport medium for the mass transport of hydroxyl and alkali ions required by the reaction. To avoid the problem of water permeation within the aggregates, we consider a saturation of the pore connectivity of aggregates and matrix. The reaction at the silica front may be considered to be almost immediate when the saturation is confirmed. This is justified by Dron and Brivot's [3, 4]observation that "the liquid film in contact with the grains of silica is at all times saturated in silica ions." Therefore, the rate of advance of the reaction front must depend solely on the rate at which the diffusion through the aggregate can supply ions to the reaction front.
- Flux is given by the following law Fick's first law:

  $J = -D.\overrightarrow{grad}\,C$

  C is the concentration of the diffusing species.

  D is the coefficient of diffusion in m^2/s and strongly depends on the temperature. Indeed $D = D_0 \exp(^{-E_a}/_{RT})$ where D_0 is a constant, R the gas constant, T the temperature in K and E_a the activation energy
- The variation of concentration in time and space is described by the Fick's second law: $div\, D\,\overrightarrow{grad}\,C = \frac{\partial C}{\partial t}$, this one rises from the conservation equation.

It is supposed that the gel creation does not affect too much the disappearance of alkalis inside a volume)

3. Boundary conditions, initial conditions

As the time of diffusion depends on the form and dimensions of the aggregates and as both strongly vary within a sample, calculations were carried out twice for two various areas in order to obtain a more correct result. In fact two areas of various SEM images of the same sample Mortar A were modelled.

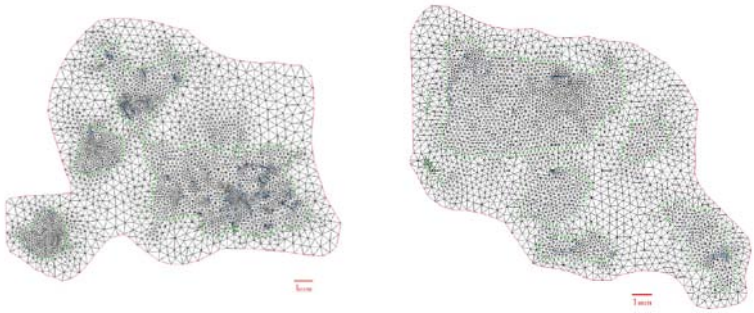

Figure 4: meshing of the domains

Calculations were performed for the mortars as a reactive medium for duration of 2 years to perform a complete reaction in all sites. Then an over scale of the samples were applied and the samples were performed in order to increase the size of the coarse aggregates in mortar to the one observed in concrete. Calculations were then carried out for the first meshing for 4.5 years duration. Simulation was made in three stages with steps of different times. A step of time of 1 hour for the 7 first days ½ day for the first year and daily for the remaining period. As the limits of the modelled area (in red) follow approximate symmetry planes, a null flux was imposed. A perfect contact between the various fields (cement paste - aggregate (green) and aggregate - reactive sites (blue)) was supposed.

4. Equivalence Chemical diffusion - thermal diffusion

The program used to carry out the calculations (calcosoft ®) was developed to solve thermal problems. On the other hand the equation for thermal diffusion

and the ionic diffusion are being equivalent if we consider the changing of phases of reactive silica is instantaneous and the gel has the same properties as the aggregate. Indeed considering a thermal process it is described by the equation:

$$div\, k\, \overrightarrow{grad}\, T = \rho C_p \frac{\partial T}{\partial t}$$

Thus if we consider T = C, K = D and R = C_P = 1 we obtain an equivalent equation which is the one of chemical diffusion:

$$div\, D\, \overrightarrow{grad}\, C = \frac{\partial C}{\partial t}$$

5. Results of simulations

To note some general features of the diffusion, we can already look at the curves isoconcentrations at various times. For a short time of diffusion we can see well that the equidistant lines between two close plans correspond to a line of symmetry (the curves of isoconcentration are perpendicular to the line). In addition, the gradient of concentration in the aggregates is higher than that in the cemented paste, the cause being that the coefficients of diffusion of the two mediums differ from two orders of magnitude.

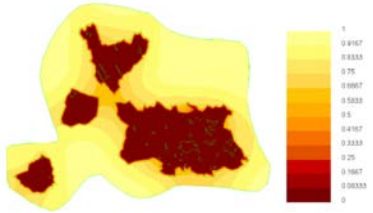

(a)

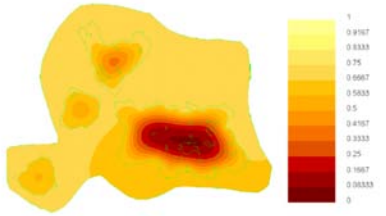

(b)

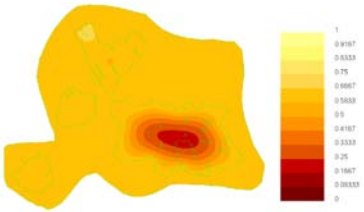

(c)

Figure 5: Profile of the concentrations after 1(a), 23 (b) and 85 (c) days.

After 22 days the profile (see figure 5) changed, the cement paste starts to be impoverished, the diffusion reached all the points of the area except the centre of the largest grain. The largest grain became the principal consumer of alkalis and the paste starts to be impoverished where the layer of cement surrounding this grain is thinnest. Consequently the symmetry planes of the diffusion are not defined any more by the equidistant lines between the aggregates.

This phenomenon becomes even more marked over of time. Indeed when the diffusion in the grains of small diameter was carried out completely, the profile of concentration will be rather parallel with the equidistant lines than perpendicular.

We see on the profile of diffusion after 85 days that the place containing the most alkalis is within an aggregate. Indeed as the aggregates have a coefficient of diffusion much smaller than the paste, the parts of the grains where the diffusion was already supplemented shows an opposite profile of concentration.

For the small grains, the time of diffusion corresponds to the time until the direction of the diffusion is reversed. For the largest grains the time of diffusion cannot be to determine so easily, as the direction of the diffusion remains always the same one. The time of diffusion is thus time or one cannot distinguish one profile any more through the grain.

6. Diffusion in the reactive site

To be able to estimate the influence of the diffusion over the reaction time the evolution of the concentration in the reactive sites was looked at.

Using the criterion given in the model principles, the volume percentages of the reactive sites having exceeded this concentration were traced on a graph according to time.

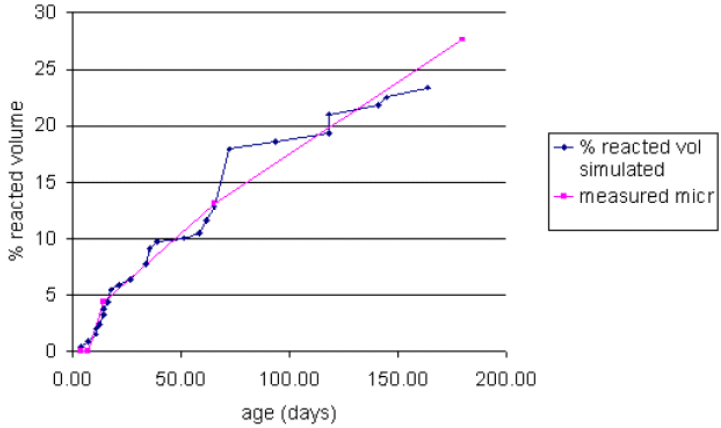

Figure 6: Volumetric percentage of the sites having reacted as observed in the microscope and as simulated.

If we compare these results with the observations made with the microscope on the same types of sample, one can note that at the beginnings the curves are almost being equivalent. For longer times the simulated diffusion is much slower than the reaction observed under the microscope.

7. Importance of the large grains on expansion

Another question which was put was to know the contribution of the aggregates size for the alkali-aggregate Na_2O_{eq}. As we said in the beginning and to solve this question, the over scale of the meshing was applied, then the contributions of the various grains to the volume of sites having exceeded the concentration 0.5 % Na_2O_{eq} were raised.

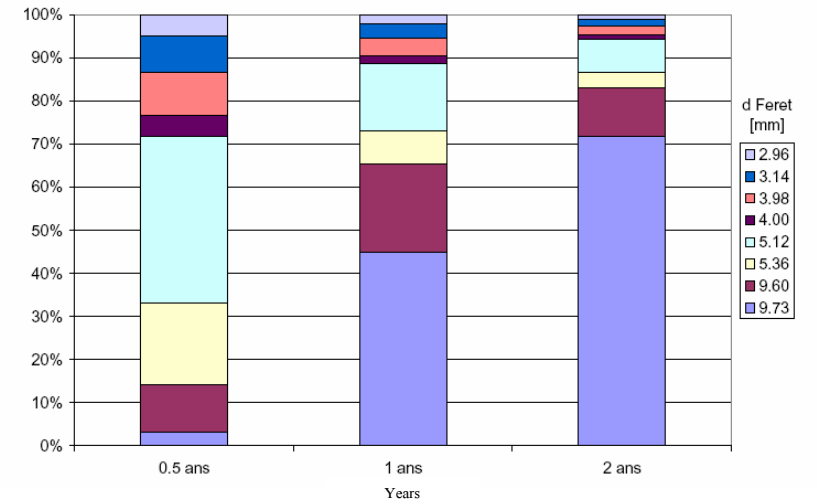

Figure 7: Contribution of the various grains size expressed as in the percentage of the reactive sites at 3 different times

It is seen that, once the diffusion is completed, the aggregates with a diameter higher than 9mm contributes more than 80 % to reactive volume. On the other hand times of diffusion are much slower in the coarse aggregates and the reaction thus occurs there more slowly (after a half years only 15 % of reactive volumes are contributed by the aggregates of diameter higher than 9 mm).

8. Discussion

As noted in the results of numerical simulation, the curve of diffusion and the curve observed under the microscope are rather similar in the beginning of the reaction.

For larger times of diffusion is much slower than the expansion. The diffusion is on the other hand influenced by the internal stresses caused by the formed gel. Indeed the cracking of the aggregates due to ASR can increase diffusion rate of alkalis towards other reactive sites. This acceleration is not taken into account at the time of simulation and explains the fact that latest reactive amount observed is bigger than the one predicted by calculation for larger time of diffusion.

As the diffusion in the small aggregates is already completed before the diffusion in the coarse ones, the direction of the gradients in these aggregates is reversed.

We can see this effect in the figure 5. Thereafter the grains of small diameter thus act like alkali tanks and thus slow down the diffusion. This can explain how these small aggregates can act when adding fine reactive to mixes to avoid alkali-silica reactions.

As we saw also that the aggregates of large diameters contribute more than 80 % of reactive volume but that the reactive sites in the large aggregates are activated later one can conclude than the addition of small diameter and fine reactive aggregate can slow down the expansion due to reaction alkali-aggregate by consuming the alkalis present.

Even if a higher number of results would be desirable to increase their precision and their significance, some characteristics and influences of the alkali diffusion in the aggregates could be noted. Firstly it was seen that the diffusion is probably accelerated over the reaction time because of the cracking of the aggregates. We note that the period of dormancy could be governed well by the diffusion of alkalis. We would on the other hand need a little more results to confirm this result

Fracture characteristics of aggregates

1. Introduction

In rock mechanics, fracture toughness is usually used as the main parameter to characterise the fracture behaviour of rocks.

In this study, the fracture behaviour of aggregates under ASR was studied. The measured parameter was the specific fracture energy because it is a global material parameter, which more efficiently captures the fracture and softening process. Also, this parameter was used as an input into an in-house numerical model specially developed for studying crack propagation and fracturing process of dam concrete. In the model, concrete is supposed to be heterogeneous material composed of elastic aggregates embedded into a viscoelastic matrix [1, 2]. The reactive sites are randomly distributed in the pre-cracked aggregates. The crack propagation which starts within the elastic aggregates may cross also the paste-aggregate interface and thus continues in the viscoelastic matrix.

Four-point bend tests were carried out to determine the fracture characteristics of these aggregates. The effect of sample immersion into an alkaline solution and the anisotropy observed in some aggregates were investigated. These properties will be used further as an input for a future study concerning the modelling of concrete fracture induced by ASR.

2. Sample preparation and experiments

A four point-loading Chevron Notched Bend Beam (CNBB) was used as a testing method for the determination of specific fracture energy G_f of various rocks from which the aggregates come, (Fig.1). A V-shaped chevron notch is used instead of straight-through notch because the V-shaped chevron notch causes crack initiation at the tip of the V and propagation in the notch plane along the specimen axis in a slow, stable and controllable manner. A second notch which starts from the chevron base up to bottom face of the specimen is also carried out to eliminate frictional effect. The four-point loading produces a constant bending moment between the support rollers and thus zero shear forces in the ligament zone which in turn allows a pure mode I crack opening.

The use of chevron-notched specimens with different dimensions may result in different monotonic crack extension and crack stability. Thus, the effect of notch

geometry on test stability was investigated with various samples in order to optimise specimen proportions . This has been done through a parametric study in terms of specimen dimensions, notch length and chevron angle, since these influence the amount of crack extension and crack area developing during the experiment. It should be noted also that the stability of the test is improved when the surface of the ligament is decreased and the thickness of the sample is reduced. In fact, the sample, which is appropriate for the controlled rupture, should show the following characteristics: a height/length ratio neither low nor high, a lowest possible thickness and a sufficiently deep notch [1]. The most stable test was obtained with samples having the following dimensions: length (L=180 mm), width (W =70 mm); thickness (b =20 mm), notch length (a=10 mm), chevron notch angle (θ=55°).

In order to study the size effect various samples of different length are cored from rocks (Table 1). The smallest samples did not have perfect geometrical similitude with largest ones because it was not possible to decrease their thickness below 10mm.

The three types of aggregates were studied. Displacement-controlled tests at the rate of 0.01 mm/s were performed on 25 samples for each case. Additional tests were also carried out to determine the elastic modulus and the tensile strength of each rock.

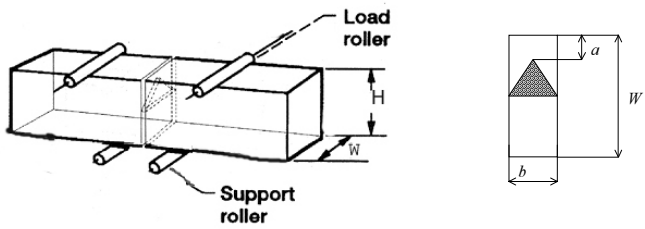

Figure 1. Chevron-notched beam in four-point bend test

Table 1: Dimensions of tested samples

Sample sizes	Length *L* (mm)	Depth *W* (mm)	Thickness *b* (mm)	Notch length *a* (mm)
Large (L)	180.00	40.00	20.00	10
Medium (M)	120.00	20.00	10.00	10
Small (S)	60.00	10.00	10.00	5

Immersion in alkaline solution

Each sample wass immersed in a saturated alkaline solution. Two initial water solutions were used: (1) pure water; (2) 0.6 M NaOH-equivalent solution. For each aggregate type, one experiment was performed at 40 °C. One set of samples was immersed for 60 days, the other for 180 days. Thus, samples were removed from the water solution and washed with alcohol.

3. Results and discussion

Table 2 presents the mechanical properties (tensile strength and the modulus of elasticity) of the various non-immersed (immersion time=0) aggregates in two orthogonal directions. Aggregate A presents a strong anisotropy (factor of 8 and 5 respectively for the modulus and the strength) whereas the aggregates B and C can be regarded as being isotropic.

Table 2: Mechanical properties of aggregates

	Aggregate A		Aggregate B		Aggregate C	
	LD	TD	LD	TD	LD	TD
σ_c (MPa)	10	1.2	11.2	10.9		10.3
E (GPa)	59.7	11	67.9	64.5	61.9	58.9

LD: longitudinal direction, TD: transverse section.

3.1. Influence of specimen size

Figure 2 shows a comparison of load-deflection curves obtained on samples of different size from aggregates A and B. For the aggregate A, it appears that increasing the sample size seems to increase the brittleness of the material. However, this tendency is less obvious for aggregate B and C (not presented here). This difference can be explained by the fact that rocks B and C are more homogeneous and less fractured than A.

The results obtained for the specific fracture energy G_f, defined as the area under load-deflection diagram per unit fractured surface, are compiled in Table 3. The statistical variability of this parameter, estimated from a set of 25 samples for each case, was found to be less than 5%. The results obtained clearly show that there is a tendency for G_f to decrease when the sample size increases. This can be explained by the fact that the larger the specimen sizes the higher pre-crack density, particularly for quasi-brittle materials such as rocks. For similar reason this is an increase of brittleness as a function of specimen size. The area under the load-deflection diagram becomes smaller for quasi-constant critical load.

Table 3: Specific fracture energy G_f [N/m] obtained under alkaline solution

	Aggregate	A			B			C		
	Immersion time (Days)	0	60	180	0	60	180	0	60	180
Sample size	Large (L)	148.3	135.9	133.5	165.3	157.6	160.1	-	-	-
	Medium (M)	165.7	155.8	149.5	169.7	160.3	162.5	158.2	154.3	151.2
	Small (S)	208.3	198.9	195.2	181.4	180.9	179.2	172.4	169.9	168.2

3.2. Influence of alkaline solution

The results on the samples immersed on alkaline solution are compiled in table 3. Fig.3 presents load-displacement curves from tests performed on samples (largest size) immersed for 6 months in an alkaline and non alkaline solutions for both aggregates A and B. This reveals that the presence of ASR product seems to increase the brittleness of the rock. On another hand, Fig.4 shows the evolution of average specific energy versus the immersion time for and also for the reactive aggregate (A) and the non-reactive one (B). It is clear that specific fracture energy decreases with increasing immersion time for the reactive aggregates - in particular for the largest samples - while there no significant effect on the non-reactive aggregate. These differences can be attributed to different amount of reaction and spatial distribution of alkali silica gel, which induces the development of microcracks along the reactive zones inside each sample as shown in Fig. 5.

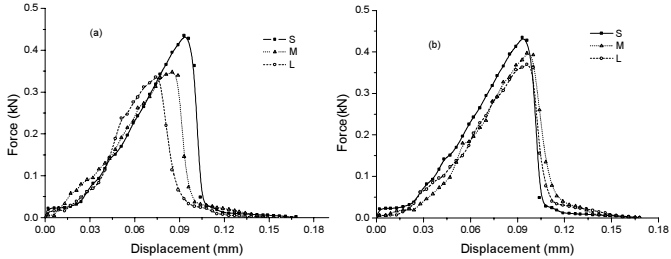

Fig. 2 Load-displacement diagram vs. specimen size before ASR

(a) Aggregate A, (b) Aggregate B

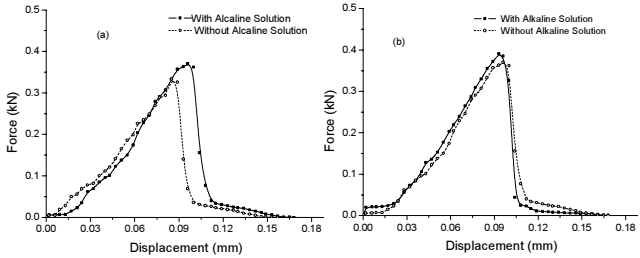

Fig. 3 Load-displacement diagrams obtained under alkaline solution and non-alkaline solution

(a) Aggregate A (reactive), (b) Aggregate B (non-reactive)

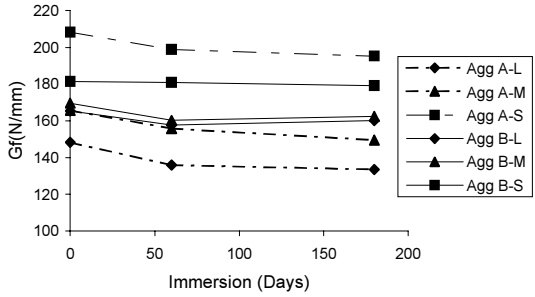

Fig.4: Specific fracture energy versus immersion time

for reactive aggregates (A) and non-reactive aggregates (B)

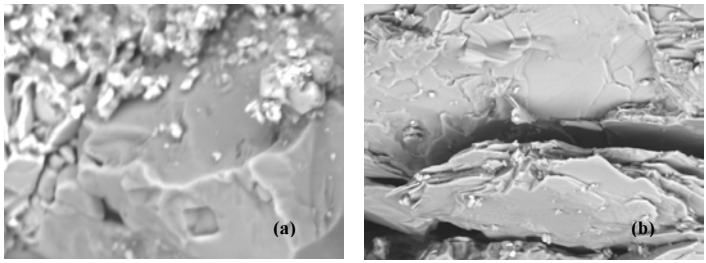

Fig. 5: Fractured surface of aggregate A: (a) before immersion, (b) After 6 months of immersion into alkaline solution

4. Conclusion

The determination of fracture properties of brittle materials through the four-point bend test has been described and specimen proportions have been optimised to ensure a stable displacement-controlled testing. The specific fracture energy has been investigated in terms of size sample and immersion time into an alkaline solution. The obtained results reveal that the fracture energy decreases and the brittleness of the rock increases as the specimen size increases. Nevertheless this size effect needs to be more deeply investigated through additional experiments in terms of sample width *W* and notch length to width ratio *a/W*. The results on the influence of immersion time also show that the ASR-induced products may reduce both the fracture energy and the brittleness of the reactive rocks.

5. References

1. Huet, C., *Méthode de détermination de l'énergie spécifique de rupture et application aux céramiques et à divers matériaux minéraux.* Cahiers français de rhéologie, 1973. **III**(3): p. 128-142.
2. Ouchterlony, F., *Fracture toughness testing of rock with core based specimens.* Engineering Fracture Mechanics, 1990. **35**(1-3): p. 351-366.

3. Chang, S.-H., C.-I. Lee, and S. Jeon, *Measurement of rock fracture toughness under modes I and II and mixed-mode conditions by using disc-type specimens.* Engineering Geology, 2002. **66**(1-2): p. 79-97.

4. Wang, Q.Z., et al., *The flattened Brazilian disc specimen used for testing elastic modulus, tensile strength and fracture toughness of brittle rocks: analytical and numerical results.* International Journal of Rock Mechanics and Mining Sciences, 2004. **41**(2): p. 245-253.

Ben HAHA Mohsen

Rte Neuve 81
Ecublens-VD 1024
Tel : +41 021/6934673
Mobile : +41 078/7630681,
Email : mohsen.benhaha@epfl.ch

Date of birth:	January 10, 1977
Place of birth:	Grombalia, Tunisia
Nationality:	Tunisian
Marital status:	Single

Education:

2002-2006	PhD studies, Swiss Institute of Technology Lausanne, in the laboratory of construction materials, group of Prof. Karen scrivener
2001	Master in hydrology and water resources management, Ecole Polytechnique fédérale de Lausanne, ETH Zürich, Switzerland
1997-2000	Engineer diploma in structural engineering, INAT, Tunisia
1995-1997	Math sup and Math spé: institut préparatoire aux études d'ingénieurs de Tunis : IPEIT
1995	Bachelor entrance exam: mathematics

Professional experience:

2001-2005	Teaching assistant, material sciences: construction material, Swiss Institute of Technology Lausanne
2000	Structural engineer
1999	Training in a dam society : engineer
1998	Training in OTD

Languages:

Arabic	Mother tongue
French	2nd Mother tongue
English	Fluent
german	Good knowledge
Italian	Good knowledge

Hobbies:

Formula 1, Football, Rugby, Music, Theater